REFERENCE NO. 64 152

COPIES

R. L. W.
V.M

~~CONFIDENTIAL~~

Unclassified

LUNAR ORBIT RENDEZVOUS REFERENCE TRAJECTORY DATA PACKAGE (U)

PREPARED UNDER CONTRACT NO. 10001
TO BELLCOMM, INC.

EXEMPLARY APOLLO MISSION PARAMETER ANALYSIS

8408-6039-RC-000 **FEBRUARY 10, 1964**

Classification changed to
UNCLASSIFIED by authority of
SCG-1, Rev. 1, 1/1/65, and
SCG-6, 8/27/64, as amended
Initials: [illegible] Date: 3-22-69
letter from R. L. Wagner
dated 3-11-69

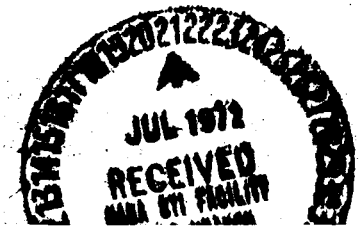

Unclassified

TRW SPACE TECHNOLOGY LABORATORIES
THOMPSON RAMO WOOLDRIDGE INC.

~~CONFIDENTIAL~~

[redacted] REFERENCE NO. 64 152

COPIES

R. L. W.

Unclassified

Copy ___ of ___

Total Pages: 146

LUNAR ORBIT RENDEZVOUS

REFERENCE TRAJECTORY DATA PACKAGE (U)

Prepared under Contract No. 10001
to Bellcomm, Inc.

EXEMPLARY APOLLO MISSION PARAMETER ANALYSIS

8408-6039-RC-000

February 10, 1964

Classification changed to
UNCLASSIFIED by authority of
SCG-11, Rev. 1, 1/1/66, and
SCG-6, 8/27/64, as amended
Initials: [illegible] Date: 3-22-69
Letter from R. L. Wagner
dated 3-11-69

Approved: F. L. Baker
F. L. Baker
Project Manager

Approved: for Edward W. Fichtl
R. M. Page
Manager
Systems Analysis Department

TRW SPACE TECHNOLOGY LABORATORIES
One Space Park
Redondo Beach, California

[redacted]

Unclassified

[redacted]

ACKNOWLEDGEMENTS

The following personnel have contributed to the preparation of this report:

J. A. Herbaugh
R. W. Johnson
L. L. Lakamp
P. A. Penzo
R. J. Schussler

CONTENTS

8408-6039-RC-000
Copy ___ of _____
Total Pages: 146

1. INTRODUCTION AND SUMMARY

In accordance with the provisions of Amendment No. 1 to Subcontract No. 10001 from Bellcomm, Inc., TRW Space Technology Laboratories is pleased to submit the first of two reports covering a generalized "Mission Parameter Analysis" of the Apollo mission. The total purpose of this analysis is to determine the behavior of mission variables, both geometric and dynamic, applicable to the moon's motion at the end of this decade. The study is to be sufficiently complete such that the quantitative characteristics of the mission, subject to certain ground rules and constraints pertinent to the present overall mission plan, will be identified for typical launch opportunities. The objectives of this first report are to:

a) identify a procedure for obtaining the results desired,

b) show the results of applying the procedure to one particular launch day,

c) present results in a coherent manner with maximum reliance on graphical presentations,

d) identify the important variables and eliminate the unimportant parameters from general consideration, and

e) provide a basis from which the final report may be constructed for maximum utility.

The complete study is to be performed by considering a minimum list of mission parameters (with a range of values for each) and a list of constraints which serve to define a basic mission plan and vehicle capability. These study ground rules are summarized in Section 2, and their interactions are noted.

In the simplest terms, the Apollo mission may be thought of as containing three principle phases:

a) earth launch, circular earth parking orbit, and a highly elliptical earth-moon transfer trajectory which, if unperturbed, would pass the moon within a certain distance,

b) deboost from the earth-moon transfer trajectory into a circular parking orbit about the moon, and a series of LEM operations culminating in rendezvous with the CM/SM which has remained in orbit,

c) transearth injection, a moon-earth transfer trajectory, and shallow reentry and landing at one of two prescribed sites.

Within each of these phases, basic constraints exist which limit operations to a range of desirable characteristics. The essential task of this study is to connect the three phases by means of calculations which will demonstrate their interrelationships quantitatively and thereby establish the trajectory dependent limits of system operation. Particular attention is to be given to the lunar landing site accessibility afforded by the Service Module in conjunction with a trajectory design.

STL's approach to the problem, as described in this report, has been to treat each of the mission phases as a separable problem and then to analyze the influence each has on the other two. A detailed analysis of the interaction among phases has been made for one assumed launch date, January 28, 1968, based on a procedure which is itself described. The results of this analysis have been applied to a discussion of the independent variables in order to confirm the adopted method. Although the analysis of one day does not allow the effects of the moon's motion to be shown, this influence is implied from previous work.

The first result that is derived from this study is that the division of the trajectory into three phases permits an analysis of the lunar operations phase independent of the other two. For example, the launch operation is completely standardized from a trajectory point of view. The degrees of freedom that exist, i.e., time of flight, launch azimuth and the length of the parking orbit will generate the launch window and translunar injection energy requirements. The lunar phase of the operation, however, is not so well defined. There is no fixed orbit altitude or landing site and, for that matter, no accepted method for deboosting into and injecting out of orbit. Also, the use of unrestricted (non-free-circumlunar) translunar orbits provides a degree of freedom which may be used to satisfy a variety of desirable constraints, such as minimizing the Service Module energy requirements, or reducing LEM rendezvous plane change. An attempt is made to solve some of these problems, or consider their significance, in Section 3.

Before deciding on a mode of operation in the lunar phase of the Apollo program, different modes must be compared. This phase of the problem is best handled if it can be divorced from the translunar and transearth phases. The concept of the approach and departure hyperbolic excess velocity vectors, described in Section 2 and analyzed in Section 3, permits such a division.

The major portion of this report is concerned with the non-free-circumlunar trajectory. An analysis of the Apollo trajectory for the free circumlunar case may be found in Reference 1. The analysis of unrestricted translunar trajectories raises a number of questions which do not arise in the free circumlunar case. Complete or partial freedom in the dimension and orientation elements of the approach hyperbola gives rise to several possible operational modes. It has been shown that unrestricted translunar trajectories possess this freedom which, in turn, is used to the fullest extent to minimize Service Module propellant weight required. The sole constraints imposed are the following:

a) The SM orbit altitude be maintained at 80 nautical miles

b) The SM circular orbit be oriented such that LEM descent, after two orbital revolutions, be in the plane of the orbit.

This minimization also assumes a single injection at deboost into and departure out of the SM orbit. It is possible that an additional injection, perhaps at a much greater distance from the moon, may result in a reduced minimum propellant weight. For the single impulse deboost and transearth injection case, however, the method described here does represent the minimum required propellant weight. Other operational modes, such as the free circumlunar case, will result in a greater SM propellant expenditure assuming that all other parametric values remain the same.

In order to illustrate the effect of lunar landing site location on the minimum propellant analysis described above, propellant weight contours have been drawn on selenographic grids. These contours are presented for a single day and include variations in translunar flight time, lunar orbit stay time and transearth flight time. Some qualitative characteristics

and trends observed for this one day may be generalized to other days when the moon has another distance and declination to the earth's equator. Also included on these contours is the effect on the lunar surface stay time imposed by a maximum of 4 degrees plane change for LEM rendezvous. The following summarize some of the more important results which have been derived for the unrestricted translunar trajectory problem:

a) For a unique set of parameters in the translunar and transearth phases of the Apollo trajectory, there exists a unique retrograde lunar orbit for which the total Service Module propellant requirements will be minimized. It follows that landing sites chosen along the trace of this orbit at the time of LEM descent can be attained for this minimum SM propellant expenditure. The mean location of this orbit is near the lunar equator.

b) For landing sites not on the trace of this optimum orbit, a greater amount of propellant will be required. However, for each such landing site a unique minimum fuel SM orbit exists if the pericynthion altitudes of the approach and departure hyperbolas are unrestricted.

c) As landing sites become further removed from the minimum locus, the SM propellant requirement may increase so as to ultimately exceed the tank capacity. That is, under certain conditions there may exist areas of inaccessible landing sites on the moon.

2. METHODS AND ANALYSIS

2.1 Introduction

The analysis reported herein will be concerned with two of the more important aspects of the mission parameter study. The first is to establish a procedure for a general parametric study which will yield a maximum amount of data. The second is to determine a plan of operation for the Service Module when the translunar trajectory is not restricted to the free circumlunar case. It will become clear with the following discussion that the solution to the first problem considerably simplifies the analysis of the second.

A simplification of the parametric study is accomplished by dividing the problem into three phases. The parameters to be studied in each of these phases are the following:

Group 1. Translunar Phase

a) Day of launch (introduces the variable lunar distance and declination).

b) Launch from Cape Kennedy with a range of launch azimuths between 72 and 108 degrees.

c) Launch into a circular parking orbit the duration of which may vary between 0.5 and 3 revolutions.

d) Translunar flight time varying from 60 up to 120 hours.

Group 2. Lunar Operations Phase

a) Circular lunar orbit altitude ranging from 50 to 150 nautical miles.

b) Lunar landing sites in the area bounded by ±45 degrees selenographic longitude and ±30 degrees selenographic latitude.

c) LEM descent on the first or second pass over the landing site from a retrograde circular orbit.

d) Stay time on the lunar surface ranging from 1 to 48 hours.

e) CM/SM injection time on the first, second, or third revolution after rendezvous.

Group 3. Transearth Phase

a) Inclination of the earth phase conic with the equator ranging from 30 to 40 degrees.

b) Transearth flight time varying from 60 up to 120 hours.

c) Earth landing site of either San Antonio, Texas, or Woomera, Australia.

d) Re-entry maneuver angle ranging from 15 to 100 degrees.

Listed in these three groups are only those parameters which are considered as variables. Those which are assumed to be constant are:

a) Launch and translunar powered flight profiles

b) Earth parking orbit altitude of 100 nautical miles

c) Δv budget of 300 feet per second for outbound and inbound midcourse correction

d) Re-entry altitude and flight path angle of 400,000 feet and 96.4 degrees, respectively.

In addition to these variable and constant parameters, the following ground rules apply to the study:

a) Patched conic techniques may be used to generate the complete free flight trajectory.

b) A true (tabulated) lunar ephemeris is to be used.

c) Hyperbolic approach to the moon and the lunar circular orbit are to be retrograde

d) Powered flight deboost and transearth injection are to be represented as impulsive maneuvers.

Before proceeding with a discussion of the particular variables listed in Groups 1, 2, and 3, the following observation on the scope of the study may be made. If reasonable increments of these parameters are taken, such as 72, 90 and 108 degrees for the launch azimuth and 60, 70, 80, ..., 120 hours for the translunar flight time, one can readily arrive at the number of possible trajectories with all possible combinations of these parameters. The answer to this calculation, which is simply the product

of the number of increments chosen for each variable, runs well over a million. If, however, it is assumed that the translunar and transearth trajectories may be computed only from the parameters in their respective groups, then this number is considerably reduced. For example, if this is the case, then varying the location of the lunar landing site will not require a recalculation of the translunar and transearth trajectories. The remainder of this section is devoted to establishing the validity of this assumption and developing the procedure by which the three phases may be parametrically combined.

The concept for the division of the Apollo trajectory into three phases is derived from the patched conic technique. Briefly reviewing this method (Reference 2), the patched conic approach assumes that earth-moon space may be divided into two inverse square force fields, the first lying within a sphere centered at the moon and such that only the moon's gravitation applies, and the second existing external to this sphere where only the earth's gravitation is considered. From this theory, the dividing surface, or the sphere, has a radius of approximately 10 earth-radii and usually is referred to as the moon's sphere of action (MSA). With this gravitational model, all free flight trajectories outside of the MSA will be conics with one focus at the earth's center and those within will be conics with one focus at the moon's center. For Apollo trajectories where a portion must lie within the MSA and a portion must lie outside the MSA, the complete trajectory is developed by matching the position and velocity of the earth-centered and moon-centered conics at the sphere, taking into account the moon's motion. Thus, the complete trajectory will be continuous in its position and velocity.

The advantage of using this model in determining lunar trajectories is that it results in high solution speed in that closed form expressions may be used to solve for specific end conditions such as those given in Groups 1, 2, and 3. Comparison of the conic parameters of such patched conic trajectories with integrated trajectories satisfying the same terminal conditions is sufficiently accurate for the parameter study.

For the set of translunar and transearth trajectories which satisfies the parametric conditions stated in Groups 1, 2, and 3, the earth-phase

conic will be an ellipse of high eccentricity, greater than 0.96, and the moon phase conic will invariably be a hyperbola. Figure 2.1-1, for example, indicates the nature of a translunar trajectory where it is assumed that the earth phase conic is launched in or very near the moon's orbit plane and satisfies a specific set of parameters in Group 1. The locus of penetration points at the MSA will result in a moon phase conic having a specified pericynthion altitude but no unique inclination. Thus, each point on the locus represents a specific approach inclination to the moon; the right half locus represents direct approaches and the left half represents retrograde approaches. A slightly larger or smaller locus will result if the pericynthion distance is increased or decreased.

This set of translunar trajectories, including those with a range of pericynthion altitude, satisfies specific conditions in Group 1, but no specific conditions in Group 2. Concerning this set, an important observation is made (it will be substantiated later):

> Only slight variations at translunar injection are required to generate any one trajectory satisfying specific conditions in the moon phase (Group 2).

For example, in Figure 2.1-1 the earth phase conic need not be more than 0.5 degree out of the moon's orbit plane to generate the loci above. Thus the earth phase conic will essentially remain in the moon's orbit plane while the moon phase conic may be polar.

A second observation, the one which forms the basis of the division of the mission parameter study into three phases, is the following:

> For the set of trajectories described above, the moon-centered velocity at the MSA does not change appreciably in magnitude or direction.

Thus, all of the hyperbolas generated in the set above emanate from the MSA with essentially the same velocity magnitude and direction. A further observation is that the direction of this velocity vector is within 0.2 degree of the direction of the hyperbolic asymptote for all of the above cases. It is therefore possible to take this direction as the velocity-at-infinity direction and compute the hyperbolic excess velocity from the vis-viva energy

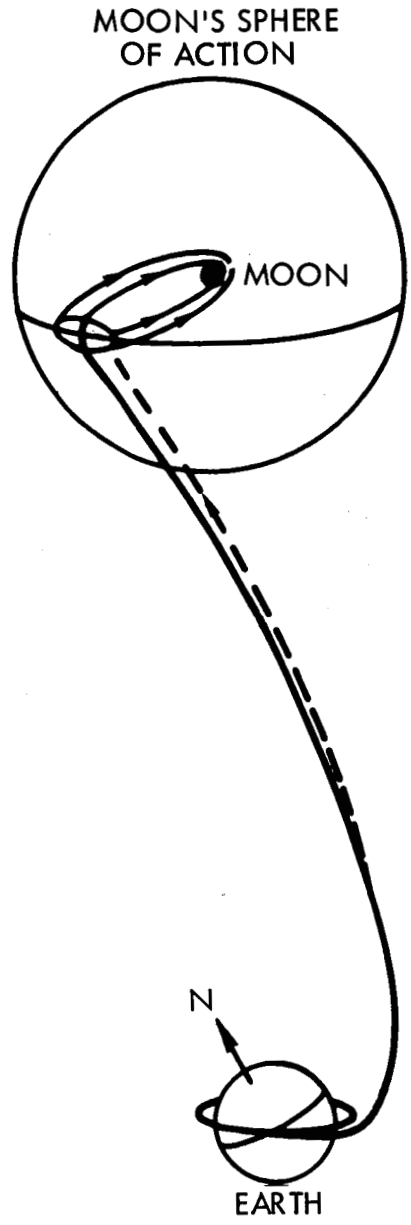

Figure 2.1-1. Geometry of a Translunar Trajectory Launched in the Moon's Orbit Plane. The Discontinuity at the Moon's Sphere of Action is Caused by Transferring from an Earth Centered to a Moon Centered Conic

equation.* The combination produces what will be referred to as the $\overline{v}_\infty$ vector, which will be considered invariant for the set of hyperbolas described above. The variation of the $\overline{v}_\infty$ vector with variations in parameters in all of the three phase groups is described in detail in Section 3.

Before describing the three-phase division of the parametric study, a word should be said concerning the transearth trajectory. All of the above discussion also applies to these trajectories due to the considerable symmetry between the translunar and transearth trajectories. The flight times lie within the same range and the characteristics of the moon-phase conics are similar. The earth-phase conics differ slightly in two respects: the perigee of the return conic is lower (about 60 nautical miles) and the range of inclinations of the outward conic is smaller (from 28.5 to 33.4 degrees). Since the conclusion above concerning the $\overline{v}_\infty$ vector encompasses these slight variations, a similar statement may be made. That is, for specific values of the parameters in Group 3 (including the day of transearth injection), all of the hyperbolic trajectories produced by satisfying the conditions in Group 2 will generate essentially the same $\overline{v}_\infty$ vector.

On the basis of this simplification, the following procedure may be used to generate Apollo trajectories for the mission parameter study:

a) Compute translunar trajectories for the complete set of variables in Group 1, but for a single case from Group 2 and assume that the incoming (to the moon) $\overline{v}_{\infty 1}$ vector applies to all cases in Group 2.

b) Similarly, generate transearth trajectories for combinations of parameters in Group 3, including the day of transearth injection, but for a single case in Group 2. Assume that the outward (from the moon) $\overline{v}_{\infty 2}$ vector applies to all cases in Group 2.

---

*This equation, in a form convenient to the analysis, is

$$v_\infty^2 = v_s^2 - \frac{2\mu}{R_s}$$

where v_s and R_s are the moon-centered velocity at the MSA and the sphere's radius, respectively.

c) Utilize only the $\overline{v}_{\infty 1}$ and $\overline{v}_{\infty 2}$ vectors generated by specific translunar and transearth phases to determine characteristics of the lunar operations phase (Group 2) of the study.

This procedure then establishes the division of the mission parameter study into the three phases. Also, it is clear that the connecting parameters between these phases are now the $\overline{v}_{\infty}$ vectors at entry and exit of the moon's sphere of action. Accompanying these vectors, but not mentioned previously, is the time of penetration for these vectors at the MSA. Thus, if a specific day of earth launch is chosen, plus other fixed parameters from Group 1; and a specific day of transearth injection is chosen (perhaps 4 days after the day of launch) plus fixed parameters from Group 3, then the penetration times will be defined. Certainly, once the translunar and transearth trajectories are computed, the times of launch and re-entry are known. Further, since the times of flight are specified in both cases, the times of deboost and transearth injection are determined. Assuming, then, that the times of flight within the MSA are independent of the values of the parameters in Group 2, the times at entry and exit of the sphere may be calculated.

In order to provide the most natural representation of moon phase results, the question remains in what coordinate system and at what time should the $\overline{v}_{\infty}$ vectors be specified. If the coordinate system is inertial, then the question of time will not arise since the two vectors are fixed in inertial space. However, as will become evident, the $\overline{v}_{\infty}$ vectors are of most direct use if they are represented in the selenographic system. Since the components in this rotating system vary with time, it will be assumed, unless otherwise stated, that $\overline{v}_{\infty 1}$ is given at the time of deboost and $\overline{v}_{\infty 2}$ is given at the time of transearth injection. Also, whenever they are graphed, the representation will be their magnitudes and selenographic longitudes and latitudes. The $\overline{v}_{\infty}$ vectors are considered as free vectors so that their position in space may be disregarded at all times.

Since the procedure for generating translunar and transearth trajectories (aside from the parameters in Group 2) is well defined, no further discussion will be given concerning them. The next two sections will be devoted to the more complex and variable problem of lunar operations.

Also, these sections will be concerned exclusively with the problem of the non-free return translunar trajectory. Some discussion on the free return trajectory will be presented in Section 4.

2.2 Optimization Theory of Service Module Performance

Having established the procedure to be used in computing the complete Apollo trajectory, it is now necessary to adapt this method to the lunar operations phase. Specifically, the problem reduces to the following:

> What characteristics should the translunar approach hyperbola, CM/SM orbit, and transearth departure hyperbola have which best satisfy a specific set of parametric constraints given in Group 2?

Before launching into the heart of this problem, which as will be seen later is the minimization of the total fuel expended by the Service Module, a brief discussion will be presented to indicate the general relationships of these three conics (the two hyperbolas and the orbit) with the $\overline{v}_\infty$ vectors and the lunar landing site.

Recall that for unique translunar and transearth trajectories, the times of deboost and injection will be specified. Hence, the length of time that the Service Module is in orbit is fixed. Thus, if the revolutions for LEM descent and rendezvous are specified, as well as the time to descend and rendezvous, then the stay time on the lunar surface may be calculated. As mentioned earlier the selenographic coordinates of $\overline{v}_{\infty 1}$ and $\overline{v}_{\infty 2}$ are specified at the time of deboost and injection respectively. The rotation of the moon will cause the $\overline{v}_\infty$ longitude components as well as the node of the circular orbit to change with time. In order to analyze the problem, it is necessary to refer the two vectors and orbit to a single reference time (or epoch) and this may be taken as the pass of the orbit from which the LEM will descend. This is convenient since at this time the orbit passes over the landing site.

Figure 2.2-1 presents a Mercator projection of the moon for a typical situation at the reference time. Disregarding the pericynthion circles for the moment, note that many possible orbits may pass over the landing site. This allows one degree of freedom to the orientation of the orbit which may

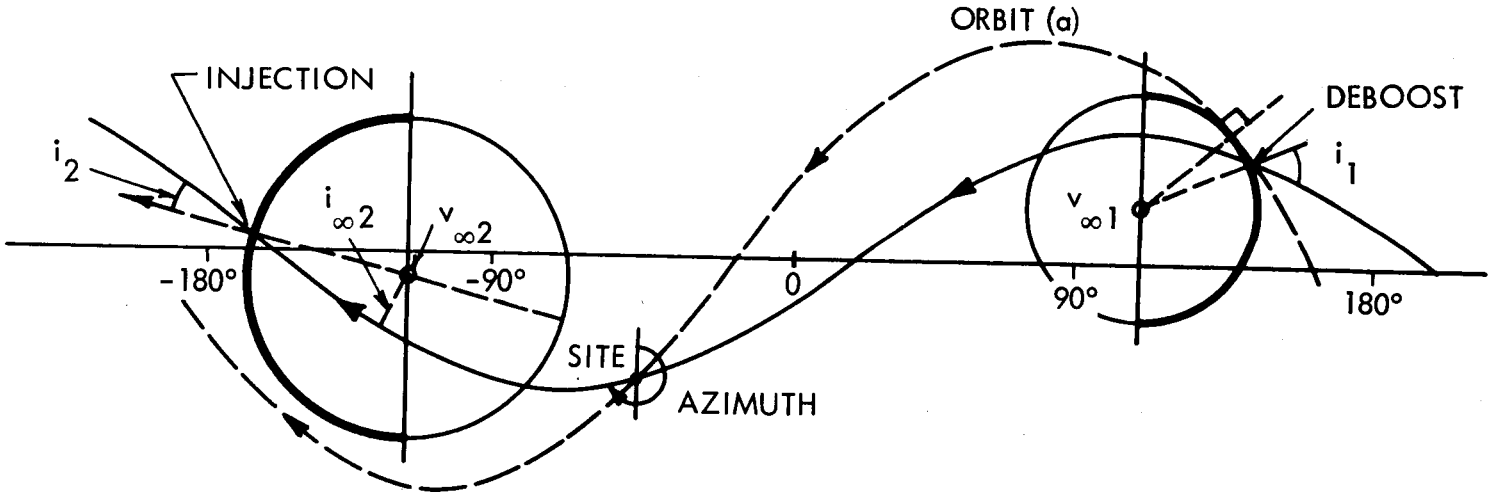

Figure 2.2-1. Mercator Projection of the Lunar Geometry for Fixed Pericynthion Deboost and Injection

be taken as the azimuth at the site. It will be shown later that this is the variable used to minimize the total SM fuel expended. For each value of this azimuth, the circular orbit will have a specific relation with the $\overline{v}_{\infty 1}$ and the $\overline{v}_{\infty 2}$ vectors. In general the orbit will not contain either vector but will be displaced from them by some angles, say $i_{\infty 1}$ and $i_{\infty 2}$.

The question now arises as to what are the characteristics of the hyperbolas necessary to deboost into and inject out of a specific SM orbit. This problem will be discussed in detail since it is directly involved in the optimization procedure. The first part of the discussion will be confined to deboosting and injecting at the pericynthion of the hyperbolas. Then it will be shown what can be gained by assuming non-pericynthion deboost and/or non-pericynthion injection. Finally, a brief discussion will be presented to indicate that minimizing total velocity impulse is not necessarily the best criterion to follow in optimizing the lunar operations phase.

Beginning with the fixed pericynthion constraint, Figure 2.2-1 shows the two loci for fixed pericynthion deboost into orbit and fixed pericynthion injection out of orbit. The smaller circle for example (the radius is determined by the magnitude of $v_{\infty 1}$) indicates the locus of pericynthions for the set of hyperbolas which have the same $\overline{v}_{\infty 1}$ vector and a fixed pericynthion altitude equal to the SM orbit altitude. In reality, the hyperbolas in this set are identical except for their orientation with the lunar equator. Thus, the pericynthion locus is generated by rotating a single hyperbola about the $\overline{v}_{\infty 1}$ vector. The shape of this hyperbola is determined only by the pericynthion altitude and the $v_{\infty 1}$ magnitude. The plane of each hyperbola would be oriented such that it would contain the $\overline{v}_{\infty 1}$ vector and the position vector to the pericynthion point. Exactly the same arguments hold for the injection pericynthion locus.

For the orbit given by the solid line, Figure 2.2-1 indicates that for pericynthion deboost and injection, the impulses must be applied at the intersection of the orbit with the pericynthion circles. Since there are two intersections for each circle, those intersections are chosen which apply to retrograde hyperbolas. That half of each locus for which the hyperbola will be retrograde is indicated by a heavier line. Also shown are the plane

changes i_1 and i_2 which will be required in each case. An alternate perspective of these points is presented in Figure 2.2-2 which views the same case from the lunar north pole. The plane changes cannot be shown in this figure; however, the location of the $\overline{v}_\infty$ vectors and the pericynthion points with respect to the earth is clearly indicated.

The impulsive maneuvers required at deboost and injection for this case are now well defined. It is necessary to deboost at the specific point shown in Figure 2.2-1 from a well defined hyperbola and with the known plane change i_1. The situation is similar at transearth injection. Thus, the two required velocity impulses Δv_1 and Δv_2 at deboost and injection, respectively, may be calculated. Also, if desired, the fuel expended by the Service Module may be determined.

In the above situation a site azimuth was chosen which resulted in an orbit intersecting both pericynthion circles. Consider an extremely poor choice for the azimuth such as one which yields orbit (a) in Figure 2.2-1. Here, the site azimuth has been chosen such that the orbit is tangent to the deboost pericynthion circle and does not touch the injection pericynthion circle at all. If the deboost hyperbola is drawn, it is seen that a plane change of 90 degrees is required to get into this SM orbit. Also, since this orbit does not intersect the injection pericynthion circle, it is impossible to effect a pericynthion injection from this orbit. Clearly, this is not a desirable SM orbit. It is equally clear that the orbit should be oriented in such a manner as to lie close to both $\overline{v}_\infty$ vectors.

It has been indicated, thus far, that the velocity impulses required at deboost and injection are extremely dependent on the orientation of the SM orbit or alternately on the site azimuth. Continuing with this line of reasoning it is possible to orient the orbit such that it contains either the $\overline{v}_{\infty 1}$ or $\overline{v}_{\infty 2}$ vector. For an arbitrary landing site it is unlikely that the orbit will contain both. If $\overline{v}_{\infty 1}$ is in the circular orbit plane then deboost will be inplane and similarly if $\overline{v}_{\infty 2}$ is in the orbit plane the injection will be inplane. It will be shown later that neither of the inplane cases by themselves is optimum, but that the azimuth should be chosen such that there is a plane change required at both deboost and injection.

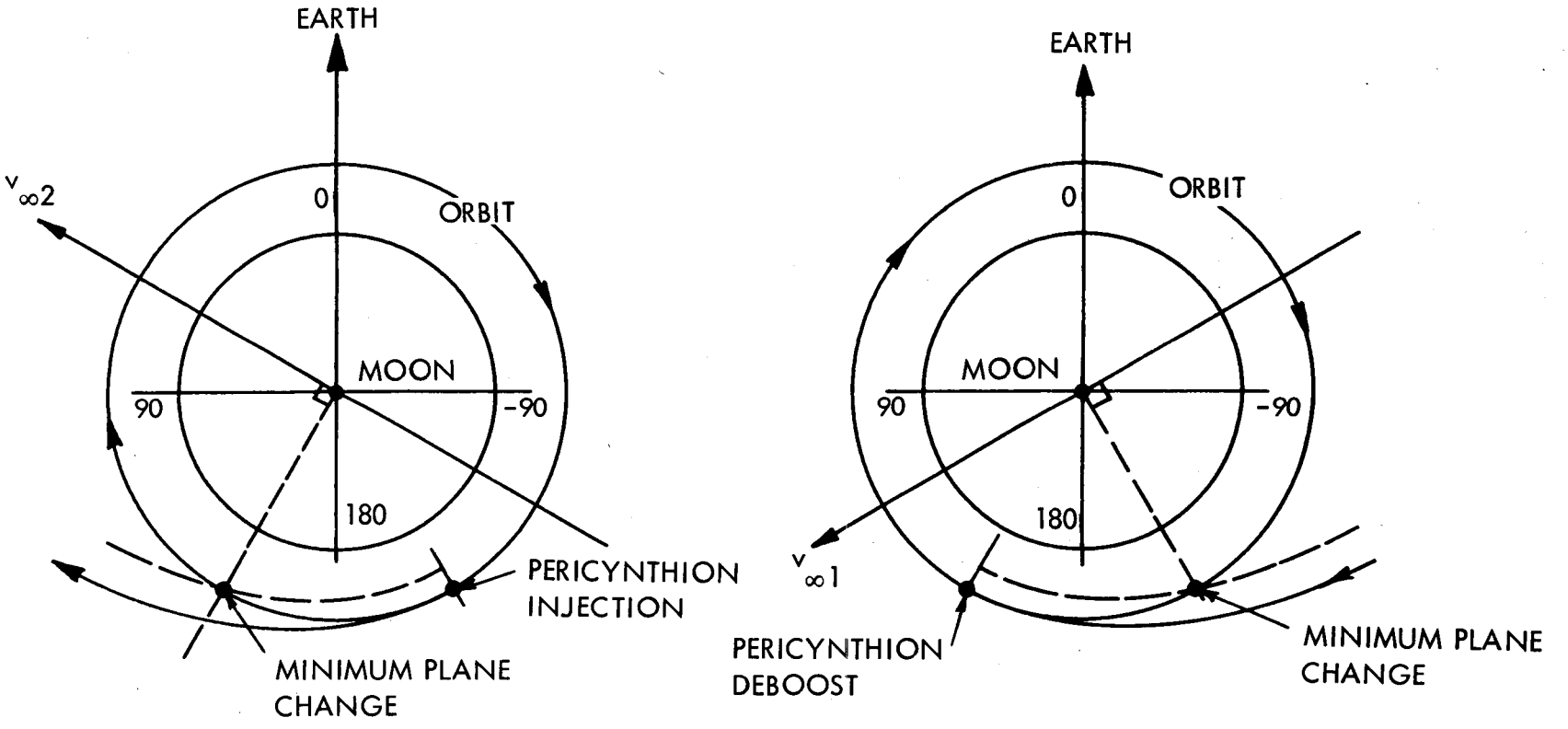

Figure 2.2-2. Polar View of Deboost and Injection Occurring at Pericynthion and at the Minimum Plane Change Points

Before discussing the complete optimization problem, some indication will be given as to what is to be gained if non-pericynthion deboost and injection are permitted. First assume that during the search for the optimum orientation, the azimuth has some fixed value. Then the SM orbit will be fixed with respect to the $\overline{v}_{\infty}$ vectors, i. e., the angles $i_{\infty 1}$ and $i_{\infty 2}$ will be fixed. If the pericynthion altitudes are allowed to vary, is it possible to find that hyperbola which will minimize the velocity impulse at deboost and similarly that hyperbola which will minimize the velocity impulse at injection? It is certainly true that the deboost and injection points will not necessarily lie on the pericynthion circles shown in Figure 2.2-1. What will be gained under these conditions is best explained with the use of Figures 2.2-2 and 2.2-3. In Figure 2.2-3 and the following discussion only the transearth injection problem is considered since the translunar deboost is completely symmetrical with this case.

Figure 2.2-3 illustrates typical geometry attending the injection out of a circular parking orbit. The problem is referenced to the circular orbit whose altitude is assumed fixed, and requires only the v_{∞} magnitude and displacement (i_{∞}) for computation of the minimum velocity impulse. No other parameters, such as the orientation of the orbit with the lunar equator need enter into the problem at this point. Any hyperbola which may be considered as a solution to the problem must satisfy the following two requirements:

a) The orientation of the hyperbola must be such that it contain the $\overline{v}_{\infty}$ vector.

b) The impulse velocity must be such that the correct v_{∞} magnitude be achieved.

Referring to Figure 2.2-3, it will be shown that specifying a single injection point on the orbit results in only one hyperbola which satisfies both of these conditions. Because there is only one plane which contains the $\overline{v}_{\infty}$ vector and the position vector to the injection point, the orientation of the hyperbola is uniquely determined. For the second requirement, it will be stated without proof that, fixing the v_{∞} magnitude, a radius vector to a point on the hyperbola, and the angle between this position vector and the $\overline{v}_{\infty}$ vector (α in Figure 2.2-3) will determine the shape of the hyperbola.

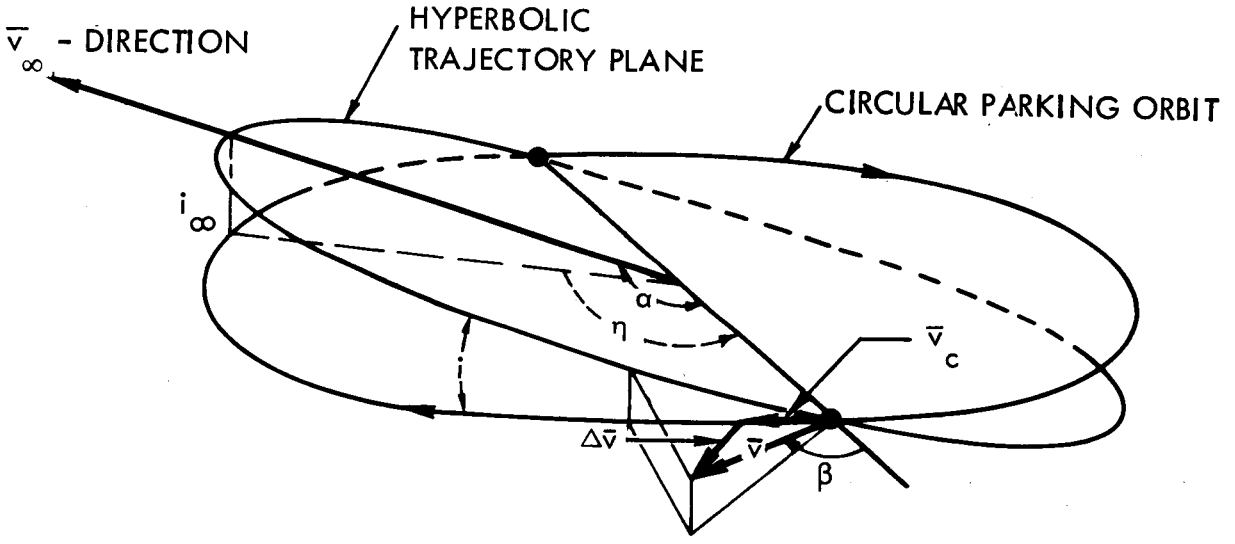

Figure 2.2-3. Transearth Injection from a Circular Parking Orbit into the Required Velocity at Infinity Direction

A unique hyperbola and a unique velocity impulse will then be associated with each point of injection on the orbit. Also, the shape of the hyperbola and hence the pericynthion altitude will change with each injection point chosen. Thus, referring to Figure 2.2-3, it is possible to restate the problem in simpler terms. That is, determine the injection position, say η, relative to the $\overline{v}_\infty$ vector which will minimize the velocity impulse Δv.

Before continuing further, it must next be established that Δv does have a minimum and that this does not occur at the pericynthion of the hyperbola. The behavior of the inclination change i and the post injection velocity flight path angle β will be discussed briefly to prove the point. The angle i is not dependent on the $\overline{v}_\infty$ magnitude but only on the displacement η of the injection point from the $\overline{v}_\infty$ vector and the inclination i_∞. The special situation when $i_\infty = 0$ will be disregarded since in this case pericynthion injection is optimum. Note that if $i_\infty \neq 0$, i will be a minimum when $\eta = 90$ degrees and that this minimum will be equal to i_∞. This is also seen in Figure 2.2-2. As the injection point moves away in either direction from $\eta = 90$ degrees, i will increase until it approaches 90 degrees when η equals 0 or 180 degrees. If plane change were the only effect on Δv, then $\eta = 90$ degrees would be the location of the injection point for minimum Δv.

The minimum value of the inclination i, however, is not the only requirement for minimum Δv. The velocity impulse is also dependent on the value of the velocity flight path angle β. To show this first note that by the vis-viva energy equation discussed earlier, the resultant velocity v (immediately after application of Δv) will be the same regardless of the injection point chosen since, for a specific case, v_∞ magnitude and the radial distance r to the injection point are fixed. Also, at each injection point, the circular orbital velocity v_c is a constant. Therefore, the velocity impulse is applied to a constant magnitude vector to achieve another constant magnitude vector. This implies that Δv will be minimum when the angle between these vectors is a minimum. This angle may be referred to as γ.

A discussion of the behavior of γ with respect to a variation in the location of the injection point will now be presented. Note from Figure 2.2-2 that the pericynthion injection on the orbit is located somewhere between η equal to 90 and 180 degrees. At this point the velocity path angle is 90 degrees. If there were no plane change or if i did not vary as the injection point moved on the circular orbit, this location would provide the minimum Δv condition because any change in the angle β from 90 degrees would increase the angle γ and hence increase the velocity impulse required. As pointed out above, however, the plane change i does vary with the injection location. For values of η less than 90 degrees, the inclination i increases and β moves further away from 90 degrees and hence γ and Δv will increase. For values of η greater than the pericynthion location, the situation is similar, again resulting in increasing γ and Δv. The injection location for minimum Δv must then lie between these two values of η.

The minimum velocity impulse is plotted in Figure 2.2-4 for various values of v_∞ and i_∞ and for a parking orbit altitude of 100 nautical miles. Also presented in this figure are the velocity requirements for a pericynthion injection or deboost, as the case may be. Except for $i_\infty = 0$, in which case pericynthion injection or deboost is optimum, the non-pericynthion launch results in considerably lower Δv for the lower values of hyperbolic excess velocity and higher inclinations i_∞. Not indicated in this figure is the fact that some combinations of i_∞ and v_∞ do not permit a pericynthion deboost or injection at all. This fact was brought out in Figure 2.2-1. Thus, considering transearth injection occurring at pericynthion, a fixed value of v_∞ magnitude will fix the radius of the pericynthion circle. Certainly, if the orbit is oriented such that the value of i_∞ is greater than this radius, as with orbit (a), no intersection occurs and therefore, no pericynthion injection is possible. A similar situation exists at deboost. The radius of the pericynthion circles and hence the maximum possible values of i_∞ are presented in Figure 2.2-5 versus the v_∞ magnitude. Any combination of i_∞ and v_∞ magnitude falling in the restricted region has no pericynthion deboost or injection possibility.

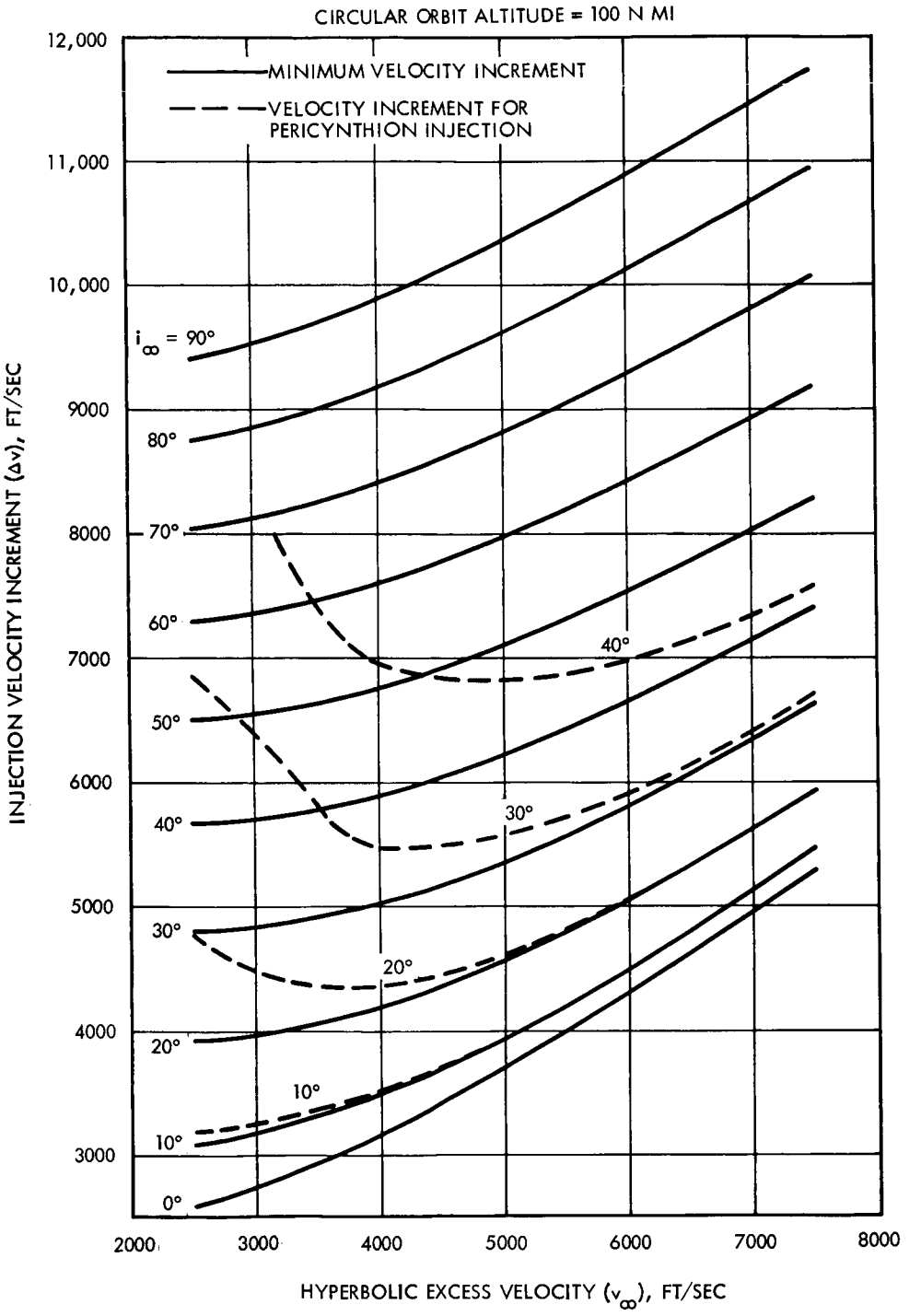

Figure 2.2-4. The Required Injection Velocity versus the Hyperbolic Excess Velocity for Various Asymptote Inclinations with the Orbit Plane

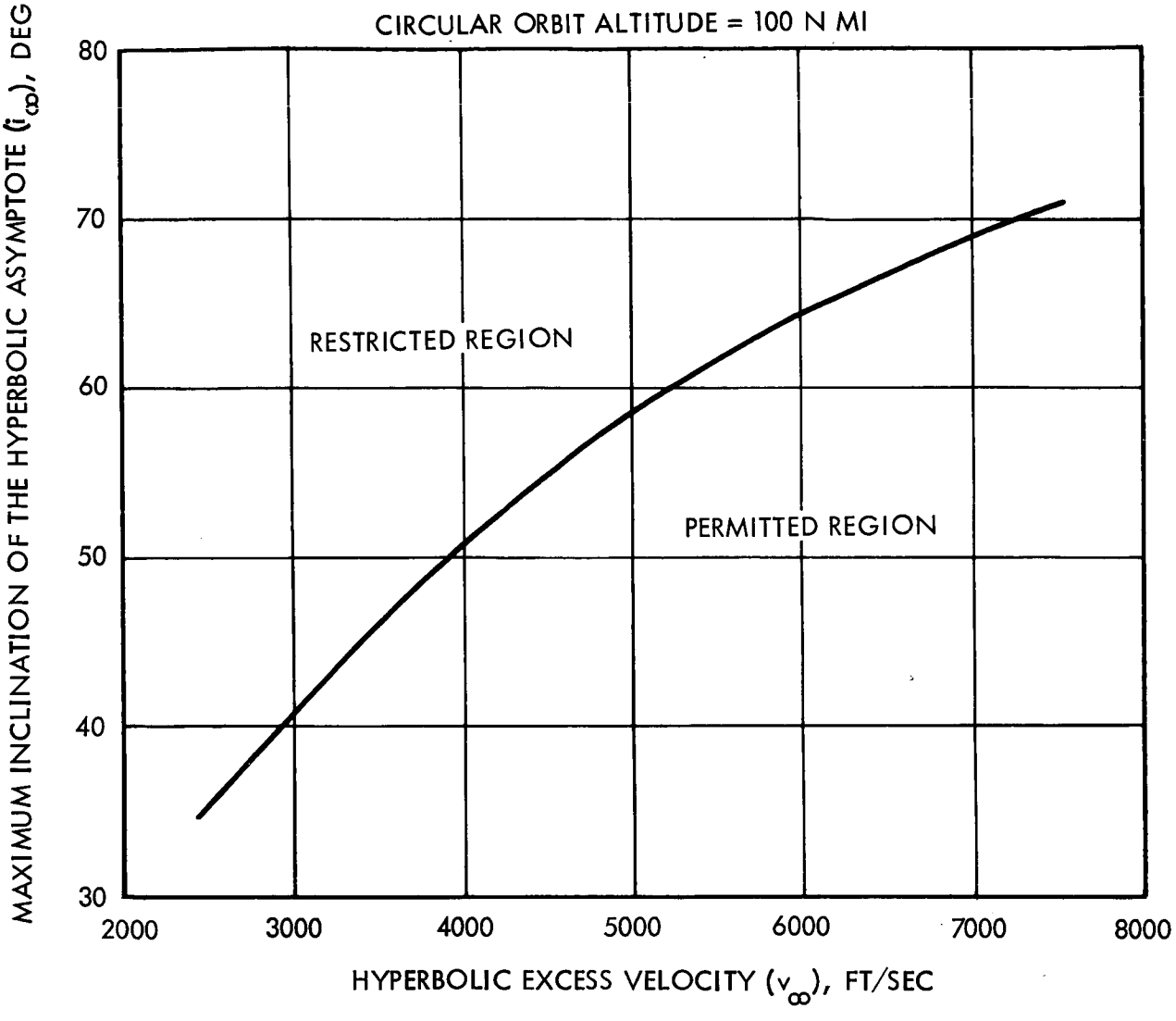

Figure 2.2-5. Maximum Possible Inclination of the Hyperbolic Asymptote with the Circular Orbit for a Pericynthion Injection

In order to relate the hyperbolic excess velocities shown here to a familiar parameter, these velocities are shown in Figure 2.2-6 as a function of the transearth time of flight. This figure applies to return trajectories lying nearly in the moon's orbit plane on return to the earth and holds approximately for translunar trajectories lying in the moon's plane. Note that the 90 hour trajectories have a v_∞ magnitude near 3000 feet per second for which case, as shown in Figure 2.2-4, a pericynthion injection has a much higher Δv requirement above an i_∞ of 10 degrees. The 50 hour trajectories on the other hand will probably permit pericynthion launches up to inclination changes of 30 degrees without great penalty.

Since the minimum Δv will usually not produce pericynthion of the hyperbola at the injection point, these pericynthion altitudes may vary significantly under certain conditions. Figure 2.2-7 indicates the pericynthion altitude of the inbound or outbound hyperbola versus the hyperbolic excess velocity and for various i_∞ values. These altitudes have no real significance for transearth injection, however, they represent the pericynthion which the translunar trajectory must have to deboost into a 100 nautical mile orbit with minimum Δv. For example, a 70 hour translunar trajectory to the moon will require pericynthion altitudes between 50 and 100 nautical miles if the i_∞ angle is restricted to less than 30 degrees. As a final note, it should be pointed out that the plane change i required for optimum transfer lies close to the value of i_∞.

All of the above discussion has applied to optimization of the deboost or injection maneuvers considered as separate problems. However, if they were separate problems, the optimum solution would be trivial since one can always find a circular orbit plane containing the landing site and the $\overline{v}_\infty$ vector (i.e., i_∞ can be made to be zero by choosing this particular plane, hence a pericynthion injection or deboost is optimum). The requirement for optimization arises because one cannot, in general, find a plane that contains both $\overline{v}_\infty$ vectors and an arbitrary landing site (see Figure 2.2-1), hence an i_∞ will usually exist for both deboost and injection. Furthermore, the values of i_∞ will depend on the orientation of the circular orbit since there can be an infinite number of planes containing the landing site. It now

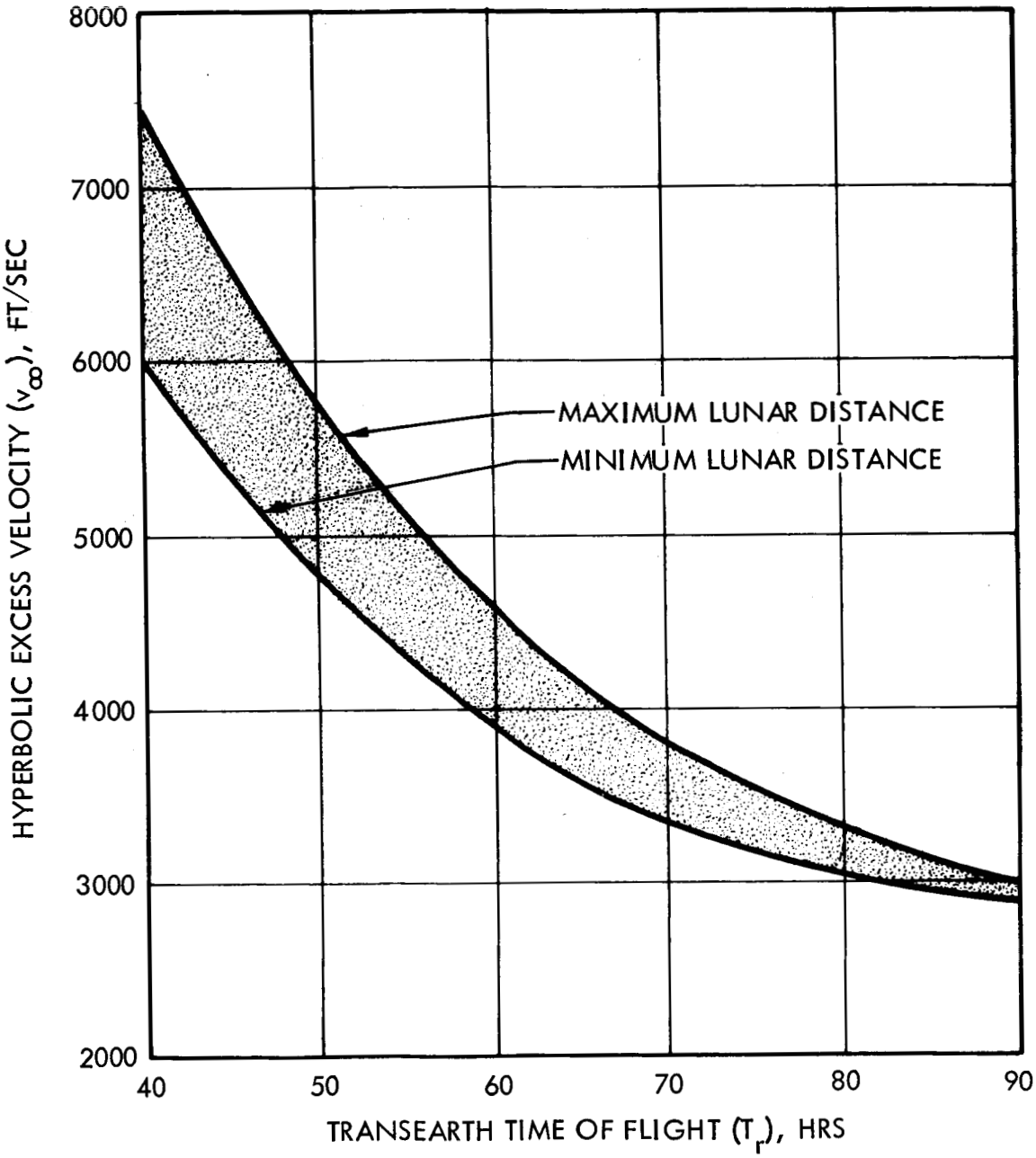

Figure 2.2-6. The Range of Hyperbolic Excess Velocity Over a Month for Various Transearth Flight Times. The Return Trajectories Lie in the Moon's Plane and Approach the Earth in a Counterclockwise Manner

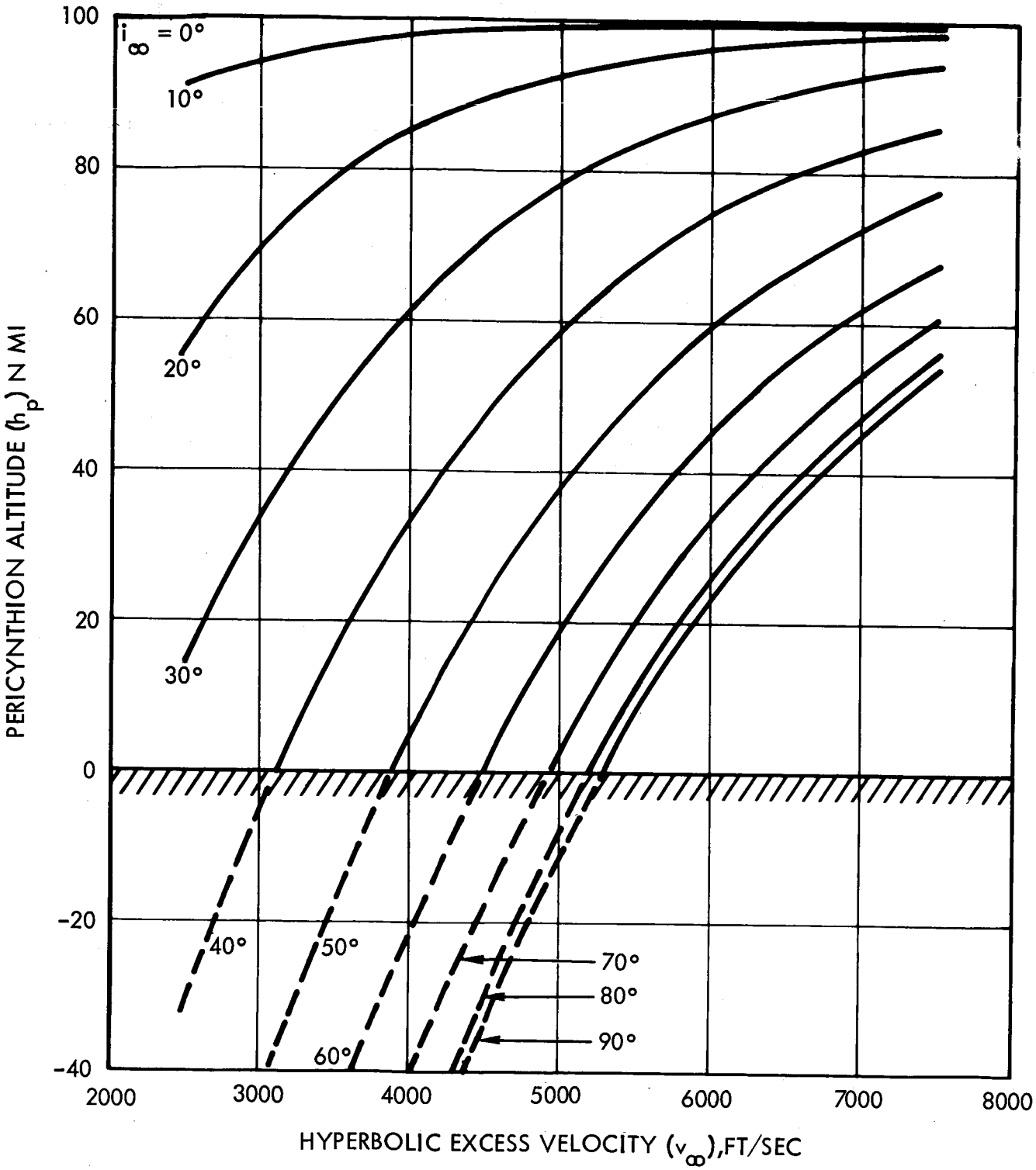

Figure 2.2-7. Hyperbolic Pericynthion Altitude versus the Velocity at Infinity for Various Inclinations of the Hyperbolic Asymptote with the Circular Orbit. Injection is from a 100 Nautical Mile Altitude Circular Orbit Resulting in the Minimum Velocity Increment

becomes apparent that a double optimization exists. First, for a given circular orbit orientation the pericynthion altitude of each hyperbolic conic may be optimized to minimize the individual deboost and injection velocity increments. But this does not imply that the circular orbit is best by some criterion. The final problem to be solved can now be stated:

> Given $\overline{v}_{\infty 1}$ and $\overline{v}_{\infty 2}$ (equivalent to a specific set of Group 1 and Group 3 parameters) and an arbitrary lunar landing site, what is the optimum circular orbit and by what criterion should the optimum be measured?

In considering the SM deboost and earth return maneuvers to be performed relative to the LOR mission constraints, it has been argued above that allowing pericynthion altitude of the incoming and outgoing lunar hyperbolic trajectories to vary permits an optimum geometrical arrangement of these conics in relation to a circular orbit plane containing the desired lunar landing site. The metric of this optimum geometrical arrangement is often taken to be the least sum of the deboost and transearth injection velocity increments. This minimization objective is solely a function of the respective orbit dynamics and does not directly specify the configuration requirements for the modular type Apollo spacecraft. An alternative minimization objective and one that is correlated directly with spacecraft design performance requirements is that optimum geometrical arrangement of the conics which requires the least total consumption of propellant. The adoption of this second criterion of merit does not help to ease the analysis problem for it can be shown that minimization of the total SM Δv required does not minimize the total propellant expended.

The problem is further complicated by the realization that propellant consumption at a fixed total Δv requirement is dependent on the SM structure weight, the LEM total weight, and the propellant specific impulse of the SM. The situation is analagous to the performance optimization of a multi-stage launch vehicle where total propellant weight may be minimized for a given performance level by appropriate weight allocation among the stages. Because the SM may be thought of as a two stage vehicle (i. e., the "first stage" propels the LEM but the "second stage" does not) one may inquire as to the effect on total propellant expenditure to varying the velocity demand in each "stage."

Velocity demand (a Group 2 parameter) becomes a mission variable both in total and in its division between the deboost and return allocation. It is the optimum proportion which will minimize propellant weight as the total velocity requirement varies.

The mechanism for obtaining the minimum propellant weight condition is the same as for obtaining the minimum total velocity increment required. Proceeding from the fact that the magnitude of $\overline{v}_{\infty}$ for each of incoming and outgoing hyperbolas remains constant for any orbit plane rotation about the vector, one seeks the orientations of the hyperbolas and the orientation of a circular orbit containing the landing site which in combination produce the desired minimum. The parameter which will be used to optimize the circular orbit orientation with respect to the $\overline{v}_{\infty}$ vectors is the azimuth of approach to the landing site. It will be shown later that the propellant weight minimum generally occurs closer to the condition of an in-plane deboost (i. e., $i_{\infty 1} \rightarrow 0$) than does the velocity minimum. The reason for this is that during the deboost the SM is carrying the LEM hence the propellant minimum would tend to be toward the condition of least deboost velocity required. Examples of the difference in propellant weight required between a total propellant weight minimum and a total velocity minimum are given in Section 2.3.

Because of the foregoing analysis and the consideration that Service Module propellant consumption is one ultimate test of launch opportunity practicality, the main body of mission analysis results have been presented with SM propellant expenditure as the dependent variable.

2.3 Service Module Performance for a Fixed Set of Mission Parameters

In the optimization of the Service Module performance, a measure of the Service Module performance must be selected and the variable mission parameters, which are available for the optimization, must be defined. It would be convenient, in meeting the first requirement, to minimize the total characteristic velocity requirement (total Δv) of the Service Module. The optimization would, as a result, be independent of the weight and specific impulse of the Service Module. However, as discussed in Section 2.2, the minimization of total Δv does not lead to the maximization of burnout weight. The most realistic approach to the optimization is, therefore, to minimize propellant weight for a fixed set of mission parameters, dependent on the spacecraft weight and propulsion characteristics. This is performed in the following exemplary analysis for the single launch date of January 28, 1968.

Those Group 2 mission parameters listed previously which can be used as variables in the optimization are most easily determined by examining the lunar phase geometry for a specified set of Group 1 and Group 3 mission parameters. As indicated previously, a completely specified set of these mission parameters define the direction and magnitude of the $\overline{v}_\infty$ vectors associated with the hyperbolic approach and departure conics. The significance of this fact to the optimization procedure is illustrated with a mercator projection of the selenographic coordinate system in Figure 2.3-1. The $\overline{v}_\infty$ vectors of the hyperbolic approach and departure conics have the locations indicated at their respective times of perifocal passage. Since the selenographic coordinate system is rotating and the stay time in lunar orbit is specified by the particular set of Group 1 and Group 3 mission parameters, a true picture of the relative positions of these vectors is obtained only if their selenographic positions are represented at a common epoch. The most convenient epoch for this situation is the time of landing, since no plane change is performed by the LEM during the landing. Thus, the $\overline{v}_\infty$ vector of the hyperbolic approach conic

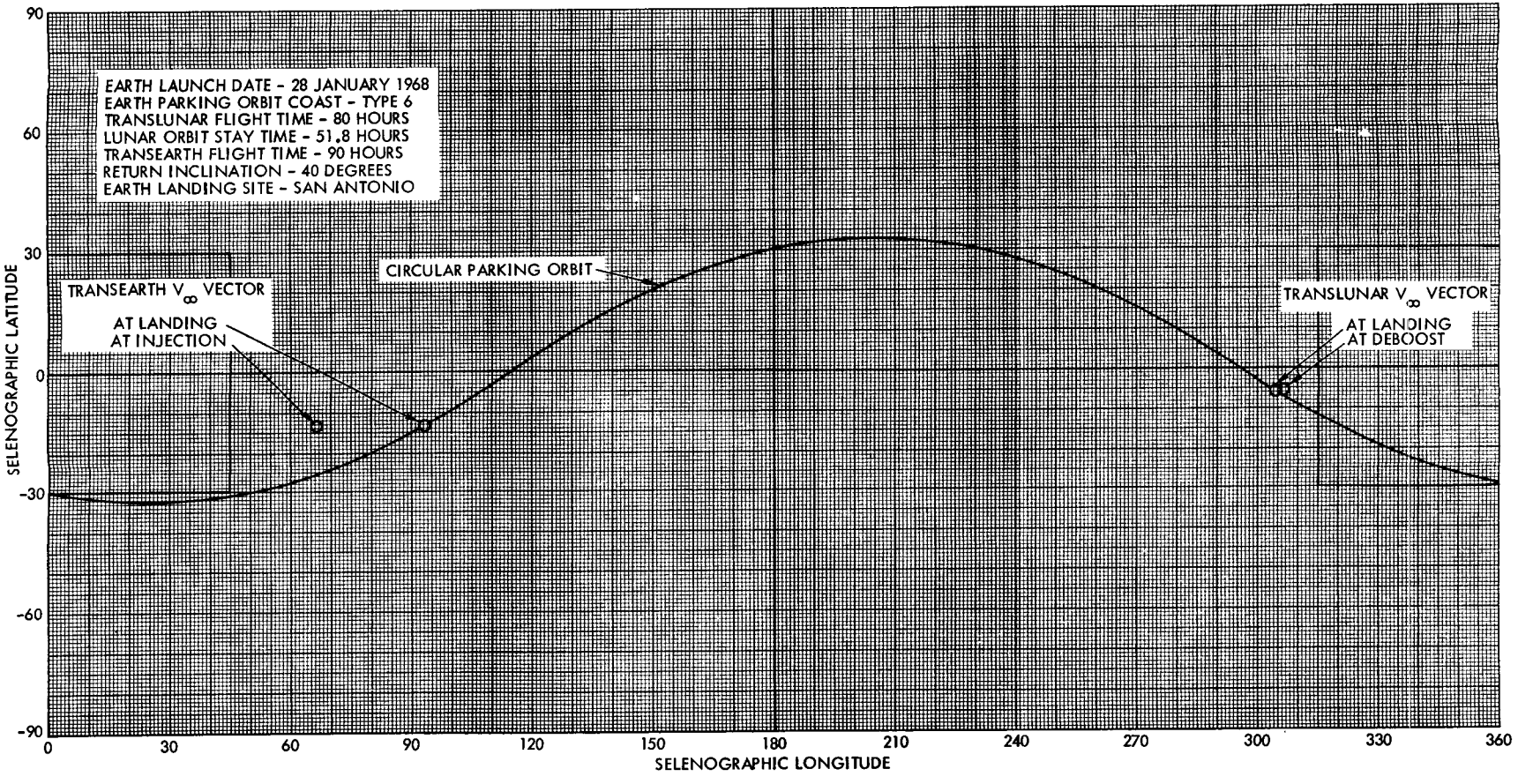

Figure 2.3-1. Moon Phase Geometry for In-Plane Deboost and In-Plane Return

is shifted in a westerly direction by the amount of the moon's rotation during the time from deboost to landing, and the $\overline{v}_\infty$ vector of the hyperbolic departure conic is shifted in an easterly direction by the amount of the moon's rotation during the time from landing to transearth injection. Having established the relative positions of the $\overline{v}_\infty$ vectors, an orbit plane represented by the ground trace, can be found which contains both vectors. With the hyperbolic conics being free to rotate about their respective $\overline{v}_\infty$ vectors, their inclinations may be adjusted such that both conics are contained in this plane. The ground trace of this plane, therefore, represents the locus of all landing sites for which no plane change at deboost or transearth injection is required. All of these landing sites are accessible with the same Service Module performance level, which is minimum for the set of mission parameters selected. This fact becomes evident by considering a landing site not in the orbit plane just described.

Figure 2.3-2 shows the same $\overline{v}_\infty$ vectors, rotated as before to their position at the time of landing, and a landing site at -45 degrees longitude and 15 degrees latitude. The orbit ground trace represents a circular parking orbit which contains the landing site and has some arbitrary azimuth of approach, such that neither $\overline{v}_\infty$ vector is contained in the orbit. The in-plane angle on a hyperbolic conic from the $\overline{v}_\infty$ vector to pericynthion is determined by the magnitude of the $\overline{v}_\infty$ vector and the pericynthion altitude (Figure 2.3-3). With the magnitudes of the $\overline{v}_\infty$ vectors determined by the mission parameters in Groups 1 and 3 and assuming that the pericynthion altitudes are equal to the circular parking orbit altitude, the rotations of the hyperbolic conics about the $\overline{v}_\infty$ vectors describe the loci of pericynthion positions as indicated in Figure 2.3-2. The impulsive deboost and return injection maneuvers are performed at pericynthion in this case and must occur at the intersections of the pericynthion loci with the circular orbit. Thus, the hyperbolic conic inclinations and the dihedral angle corrections at deboost and return injection are unique to the set of parameters described. The ground traces of the hyperbolic approach and departure conics which have pericynthion altitudes equal to 80 nautical miles are illustrated by the dashed lines between the $\overline{v}_\infty$ vectors and the pericynthion loci.

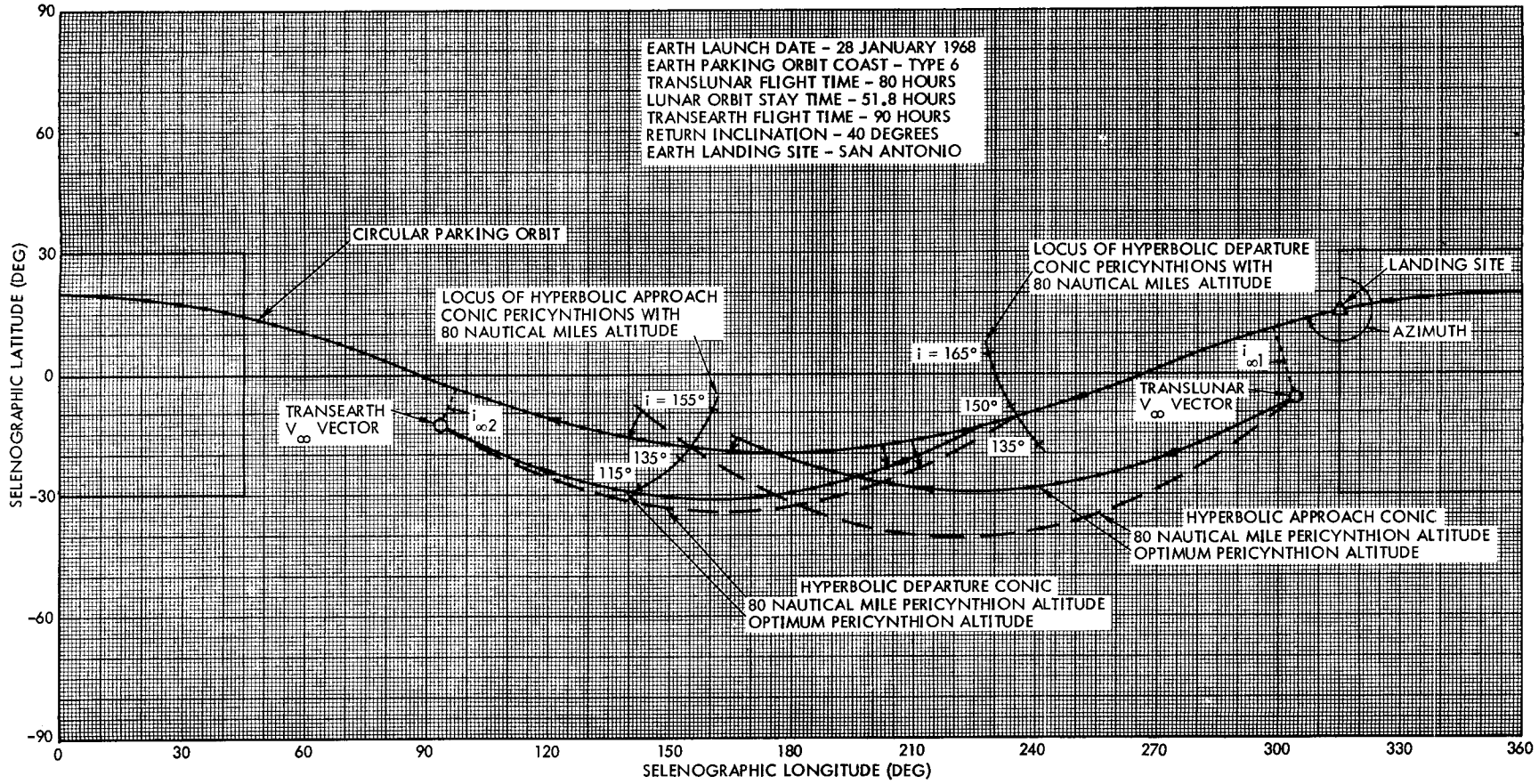

Figure 2.3-2. Moon Phase Geometry for an Arbitrary Landing Site

Each of the included angles, $i_{\infty 1}$ and $i_{\infty 2}$, which passes through a $\bar{v}_\infty$ vector and is normal to the circular orbit defines the minimum dihedral angle which can be achieved between a hyperbolic conic and the circular orbit. This minimum is approached as the inplane angle from the $\bar{v}_\infty$ vector to the intersection with the circular orbit approaches 90 degrees. Figure 2.3-3 indicates that the inplane angle from the $\bar{v}_\infty$ vector to pericynthion varies from 125 to 150 degrees for all hyperbolic conics in the range of $\bar{v}_\infty$ vector magnitudes expected. This figure also indicates that lowering the circular orbit altitude would have little effect on the inplane angle for maneuvers performed at pericynthion. The alternative is to maintain the circular orbit altitude at a fixed value (in this study 80 nautical miles), and reduce pericynthion altitude such that the intersection of the hyperbolic conic with the circular orbit occurs at a lesser inplane angle relative to the $\bar{v}_\infty$ vector. The variation of the inplane angle from the $\bar{v}_\infty$ vector to the 80 nautical mile altitude is shown in Figure 2.3-4 as a function of pericynthion altitude at various magnitudes of the $\bar{v}_\infty$ vector. It can be seen that a reduction of 80 nautical miles in the pericynthion altitude (to the surface of the moon) provides about 30 degrees reduction in the inplane angle from $\bar{v}_\infty$ vector to the circular orbit altitude.

As described earlier, the magnitude of the velocity vector at 80 nautical miles on the hyperbolic conic does not change as pericynthion altitude is decreased. Thus, the impulsive velocity requirement for transfer between a hyperbolic conic and the circular orbit in such a situation is a function only of the angle between the hyperbolic conic and circular orbit velocity vectors at their intersection. Minimization of this angle will minimize the velocity impulse requirement. This angle, γ, is the resultant of two components, the dihedral angle between the hyperbolic and circular orbit planes and the flight path angle on the hyperbolic conic. As pericynthion altitude is decreased relative to the altitude of the circular orbit the two components of the γ behave as follows:

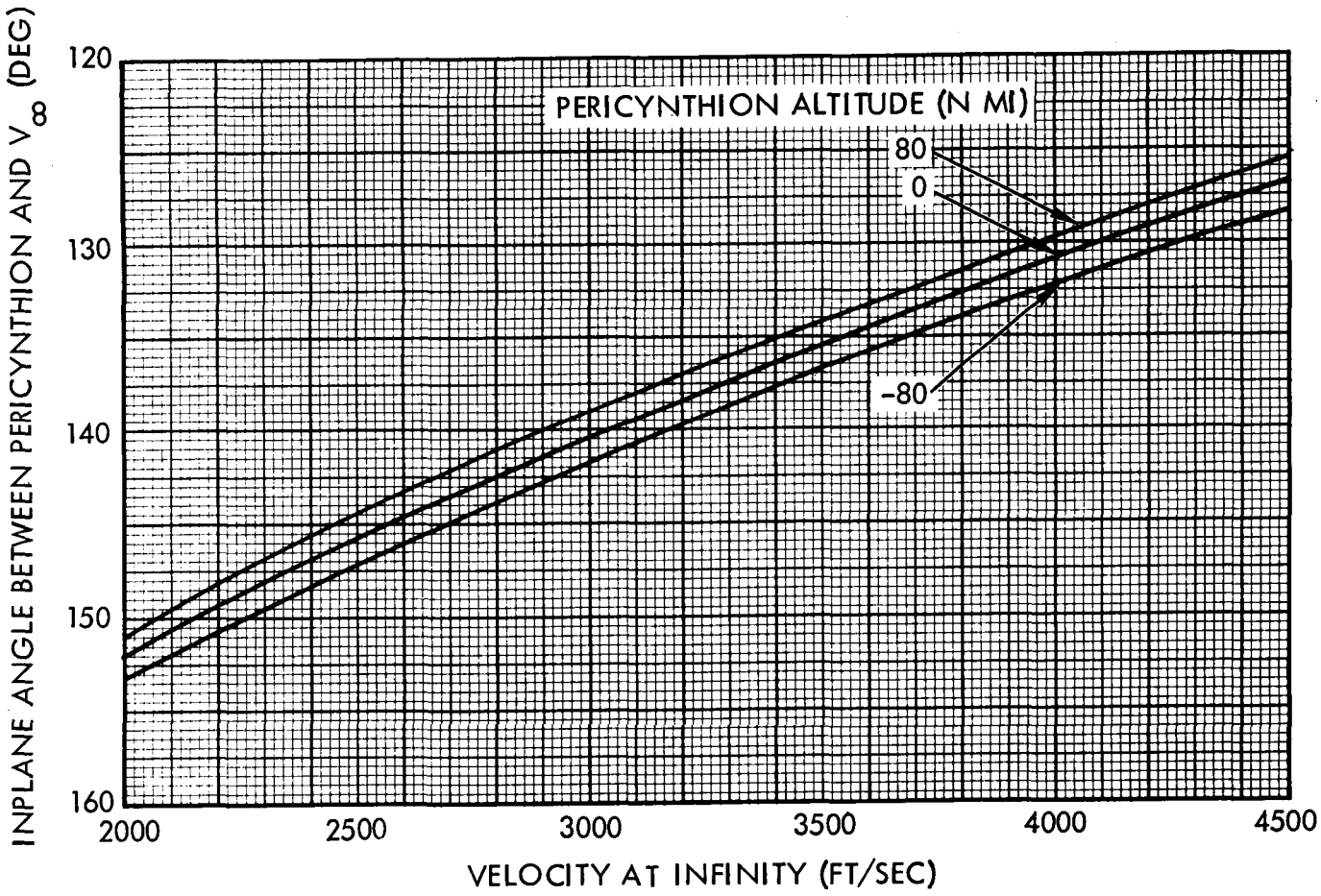

Figure 2.3-3. Angle Between the $\overline{V}_\infty$ Vector and Pericynthion on a Hyperbolic Conic

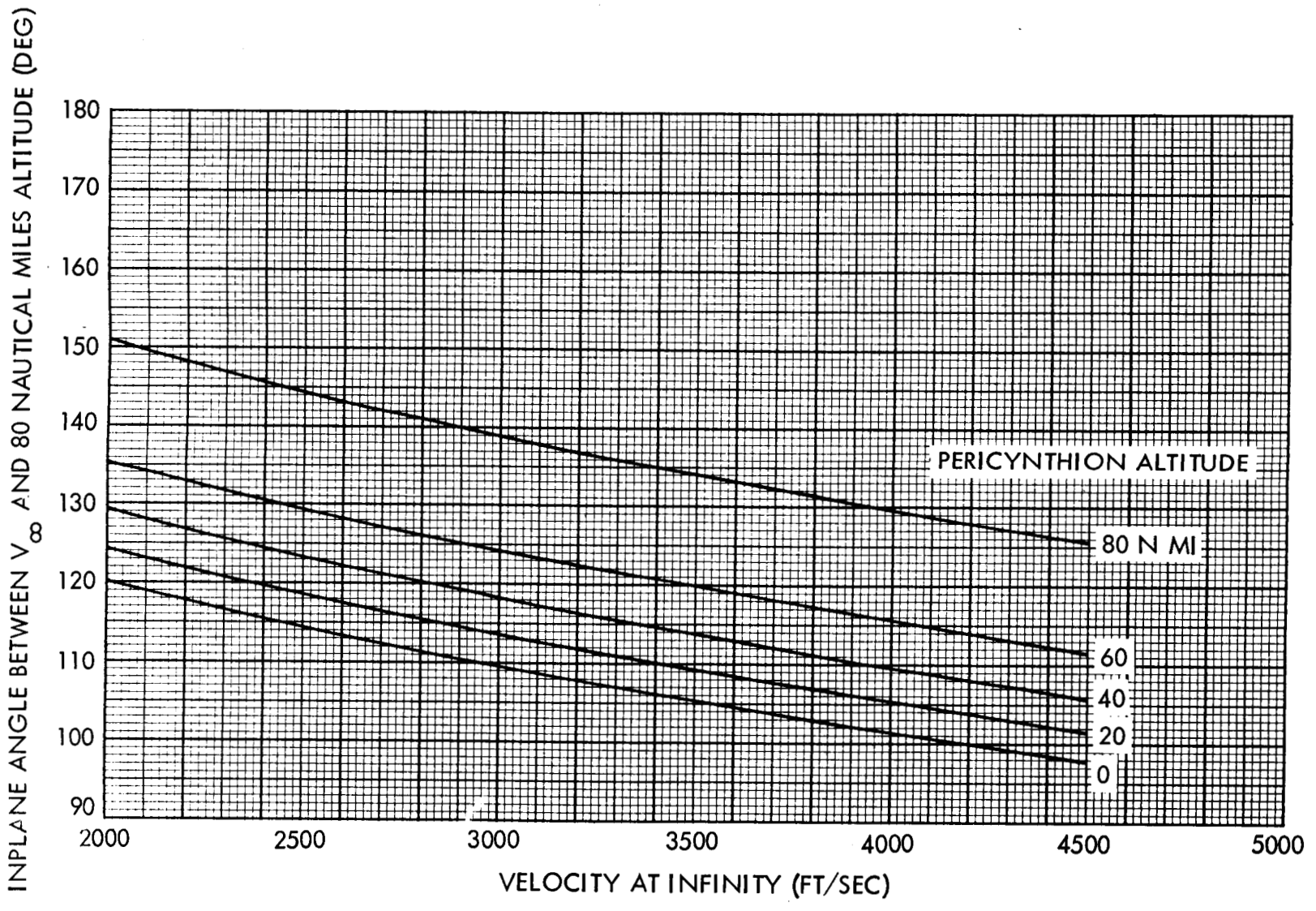

Figure 2.3-4. Angle Between the $\overline{V}_\infty$ Vector and 80 Nautical Miles Altitude on a Hyperbolic Conic with a Lower Pericynthion Altitude

a) The dihedral angle between the hyperbolic and circular orbit planes decreases to the minimum as the inplane angle from the $\overline{v}_{\infty}$ vector to the deboost point approaches 90 degrees.

b) The flight path angle on the hyperbolic conic relative to the local vertical and the circular orbit increases from 90 degrees to 180 degrees as a rectilinear orbit is approached.

The combined behavior of these components results in a minimum angle γ, and therefore in a minimum Δv requirement, which is found by varying the pericynthion altitude of the hyperbolic conic. The position of this minimum has been discussed in detail in Section 2.2. In Figure 2.3-2 the ground traces of the hyperbolic conics for which the pericynthion altitudes have been optimized are illustrated by the solid lines between the $\overline{v}_{\infty}$ vectors and the circular orbit. The optimum pericynthion altitudes are determined by the magnitude of the $\overline{v}_{\infty}$ vector and the i_{∞} angles. Thus, for a fixed set of mission parameters and a fixed circular orbit, there are unique pericynthion altitudes associated with the hyperbolic approach and departure conics, which result from minimization of the individual impulsive velocity requirements of the deboost and return injection maneuvers. The velocity increments can then be used to compute the associated SM propellant expenditure. A realistic lower limit must, however, be placed on the pericynthion altitude of the hyperbolic approach conic so that it will not impact the moon should that be the optimum case.

The azimuth of approach in the circular parking orbit at the landing site, having been arbitrarily selected, can be varied and the pericynthion altitude optimizations repeated for each value selected. The effect of azimuth variation on <u>total</u> characteristic velocity requirement and <u>total</u> propellant requirement is realized by considering the case in which the azimuth of approach is such that the circular parking orbit contains one of the $\overline{v}_{\infty}$ vectors. For example, if the circular parking orbit contains the $\overline{v}_{\infty}$ vector of the hyperbolic approach conic, no plane change is required in the deboost maneuver and a large plane change is required in the return injection. The converse is true of course if the parking orbit contains the $\overline{v}_{\infty}$ vector of the hyperbolic departure conic. The plane change required at the re-

turn injection for an inplane deboost is not necessarily equal to that required at deboost with an inplane return. The magnitudes of the plane change in these two cases are determined by the relative positions of the $\bar{v}_{\infty}$ vectors and the landing site. Thus, it is seen that as the azimuth of approach to the landing site is varied between limits defined by the two inplane maneuvers, the total characteristic velocity impulse must change since, in general, the sum of the two plane changes is not constant. The percentage of the total Δv expended in each maneuver must also change with azimuth variation. It is the effect of the variation of these two quantities, total Δv and percentage Δv expended in each maneuver, that combine to determine the azimuth of approach which minimizes total propellant weight.

Two typical optimizations with respect to azimuth of approach at the landing site are shown in Figures 2.3-5 and 2.3-6. The optimization presented in Figure 2.3-5 is for the set of mission parameters illustrated in Figure 2.3-2. Both the total Δv and propellant weight minimize at azimuths of approach near the inplane return. The propellant requirement is about 140 pounds greater at the azimuth of approach corresponding to the minimum total Δv than at the actual minimum. The optimization presented in Figure 2.3-6 illustrates the effect of the relative positions of the $\bar{v}_{\infty}$ vectors and the landing site. The mission parameters for this optimization differ from those of Figure 2.3-5 only in the latitude of the landing site and the stay time in lunar orbit. Here, the inplane angle between the $\bar{v}_{\infty}$ vectors is smaller due to the shorter lunar orbit stay time, and the landing site is displaced farther from the plane containing the two $\bar{v}_{\infty}$ vectors due to its more positive latitude. The total Δv is minimum at an azimuth near the inplane return while total propellant is minimum at an azimuth near the inplane deboost. In this case, the propellant requirement is 960 pounds greater at the azimuth corresponding to the minimum total Δv than at the actual minimum.

The variations in the optimum pericynthion altitudes with azimuth of approach to the landing site are presented in Figures 2.3-7 and 2.3-8 for

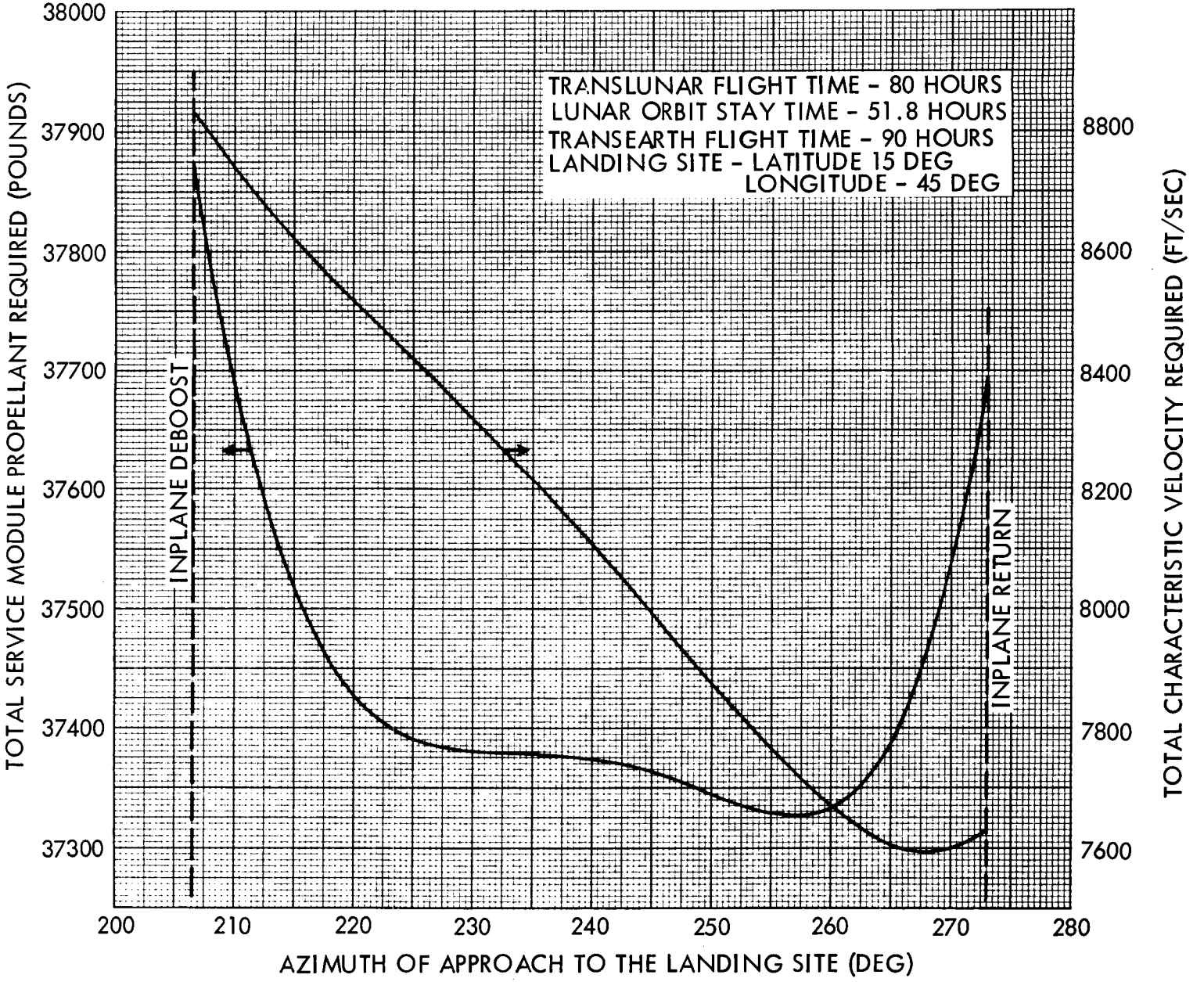

Figure 2.3-5. Service Module Optimization with Respect to Landing Site Approach Azimuth

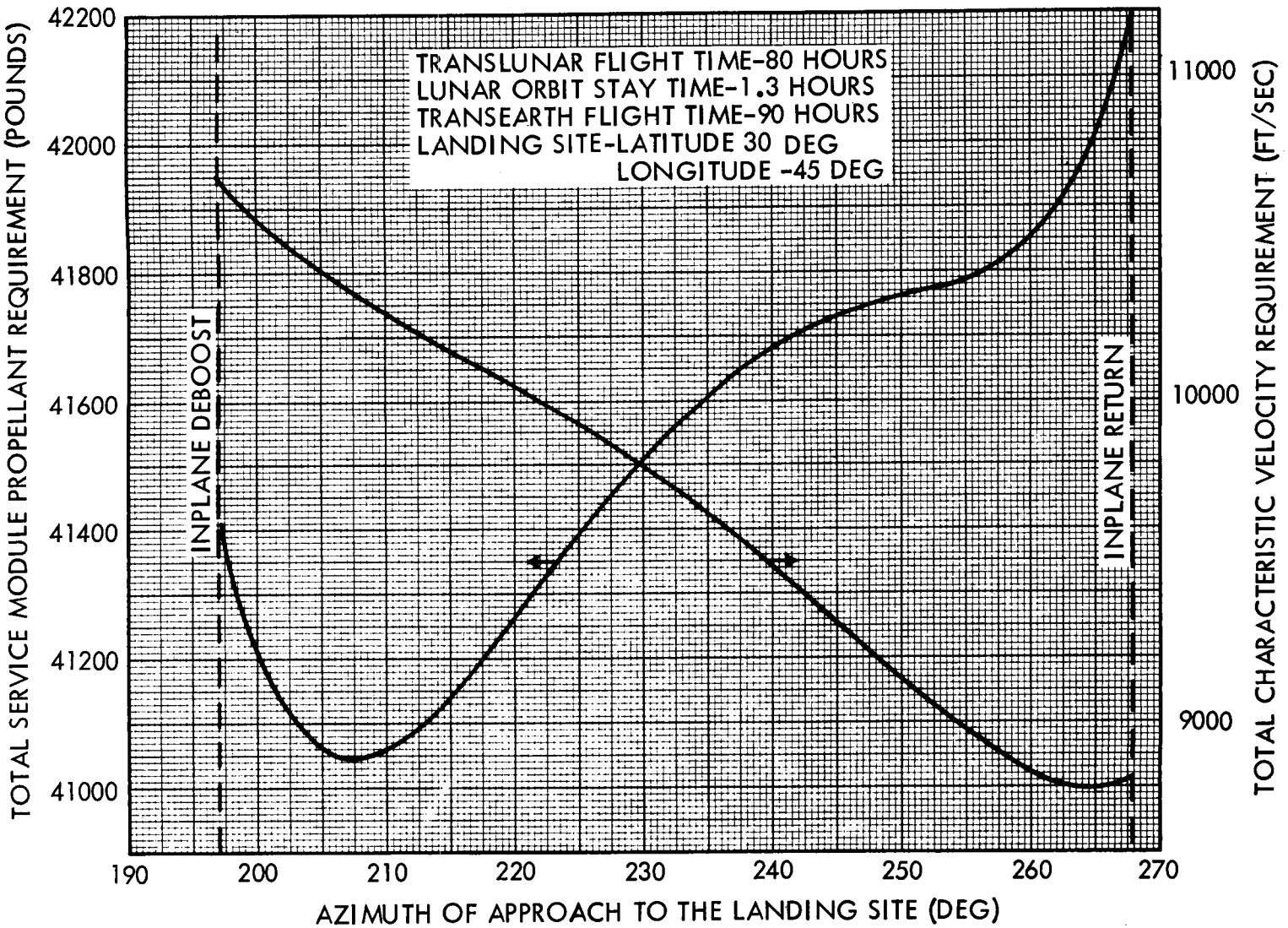

Figure 2.3-6. Service Module Optimization with Respect to Landing Site Approach Azimuth

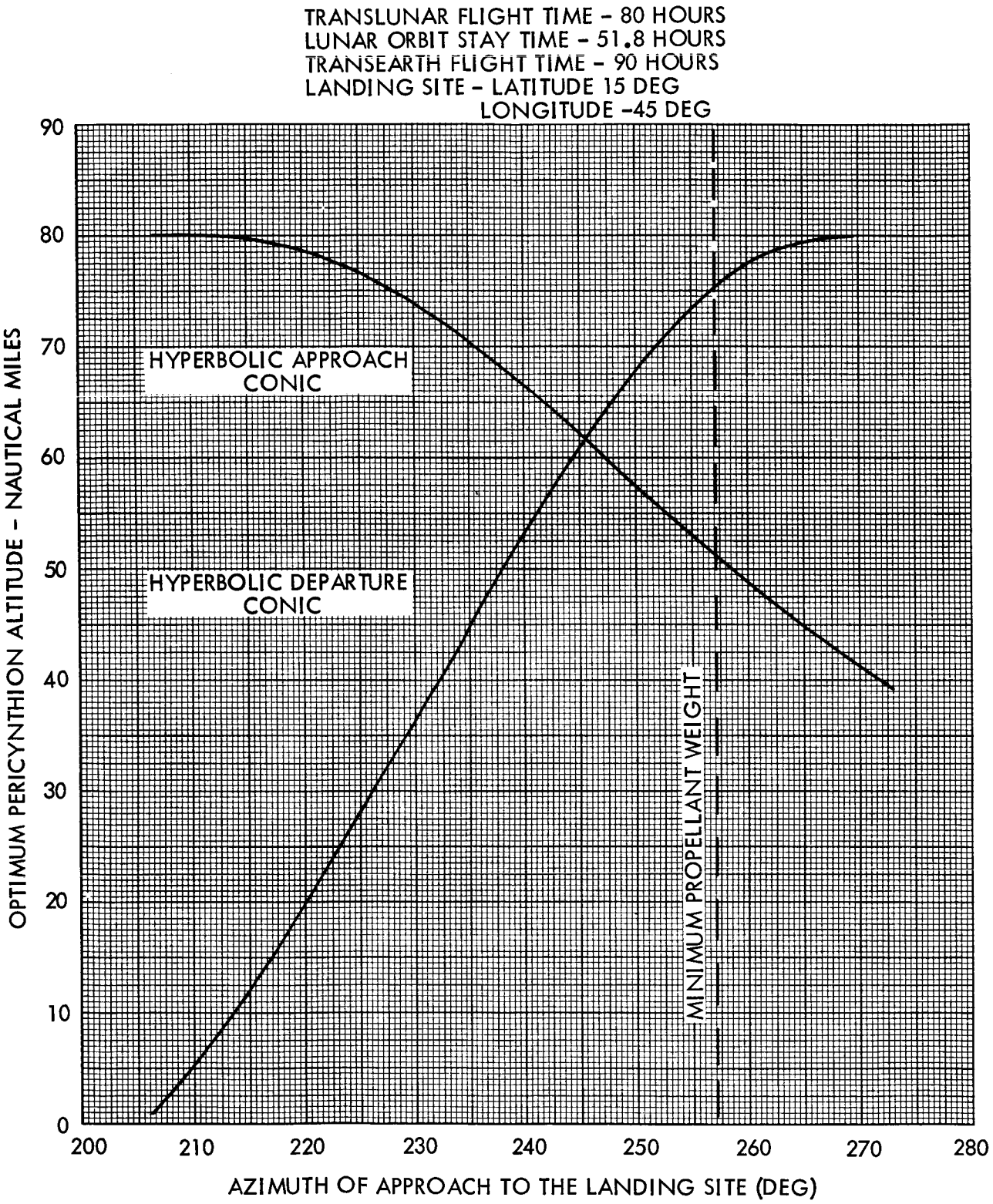

Figure 2.3-7. Optimum Pericynthion Altitude Variations

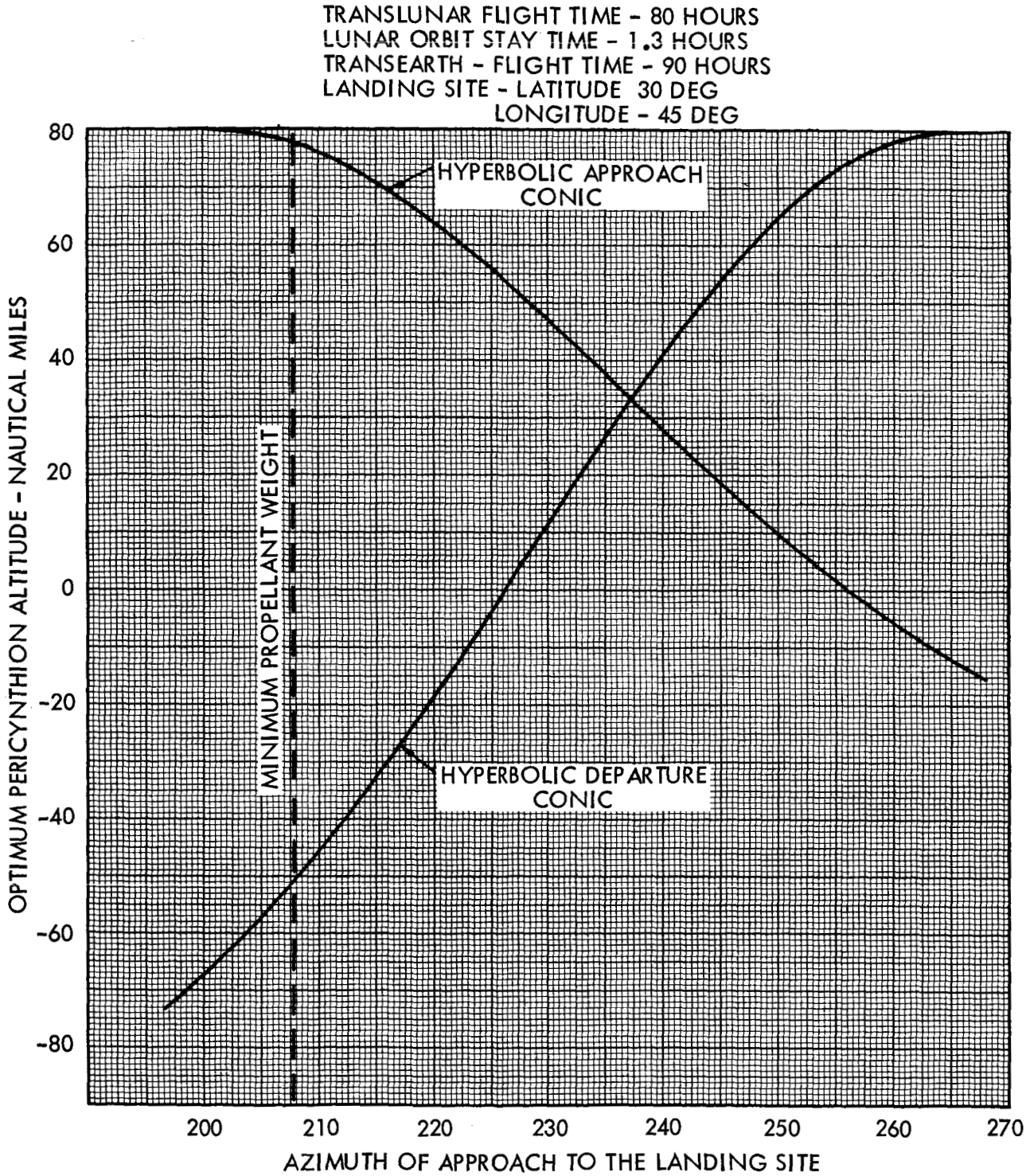

Figure 2.3-8. Optimum Pericynthion Altitude Variations

the two cases just discussed. When the azimuth of approach is such that one of the maneuvers is performed in-plane, the optimum pericynthion altitude of the hyperbolic conic associated with that maneuver is equal to the altitude of the circular orbit. As the azimuth of approach to the landing site is varied from the inplane deboost to the inplane return, the optimum pericynthion altitude of the hyperbolic approach conic decreases from 80 nautical miles and the optimum pericynthion altitude of the hyperbolic departure conic increases toward 80 nautical miles. The greater range of pericynthion altitudes covered in Figure 2.3-8 is due to larger dihedral angle components which are required at any azimuth of approach for the higher latitude landing site.

To summarize the optimization of the Service Module performance for a fixed set of mission parameters, the foregoing discussion has revealed the following:

a) Total propellant expenditure must be used as a measure of performance in the optimization of the Service Module due to the weight loss of the LEM.

b) The orbit plane, containing the $\overline{v}_{\infty}$ vectors of the hyperbolic approach and departure conics at the time of landing, describes the locus of landing sites for which no plane change is required in either the deboost or transearth injection maneuver. It is therefore the unique locus for which both the total velocity increment and the total propellant expenditure are minimum.

c) The optimum pericynthion altitudes for the hyperbolic conics in the above case are equal to the altitude of the circular orbit since the plane change requirements are zero in both maneuvers.

d) The Service Module propellant required to achieve a landing site not in the locus just described must be greater due to the plane changes required.

e) For a given landing site not in the locus of minimums and a given approach azimuth to that site, the velocity impulses (and hence the total propellant) required at deboost and injection may be independently minimized by freeing the hyperbolic pericynthion altitudes.

f) The total propellant required to achieve the above landing site may be further minimized with respect to the approach azimuth. In this process, the azimuth resulting in minimum total propellant is not usually the azimuth resulting in minimum total velocity impulse.

g) Since the azimuth of approach to the landing site also can be used to control LEM ascent plane change, it may be operationally constrained to exclude that value which produces the minimum total propellant expenditure.

The discussion of the Service Module optimization procedure has isolated the Group 2 mission parameters which are unique to the optimization of Service Module performance. The next task is to determine the minimum number of combinations of all of the remaining mission parameters required to define the significant variations in Service Module performance. The objective is to generate contours of total Service Module propellant requirements over the range of landing sites requested.

It is of interest to note that the mission parameters of Group 2, which are not constrained by the optimization procedure, are those which determine the allowable stay time of the SM in the lunar parking orbit. The analyses of the translunar and transearth phases are conducted independently to determine the arrival and departure times at the moon for each set of Group 1 and Group 3 parameters. The problem, therefore, is to select combinations of Group 3 parameters which permit departure times within the allowable range of lunar orbit stay time for the arrival times determined by each set of Group 1 parameters.

The assumption is made in the lunar phase analysis that the arrival and departure times are determined by the times of perifocal passage on the hyperbolic approach and departure conics. This assumption is not precisely correct in that the Service Module optimization produces non-pericynthion deboost and transearth injection maneuvers. The differences in arrival and departure time between the pericynthion and non-pericynthion maneuvers are, however, small enough to be neglected.

The range of allowable lunar orbit stay time is determined by the permissible ranges of variation of the unconstrained Group 2 parameters. Each

lunar orbit stay time is fixed by the time from deboost to landing, the surface stay time, and the time from takeoff to return injection. The time from deboost into circular orbit to landing is minimum when the final descent is initiated on the first opportunity in the equiperiod orbit, and is equal to 3 hours. The minimum surface stay time is 2 hours since launch opportunities nominally occur once in each orbit of the CM/SM. The time from takeoff to rendezvous is 1 hour with the first transearth injection opportunity occurring about 2 hours later. Thus, the minimum lunar orbit stay time is 8 hours. The maximum time from deboost to landing is 5 hours for descent initiation on the second opportunity. With a maximum surface stay time of 48 hours and with an additional 4 hours allowed for transearth injection on the third opportunity, the maximum CM/SM stay time in the circular orbit is 60 hours. Therefore, the examination of a range of circular orbit stay times from 8 to 60 hours will provide the complete range of variations of the unconstrained mission parameters of Group 2.

The number of combinations of Group 3 parameters required to show the significant variations in service module performance within the allowable range of lunar orbit stay time is best determined by examining the translunar and transearth data in the form presented in Figure 2.3-9. The transearth flight times associated with each departure time from 30 January 1968 to 5 February 1968 are shown for an earth landing site at San Antonio and a return inclination of 40 degrees. The arrival times at the moon for various combinations of Group 1 parameters are shown relative to departure time as the zero references for lunar orbit stay time. The arrival times for the Type 6 translunar trajectories are seen to occur 20 hours later for each 20 hour increase in translunar flight time. This results from the fact that the Type 6 translunar trajectories are in-plane and the time of launch remains essentially constant. The arrival times for the Type 5 trajectories, however, change slightly more than 20 hours for each 20 hour increase in flight time. These changes indicate the necessity to vary launch time for the out-of-plane translunar trajectories.

With a transearth flight time variation of 2.5 days, and a lunar stay time variation of 2 days, it can be seen that any given earth launch day and fixed outbound flight time could result in landing at earth on any of 4 consecutive days. Therefore, with any specific set of Group 1 parameters, four total mission durations are possible each separated by approximately 1 day. The transearth flight time has a strong influence on the magnitude of the $\overline{v}_{\infty}$ vector associated with the hyperbolic departure conic and therefore the Service Module propellant requirement. It is of interest, of course, to show the effect of both of these parameters on the optimized Service Module performance. To determine Service Module performance variation for one total mission time, it is necessary to optimize its performance for at least three transearth injection opportunities associated with one earth landing date. Twelve injection opportunities within the allowable range of lunar stay time must be analyzed to show the variations of Service Module performance for the four total mission durations possible. Since the data presented in Figure 2.3-9 is in no way dependent on choice of lunar landing site, the twelve transearth injection opportunities for each set of Group 1 mission parameters must be analyzed at a sufficient number of lunar landing sites to permit the generation of propellant weight contours. In addition, the effects of varying earth landing site and return inclination must be determined.

All of the mission constraints, with exception of that imposed by the LEM ascent plane change capability, are imbedded in the independent analyses of the various phases. This constraint may impose a lunar surface stay time restriction which is less than the maximum allowed for a specified lunar orbit stay time. The lunar surface stay time for an ascent plane change capability of 4 degrees is determined as a function of latitude of the landing site and circular orbit inclination by the method discussed in the appendix. Where the LEM ascent plane change becomes limiting, stay time contours can be determined in addition to propellant weight contours. When the LEM ascent plane change limitation becomes a factor, there are four alternatives open:

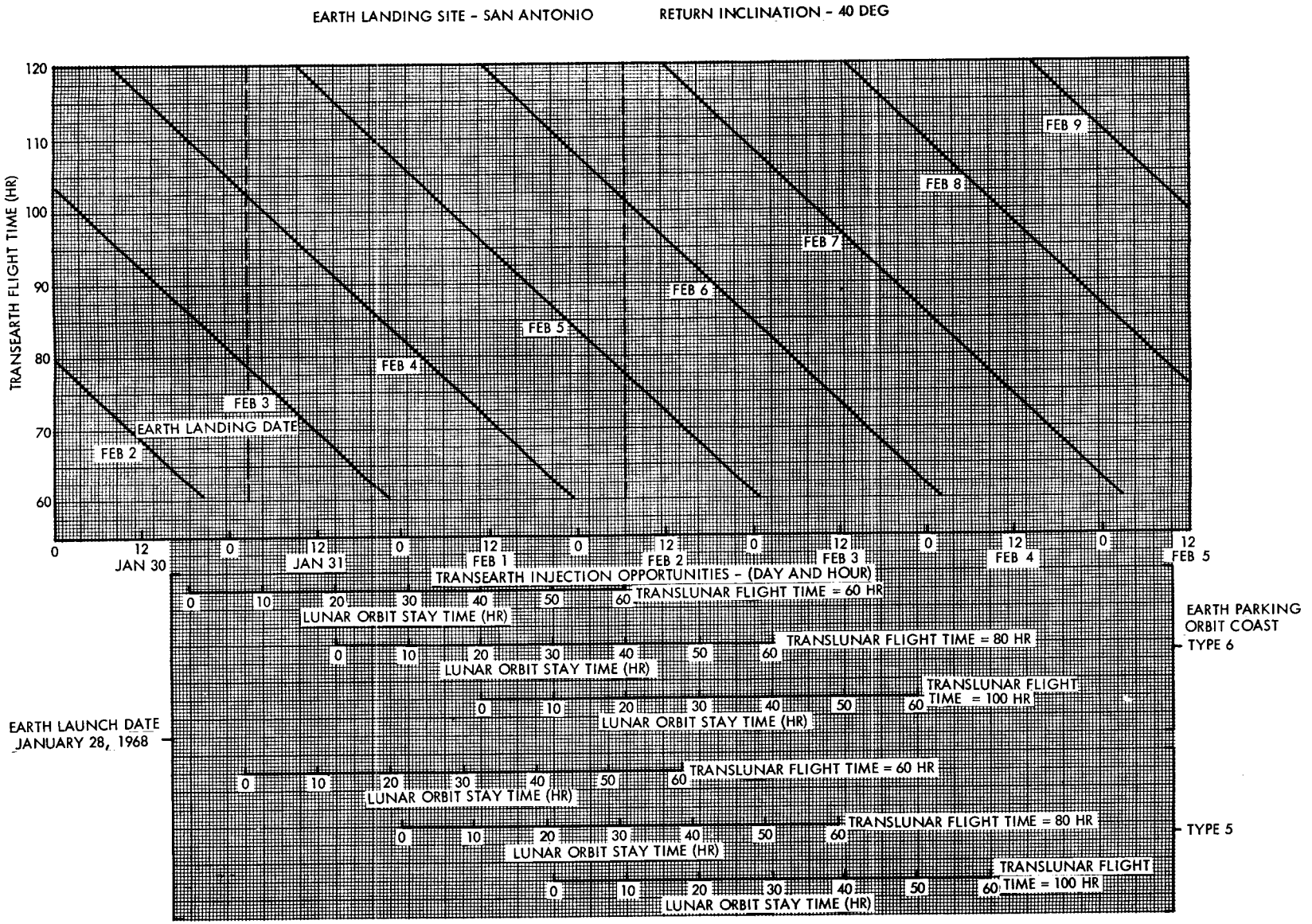

Figure 2.3-9. Relative Relationships of the Transearth Flight Time with the Deboost, Lunar Stay Time and Transearth Injection Time

1) Lunar surface stay time can be cut short

2) The minimum propellant weight geometry can be sacrificed to remove the plane change limitation

3) That particular landing site can be dismissed

4) A judicious selection of Group 1 and 3 parameters may be made.

3. RESULTS

3.1 Introduction

A method of separating the mission parameter study into three independent phases has been proposed and, on the basis that this procedure would generate satisfactory results, an analysis of the lunar operations phase was developed. This section proposes to substantiate the assumption required in that analysis, i.e., that the lunar phase parameters (Group 2) have little effect on the position and magnitude of the incoming and outgoing $\overline{V}_\infty$ vectors. This is done in detail for the single launch date of January 28, 1968. In addition, gross variations of the $\overline{V}_\infty$ vectors with the more significant translunar and transearth parameters are indicated for a typical lunar month. The parameters being considered will fall into three categories as to their effects on the $\overline{V}_\infty$ vectors. These are:

a) Those parameters which have insignificant effects on the position and magnitude of the $\overline{V}_\infty$ vectors, i.e., less than a degree and about 20 feet per second, respectively. These are found to be the lunar phase or Group 2 parameters.

b) Those parameters which have significant but relatively small effects on the $\overline{V}_\infty$ vectors, or approximately three degrees in position and about 100 feet per second in magnitude, such as the launch azimuth and the return inclination to the earth's equator. Variations in these parameters may be neglected in a limited parametric study.

c) Those parameters whose values essentially determine the position and velocity of the $\overline{V}_\infty$ vectors. These include the day of launch (or position of the moon) and the times of translunar and transearth flight.

The latter part of this section is concerned with the application of the analysis developed in Section 2.3 to the parametric generation of Service Module propellant requirements. Minimum propellant contours are drawn on the lunar surface for a single launch date and several outward and return times of flight and lunar stay times. Some general characteristics and trends of these contours are presented for this one day. An indication of the trends that may be expected on other launch dates is also discussed.

3.2 Effects of Translunar Parameters on the $\overline{v}_\infty$ Vector

The outbound trajectory parameters, listed in Table 3.2-1, which can be considered in the analysis of the Apollo mission, are many and the purpose of this study is to eliminate and/or limit these parameters. The trajectories considered here are for one day, January 28, 1968, launched from Cape Kennedy with an analytic (patched conic) simulation of the trajectory from launch site to pericynthion. The approach to the study, described in Section 2.1, considers only those variables which significantly influence the magnitude and position of $\overline{v}_\infty$ vector at the moon. The launch window at the earth for the outbound trajectories will be generated by varying the launch azimuth and the outward trip time. These windows can be determined independently of any other mission analysis if necessary.

The analysis for January 28, 1968, will be representative, but a correlation with other combinations of declination and distance will be made. The changing declination and distance of the moon for the lunar month, which includes January 28, are given in Figure 3.2-1. For launches occurring on January 28, the moon's distance is near its average value at arrival of the spacecraft. The moon's declination is near its minimum value of -28° at departure and increases toward the node as the trip time increases.

The following parameters were arbitrarily ordered to discuss a number of interrelated effects and to attempt to justify exclusion of some of them. To accomplish this, a degree of freedom must be given up for each parameter analyzed, but in total the effects and trends can be seen. First, the trip time, launch azimuth, length of earth parking orbit, and pericynthion altitude will be analyzed for a fixed lunar landing site. The fixed site means that all incoming hyperbolic planes are oriented such that an in-plane deboost at pericynthion will result in SM parking orbit which passes over this site. Secondly, the effect of moving the landing site to any point in the acceptable region will be examined for a constant flight time. Then with a fixed flight time and fixed landing site the effects of changing lunar geometry will be shown for one lunar month.

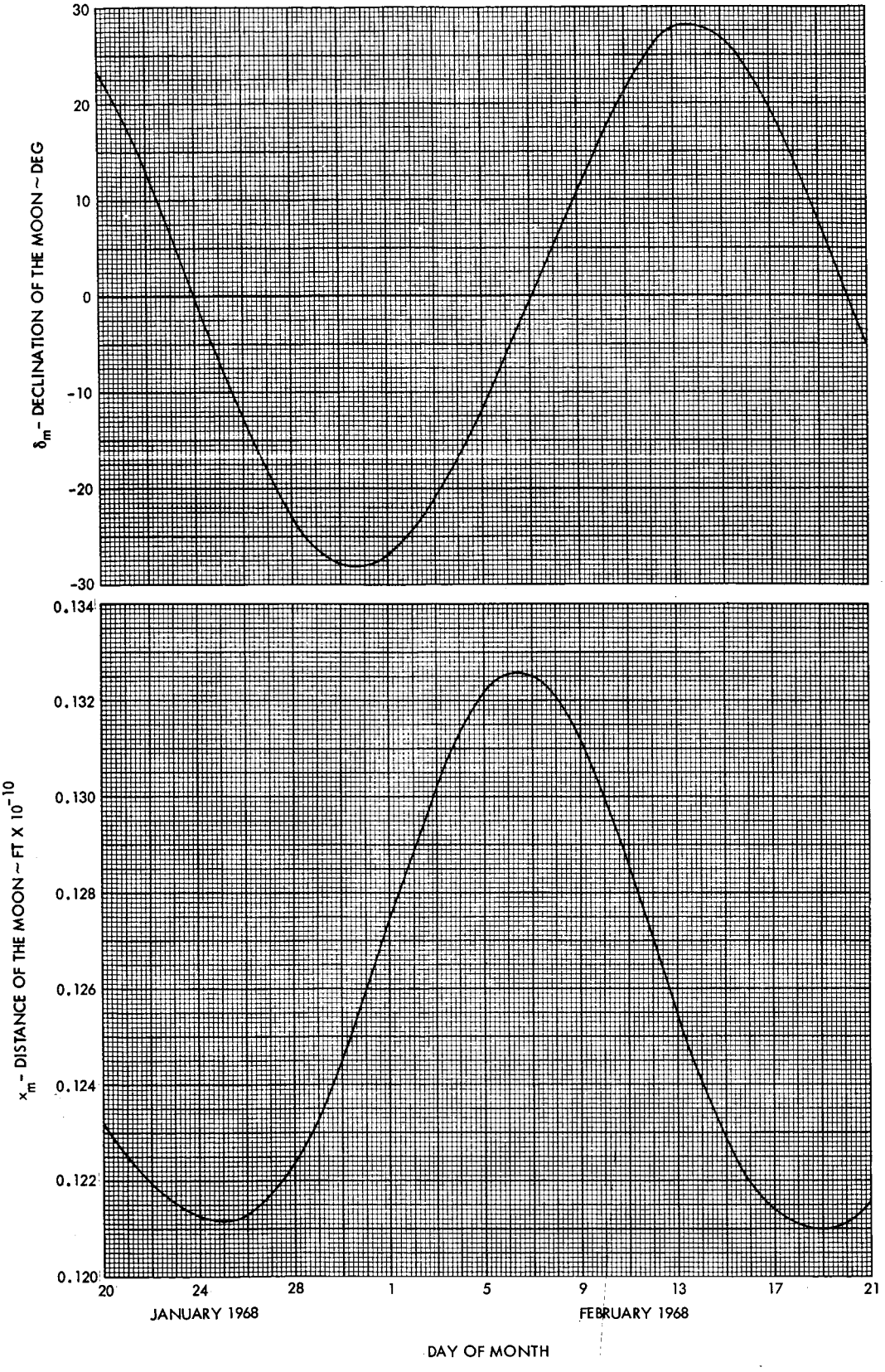

Figure 3.2-1. Declination and Distance of the Moon

Table 3.2-1. Outbound Trajectory Parameters

Launch Date	January 28, 1968
Launch Site	Cape Kennedy
Launch Azimuth	72 to 108 degrees
Powered Flight (both burns)	51.65 degrees in 17.09 minutes
Parking Orbit	100 nautical miles
Parking Duration	0.5 to 3.0 revolutions
Injection Altitude	157 nautical miles
Injection Flight Path Angle	83.44 degrees
Outbound Flight Time	60 to 120 hours
Pericynthion Altitude	50 to 150 nautical miles
Lunar Landing Site	-45 to +45 degrees selenographic longitude -30 to +30 degrees selenographic latitude

One further item bears explanation before the parameters are described. That concerns the designation of trajectory types, which is necessary because there are two launch windows occurring each day, which result in significantly different trajectories. The type 5 trajectory is defined to be in an earth parking orbit from 1.5 to 2.0 revolutions and intercepts the moon on a downward pass of the trajectory (referenced to the earth's equator). The type 6 trajectory parks from 2 to 2.5 revolutions and intercepts the moon on an upward pass. Figure 3.2-2 shows the monthly variation of the outbound trajectory's inclination to the lunar plane for the two trajectory types. This inclination is derived from a 90-degree launch azimuth; at azimuths of 70 and 108 degrees, the inclinations are from 5 to 6 degrees higher.

The trip time (translunar time of flight) is to range from 60 to 120 hours, and is defined as the time from injection out of earth parking orbit to arrival at pericynthion at the moon. On January 28, this time is limited to a maximum of somewhat less than 110 hours because of the relatively short lunar distance. Flight times of 120 hours will only be

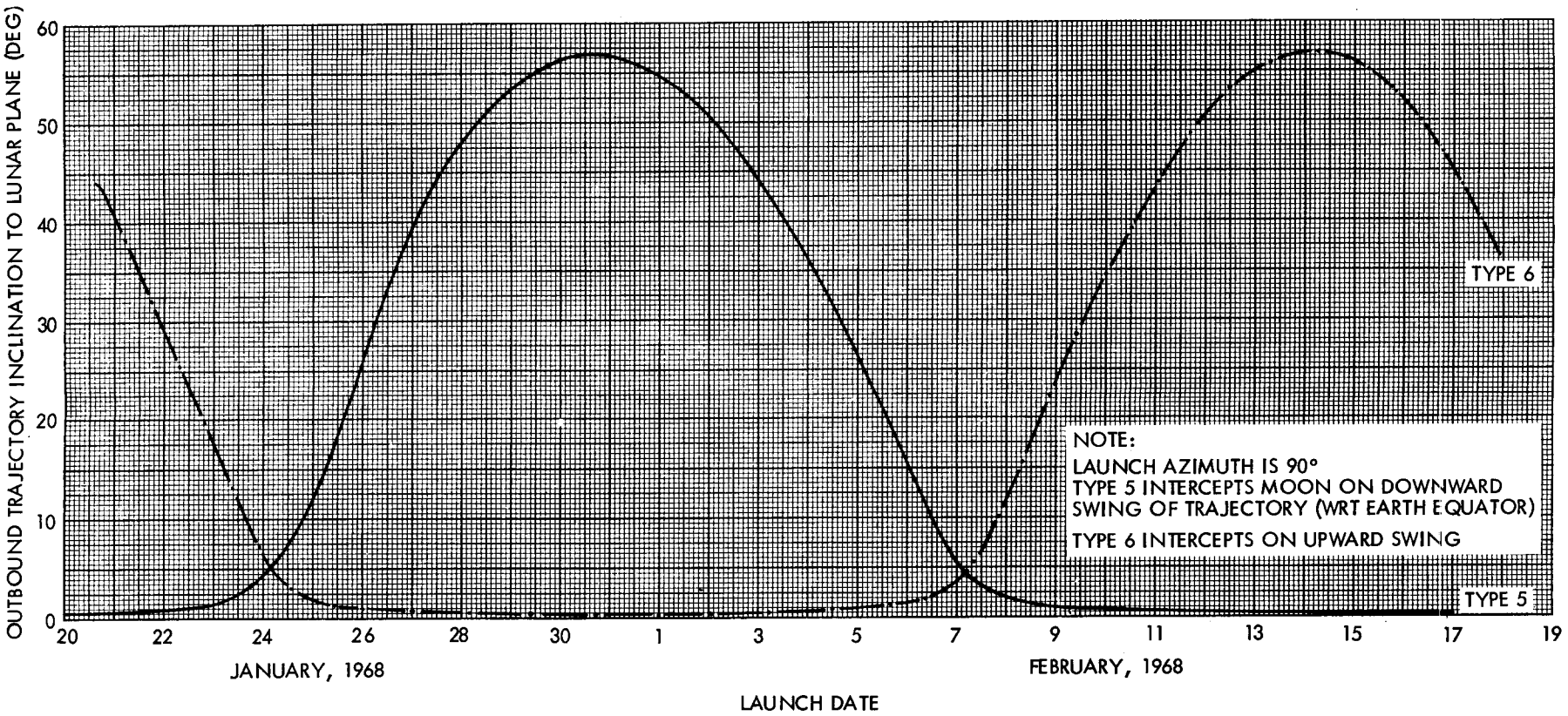

Figure 3.2-2. Inclination of the Outboard Trajectory to the Lunar Plane

possible when the moon is at its maximum distance. Trip time, as a variable, will be an important parameter in this analysis as it essentially controls the magnitude of the $\overline{v}_{\infty}$ vector.

In Figure 3.2-3, $\overline{v}_{\infty}$ magnitude is shown as a function of trip time for the two types of trajectories. Recall from Figure 3.2-2 that type 6 trajectories are in the moon's plane and the type 5 are out-of-plane on January 28. For trip times near 60 hours, the difference in the magnitude $\overline{v}_{\infty}$ between the two types is less than 200 ft/sec but increases to over 300 ft/sec at 100 hours flight time. These values are determined for an earth launch azimuth of 90 degrees, a single lunar site at 45 degrees east longitude and on the moon's equator, and a pericynthion altitude of 80 nautical miles.

The $\overline{v}_{\infty}$ vector defines the approach hyperbola to the moon and is described by its magnitude and position in terms of selenographic longitude and latitude. The magnitude of $\overline{v}_{\infty}$ is dependent on the outward trip time, the position and velocity of the moon, and the inclination of the outbound trajectory to the moon's plane. The latitude of the $\overline{v}_{\infty}$ vector is shown in Figure 3.2-4 for the range of trip times and both trajectory types. The in-plane (type 6) trajectories fall about 6 degrees below the lunar equator while the out-of-plane (type 5) lie from 12 to 16 degrees below. The longitude of the $\overline{v}_{\infty}$ vector, which is shown in Figure 3.2-5, indicates a much more pronounced change with trip time but the difference between the two trajectory types becomes less significant.

The range of launch azimuth is a determining factor in finding the launch window available for a particular mission. However, for the range of azimuths considered here, the outbound trajectory inclinations will change only about 6 degrees. Since this is the case, the effects of launch azimuth on parameters in the moon phase of the trajectory will be small, making it expedient, perhaps, to restrict further analysis to a single value of launch azimuth. Figures 3.2-6 and 3.2-7 show the v_{∞} magnitude for the range of launch azimuths at various flight times. The out-of-plane (type 5) trajectories, which are at a higher velocity level, may reach a difference of up to 50 ft/sec at the extreme azimuths for a constant trip time. On the other hand, the in-plane (type 6) trajectories vary by less than 10 ft/sec.

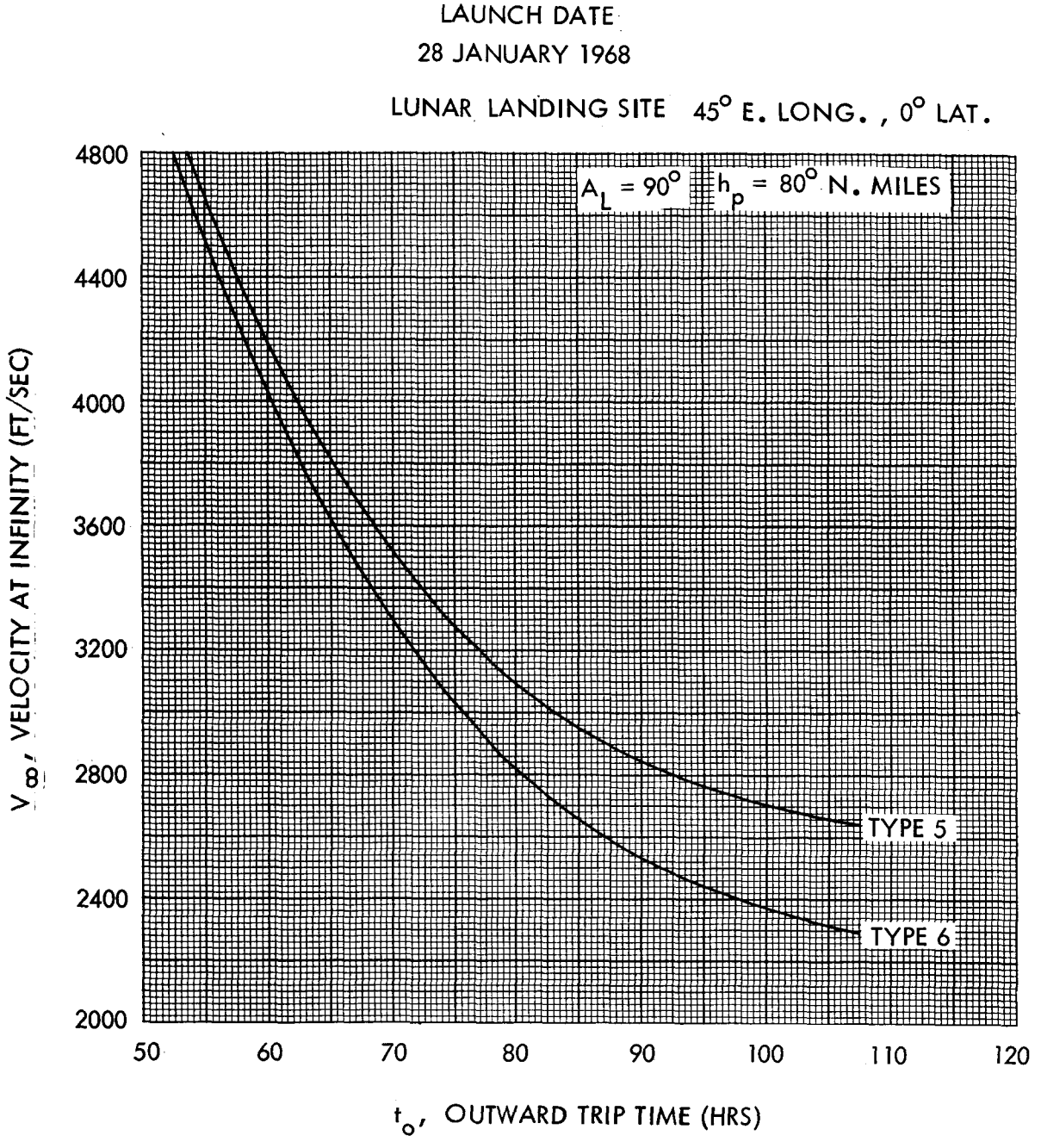

Figure 3.2-3. Velocity at Infinity of the Moon as a Function of Outward Trip Time

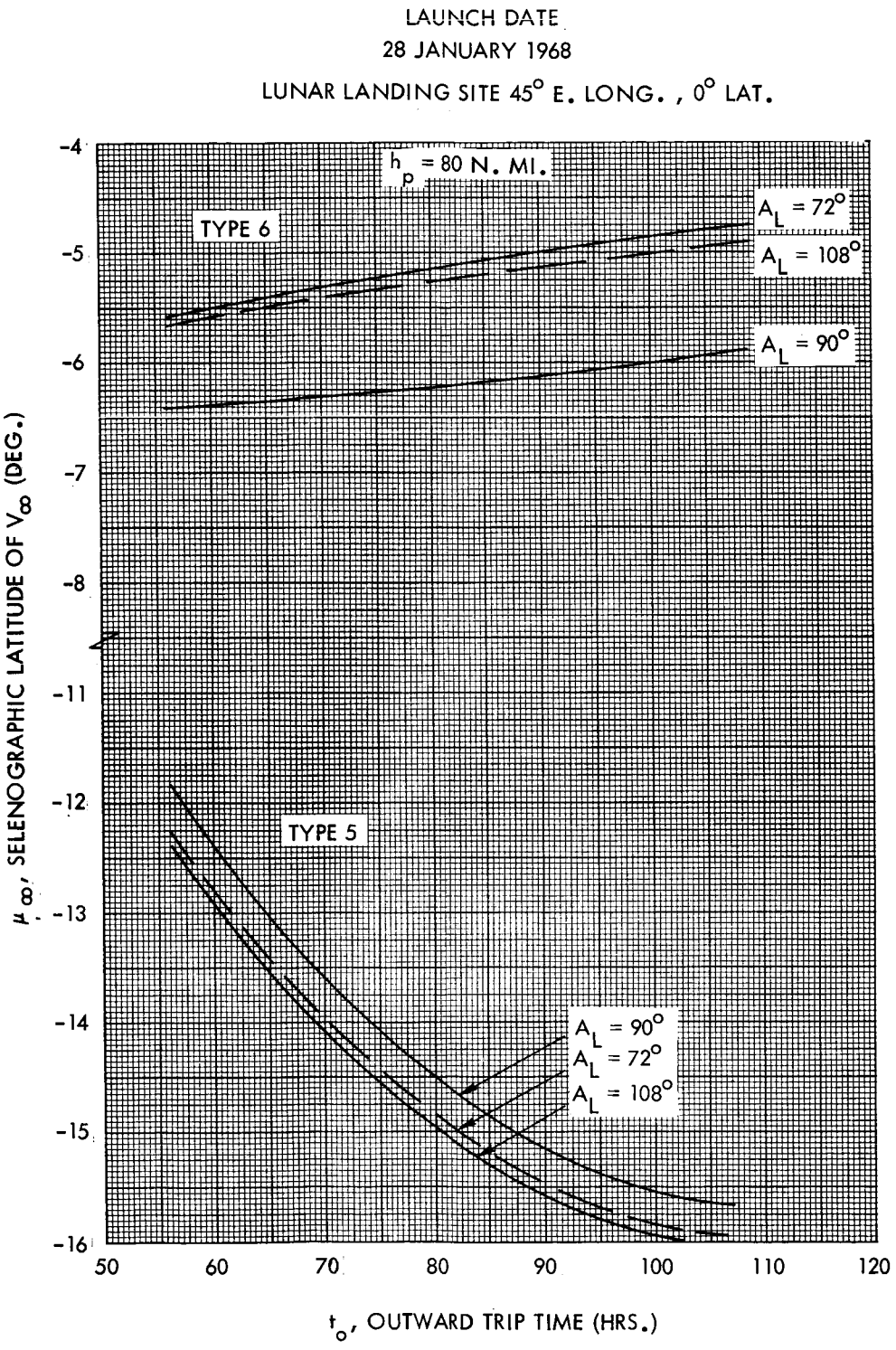

Figure 3.2-4. Latitude of V_∞ at the Moon as a Function of Outward Trip Time

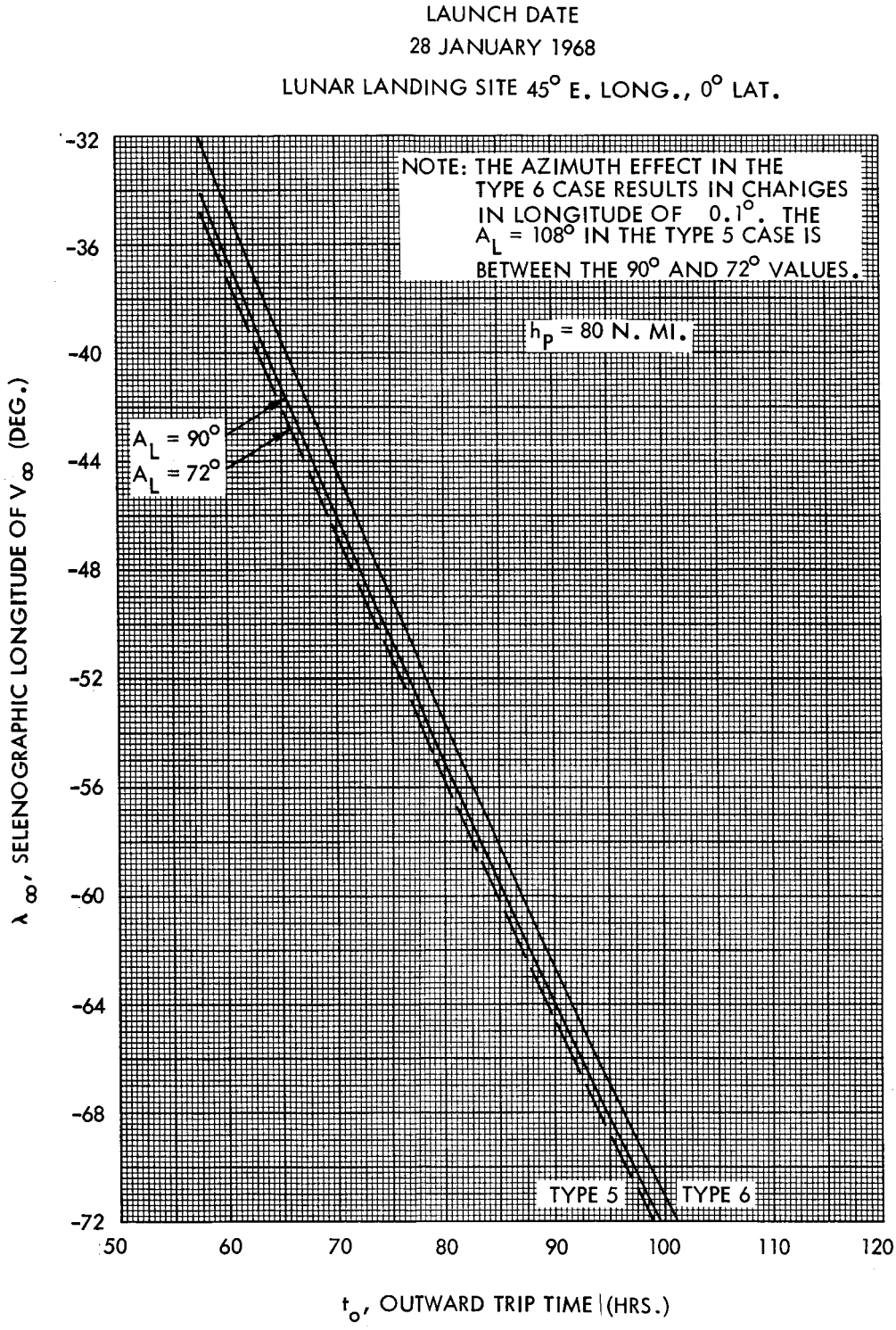

Figure 3.2-5. Longitude of V_∞ at the Moon as a Function of Outward Trip Time

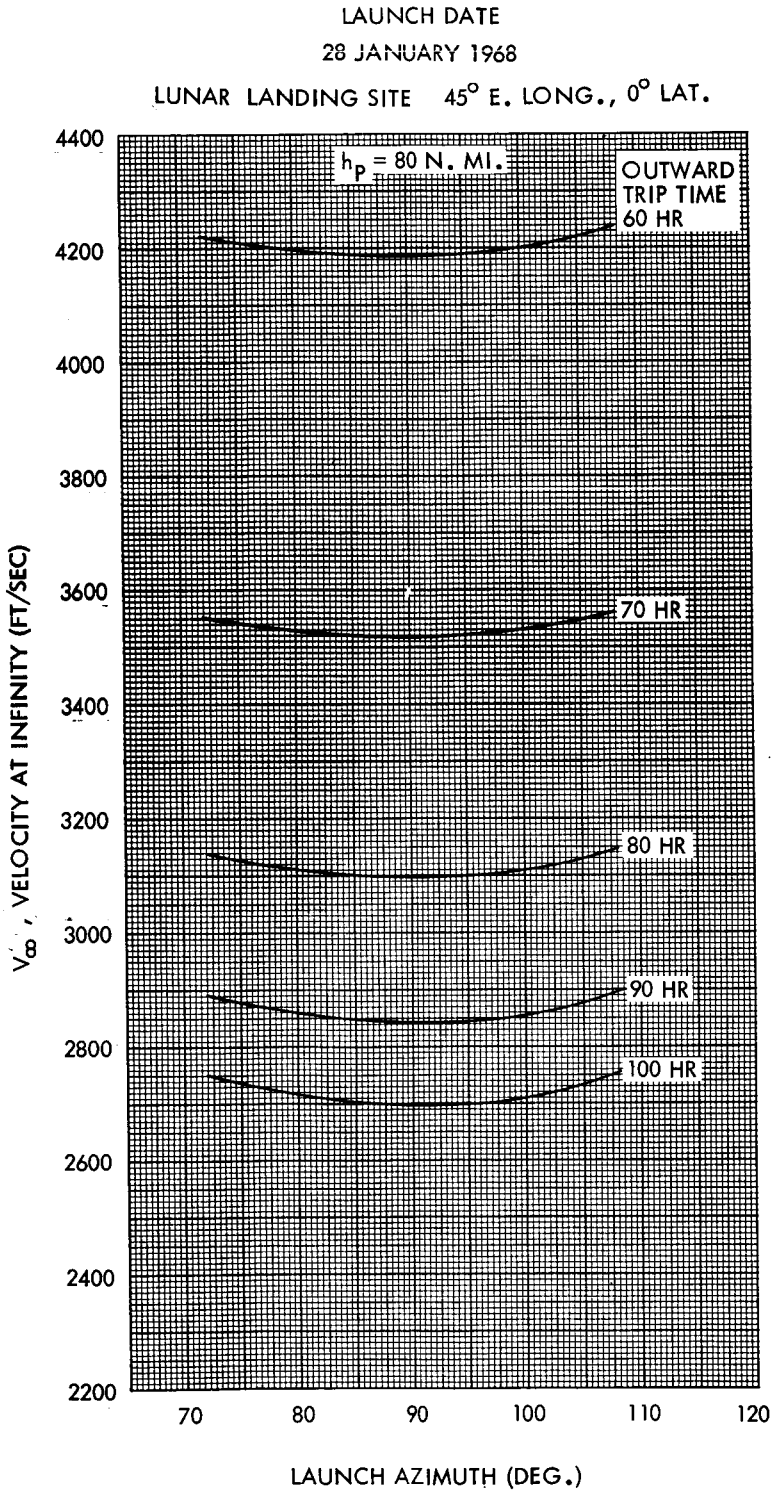

Figure 3.2-6. Effect of Launch Azimuth on V_∞ at the Moon (Type 5)

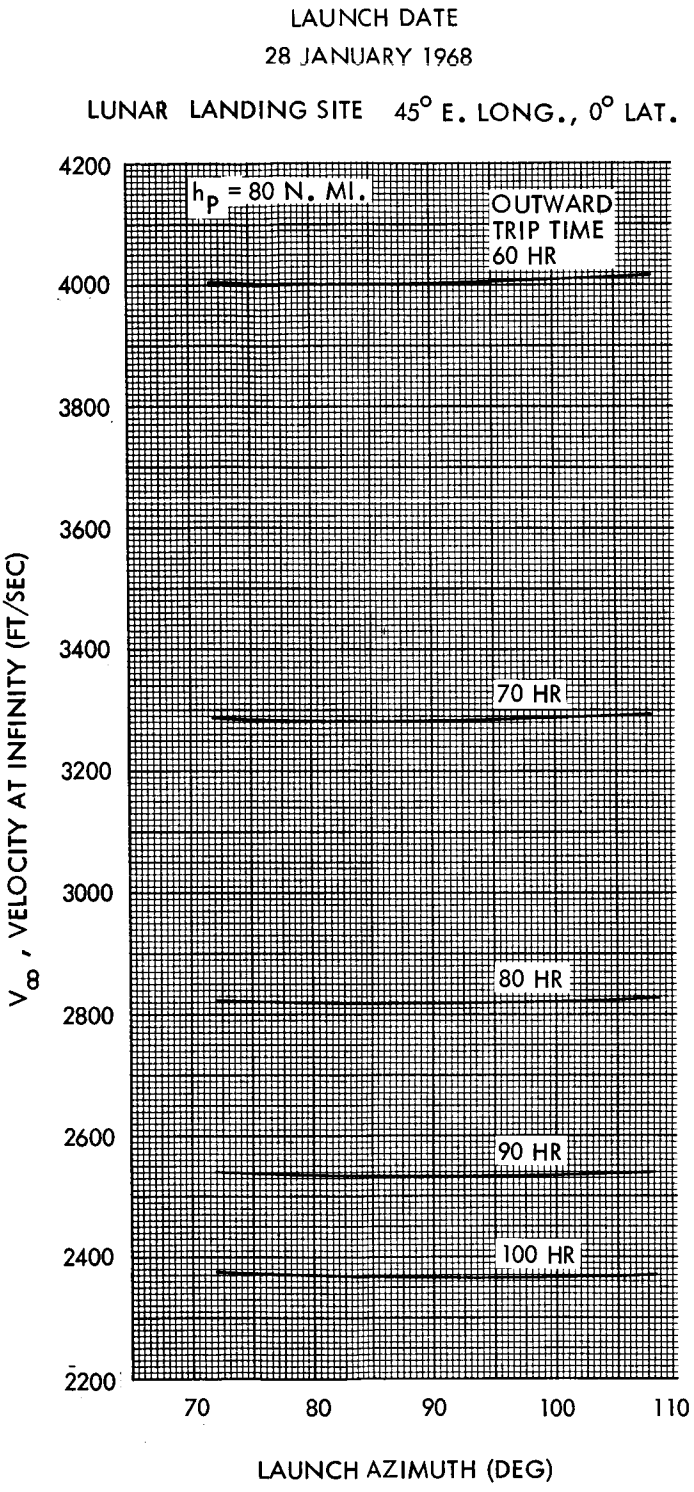

Figure 3.2-7. Effect of Launch Azimuth on V_∞ at the Moon (Type 6)

The effect of launch azimuth on the selenographic latitude and longitude position of the $\overline{v}_{\infty}$ vector has been indicated on Figures 3.2-4 and 3.2-5 respectively. The latitude changes by about 0.33 degrees in the type 5 case and by up to one degree in the type 6 case for constant trip times. The longitude of the $\overline{v}_{\infty}$ vector varies by 0.6 degrees for type 5 trajectories and 0.14 degrees for the type 6 case. The effect of these variations becomes negligible in the moon phase analysis.

The type of trajectory flown and the duration of the parking orbit phase are interrelated. The two types of trajectories were described above as types 5 and 6, for out-of-plane and in-plane respectively. These differ by approximately one-half a revolution in the time spent in earth parking orbit. Thus, any trajectory which differs by one whole revolution from either of these will be similar. In the numbering system adopted, the odd type numbers result in trajectories out of the moon's plane for January 28 launches, and the even numbers result in in-plane trajectories. Then in comparing trajectories, Figure 3.2-8 indicates that the odd numbered cases differ by only 8.65 ft/sec by increasing the parking orbit 2 revolutions from 0.75 revolution minimum (type 3). The in-plane (even numbers) differ even less; by 5.17 ft/sec when the parking duration is increased by 3 revolutions over the minimum of 0.07 revolutions (type 2). It is obvious that there is no significant penalty by limiting the analysis to two adjacent types of trajectory such as 5 and 6 which are mid-range values and thus further lessen the difference from the extremes.

Changing pericynthion altitude has a negligible effect on the $\overline{v}_{\infty}$ vector as is illustrated in Table 3.2-2. For a small change (100 nautical miles) relative to the radial distance from the moon's center, very small variations in velocity, latitude and longitude of the $\overline{v}_{\infty}$ vector are experienced. The maximum change in velocity is slightly over 3 ft/sec which occurs near the 60-hour flight times. The latitude varies by 0.009 degrees and the longitude by 0.08 degrees at the longer flight times. These values are for increasing the pericynthion altitude from 50 to 150 nautical miles. If 80 nautical miles values are used the variation from the extremes will be even less.

With such a wide region of landing sites available at the moon, it is necessary to show the effect on the $\overline{v}_{\infty}$ vector for in-plane overflights of

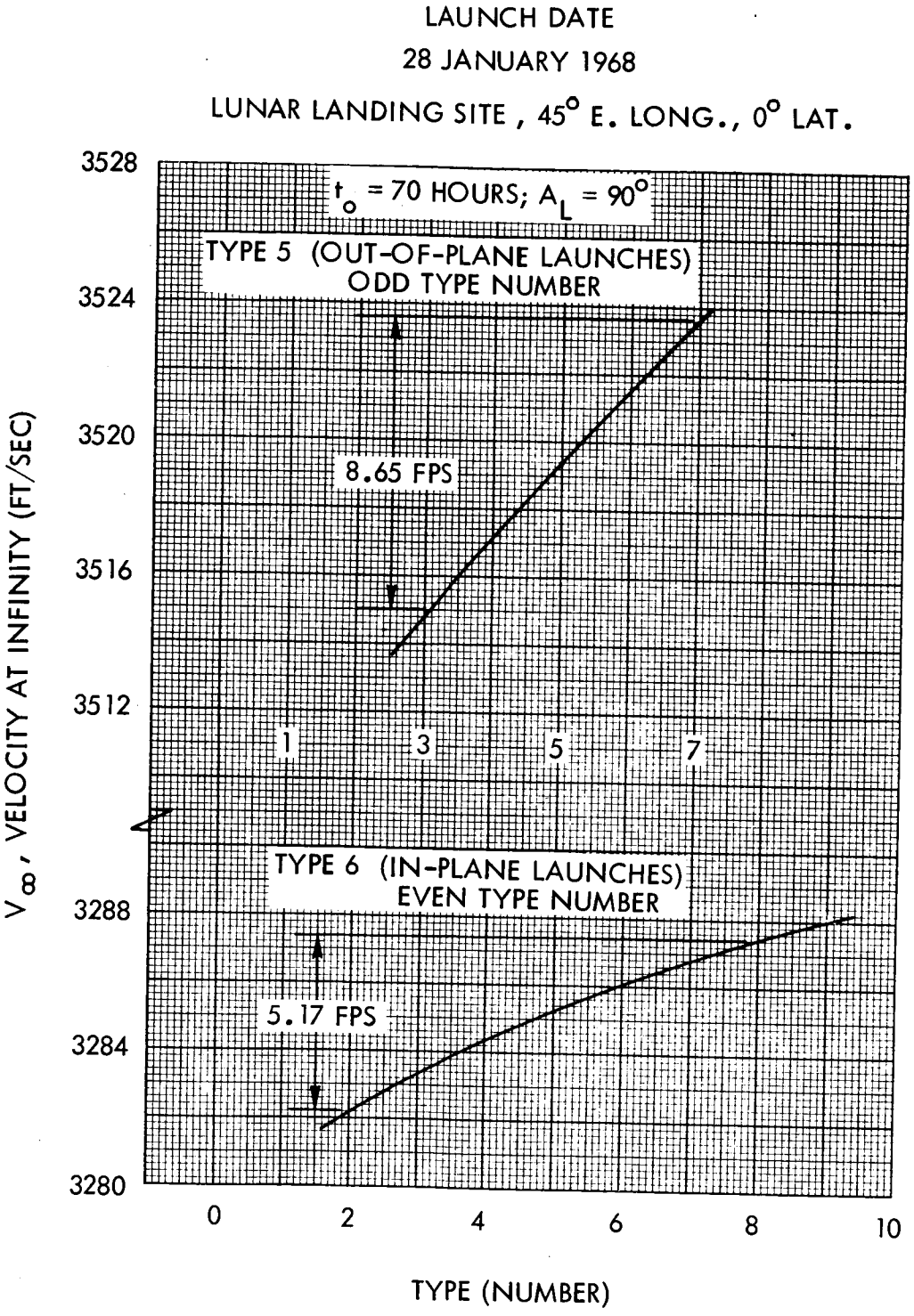

Figure 3.2-8. Effect of Parking Orbit Duration on V_∞ at the Moon

Table 3.2-2. Effect of Changing Pericynthion Altitude

		Type 5			Type 6		
t_o	h_p	v_∞	μ_∞	λ_∞	v_∞	μ_∞	λ_∞
60	50	4189.10	-12.387	-36.145	4005.18	-6.396	-34.431
	80	4190.18	-12.385	-36.130	4006.31	-6.396	-34.416
	150	4192.24	-12.381	-36.099	4007.82	-6.396	-34.395
	Δ	+ 3.14	+ 0.006	+ 0.046	+ 2.64	0	+ 0.036
80	50	3098.65	-14.493	-55.053	2820.61	-6.234	-53.255
	80	3099.30	-14.491	-55.035	2821.37	-6.234	-53.208
	150	3101.35	-14.484	-54.980	2823.73	-6.235	-53.152
	Δ	+ 2.70	+ 0.009	+ 0.073	+ 3.12	-0.001	+ 0.073
100	50	2700.66	-15.534	-72.036	2368.50	-6.012	-71.030
	80	2700.98	-15.533	-72.020	2368.91	-6.013	-71.013
	150	2701.94	-15.529	-71.965	2370.24	-6.015	-70.951
	Δ	+ 1.28	+ 0.004	+ 0.071	+ 1.74	-0.003	+ 0.079

t_o = trip time (outbound) ~ hours

h_p = pericynthion altitude ~ n.mi.

v_∞ = velocity at infinity of moon ~ ft/sec

μ_∞ = selenographic latitude of v_∞ ~ deg

λ_∞ = selenographic longitude of v_∞ ~ deg

Δ = difference between values of h_p of 150 and 50 n.mi.

any particular site. This can be done by varying the selenographic orbit inclination to provide this coverage. The inclination is constrained to retrograde orbits which have inclinations greater than 90, but less than 180 degrees. These inclinations have been generated for an 80 nautical mile pericynthion altitude, launch azimuth of 90 degrees and the range of trip times from 60 to 100 hours. The effect on position and magnitude of the $\overline{v}_{\infty}$ vector versus the selenographic orbit inclination is shown in Figures 3.2-9, 3.2-10, and 3.2-11 for $\overline{v}_{\infty}$ magnitude, latitude and longitude respectively. The change in magnitude is barely discernable, although it varies by 23 to 29 ft/sec over a 90-degree range in inclination. The change in latitude and longitude are similarly small, although the latitude drops off about one-half a degree at an inclination of 180 degrees for both types of trajectories. For practical purposes, it is possible to assume that the position and magnitude of the $\overline{v}_{\infty}$ vector are independent of selenographic inclination. This means selection of any one site in this region with trajectories providing a type 5 and type 6 overflight in the range of trip times required will be sufficient to determine the two values of the $\overline{v}_{\infty}$ vectors on any day.

The small effects of the hyperbolic approach inclination may also be seen by plotting the selenographic locations of the $\overline{v}_{\infty}$ vectors as this inclination is varied. Figures 3.2-12 and 3.2-13 present these locations for type 5 and 6 trajectories, respectively. The translunar trajectory chosen is for a 70-hour flight time which is shown on the previous three figures. The variations will be approximately the same at other flight times with longitude increasing in a westerly direction as flight time increases.

It is also of interest to overlay the lines of constant v_{∞} magnitude on the grid of landing sites available to see if any site displays singularities. In Figures 3.2-14 and 3.2-15, again type 5 and type 6 trajectories respectively, the variation of the v_{∞} magnitude over the landing sites is similar to the in-plane inclination required. That is, for landing sites near the western edge of the region, the inclination of the orbit approaches 90 degrees whereas sites at the easternmost edge require inclinations nearer 180 degrees. In both figures the higher velocity occurs at the easternmost

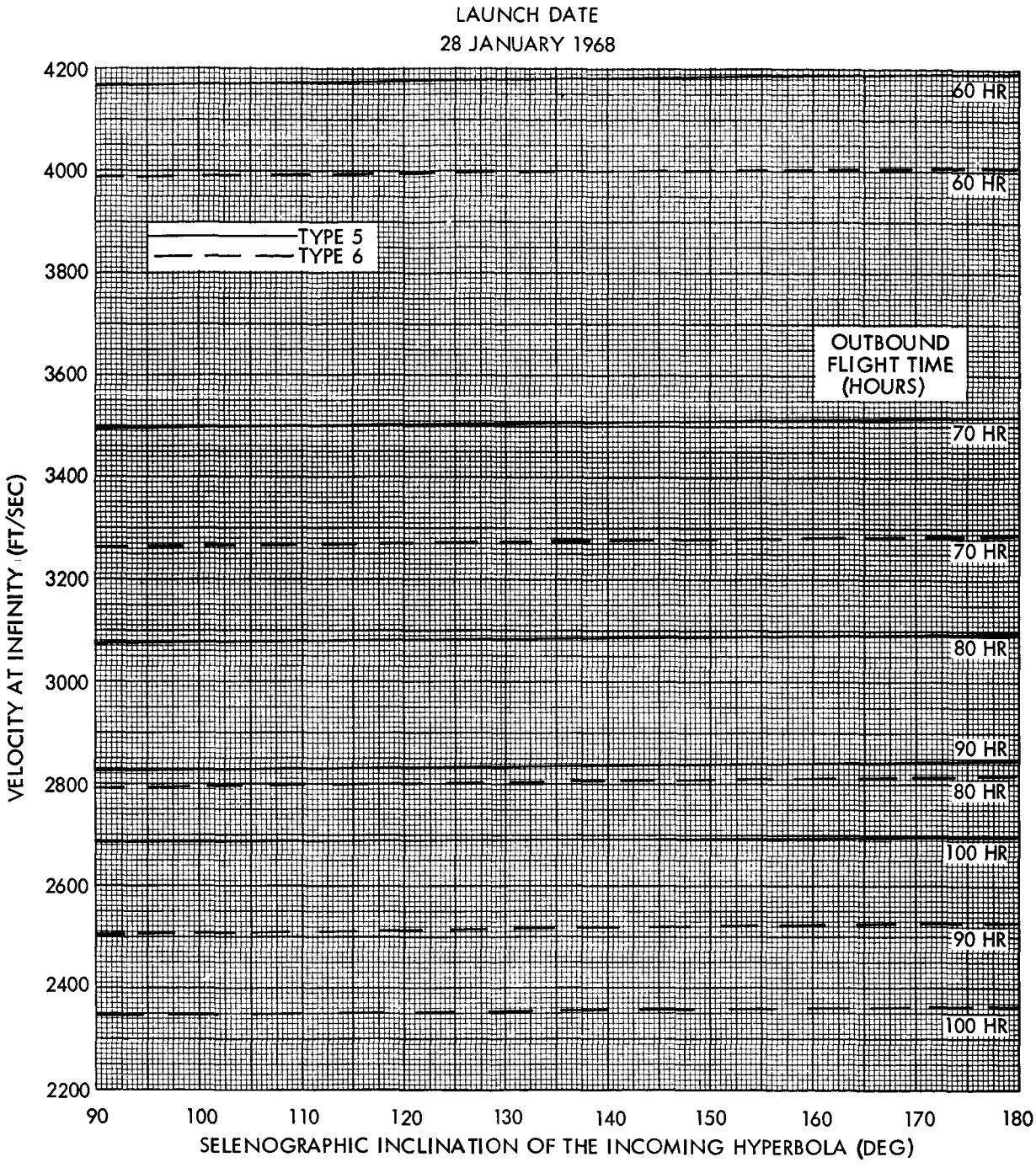

Figure 3.2-9. Effect of Selenographic Inclination on V_∞ at the Moon

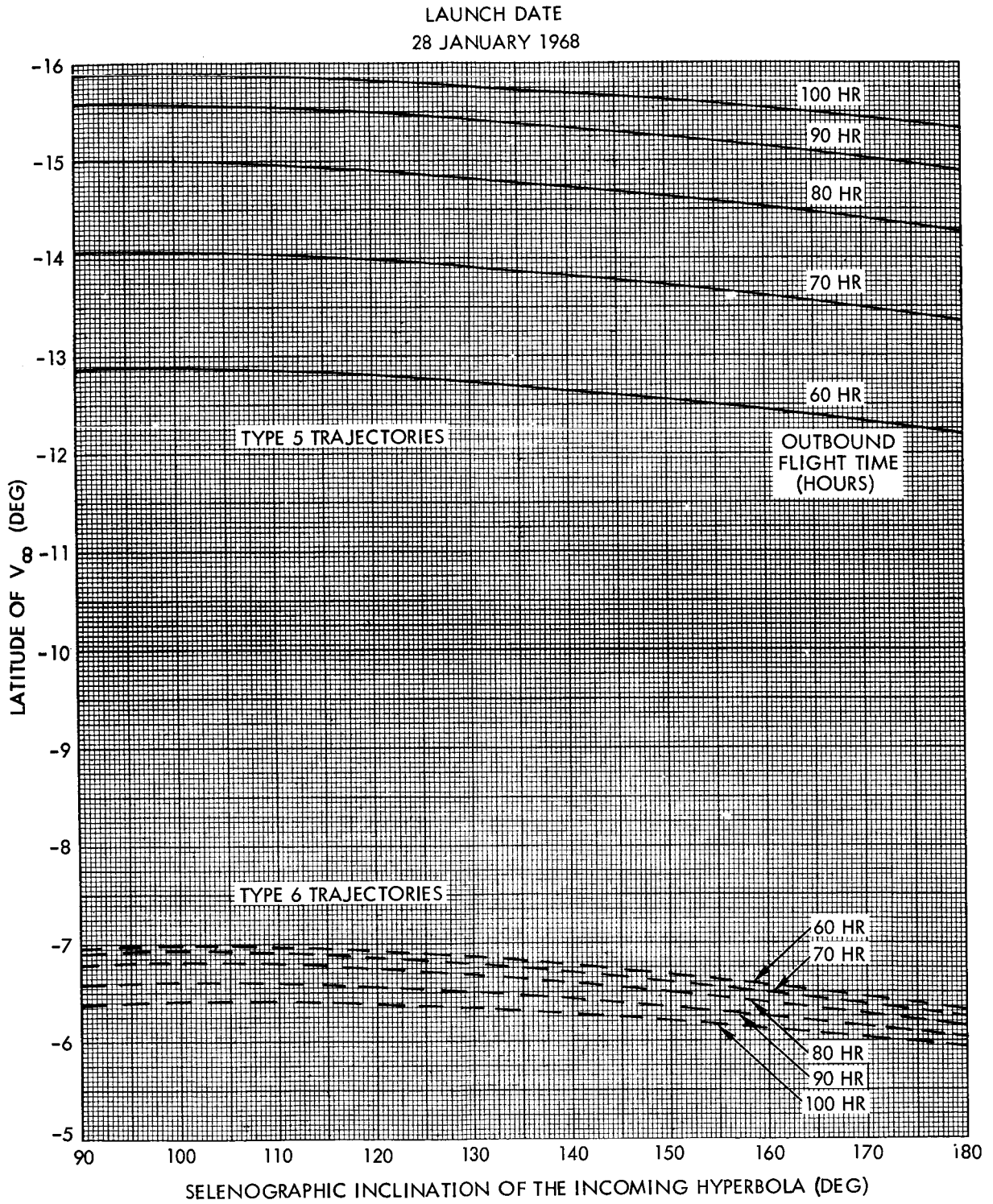

Figure 3.2-10. Effect of Selenographic Inclination on Latitude of V_∞

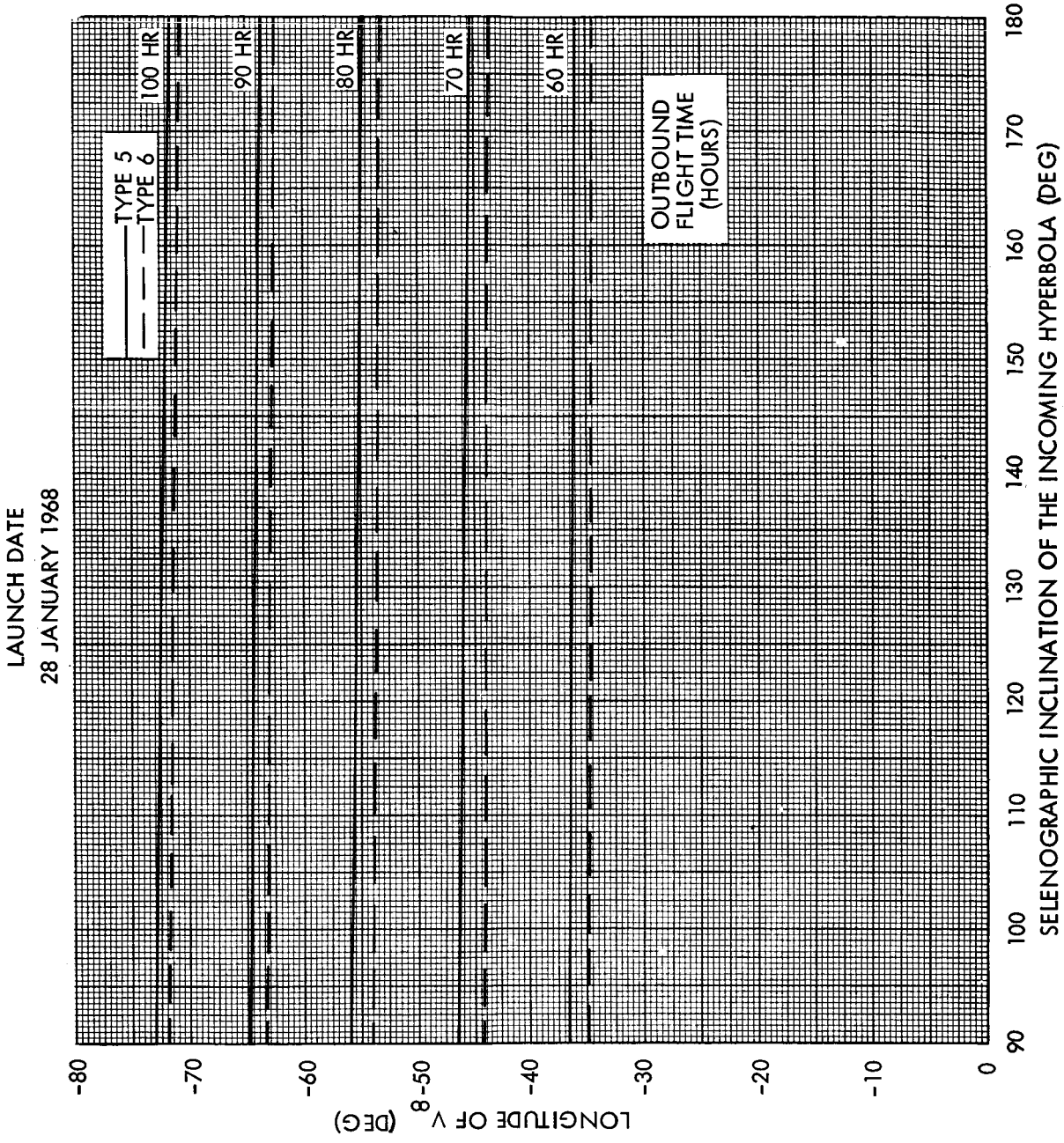

Figure 3.2-11. Effect of Selenographic Inclination on Longitude of V_∞

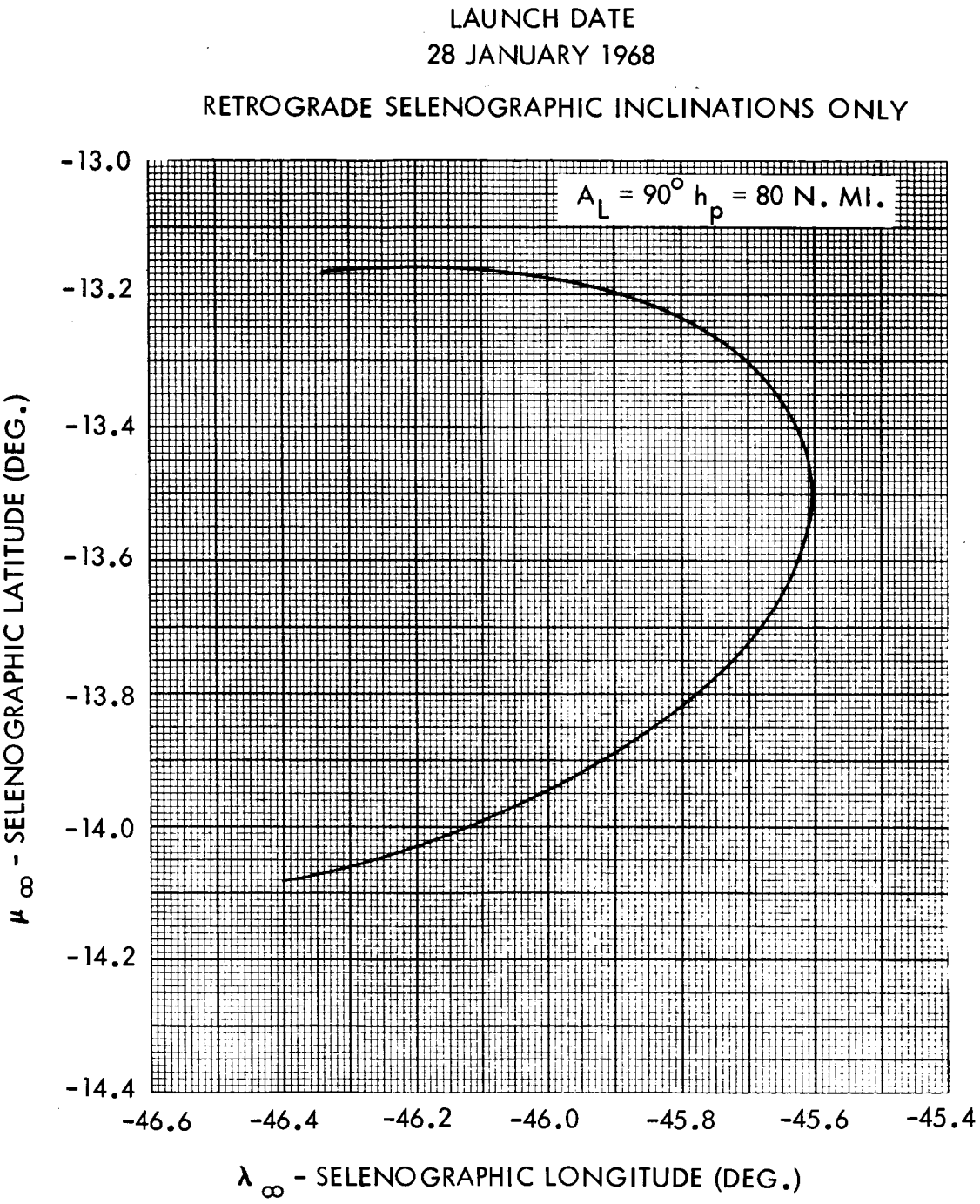

Figure 3.2-12. Locus of the V_∞ Position for a 70-Hour Outward Trip Time (Type 5)

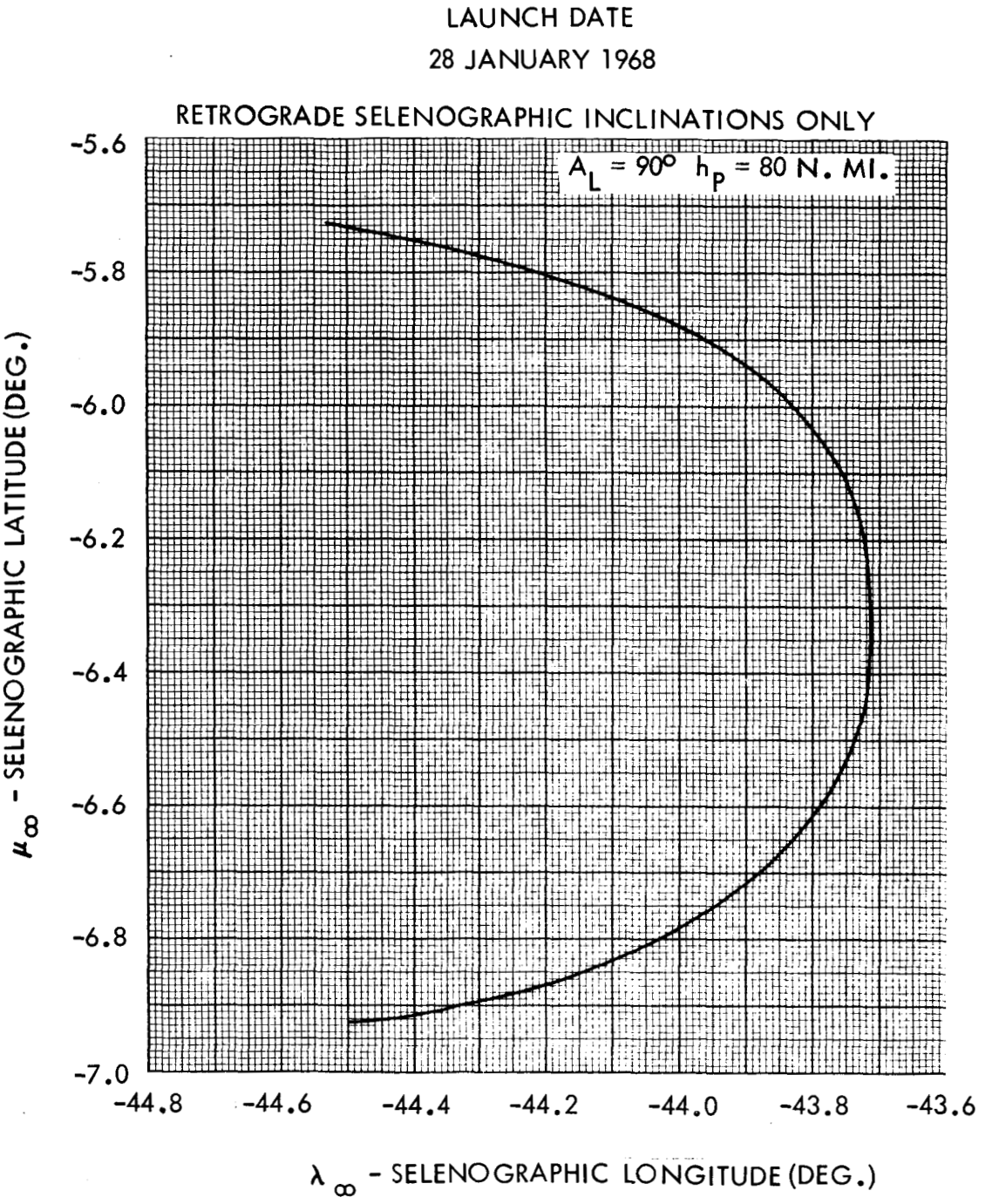

Figure 3.2-13. Locus of the V_∞ Position for a 70-Hour Outward Trip Time (Type 6)

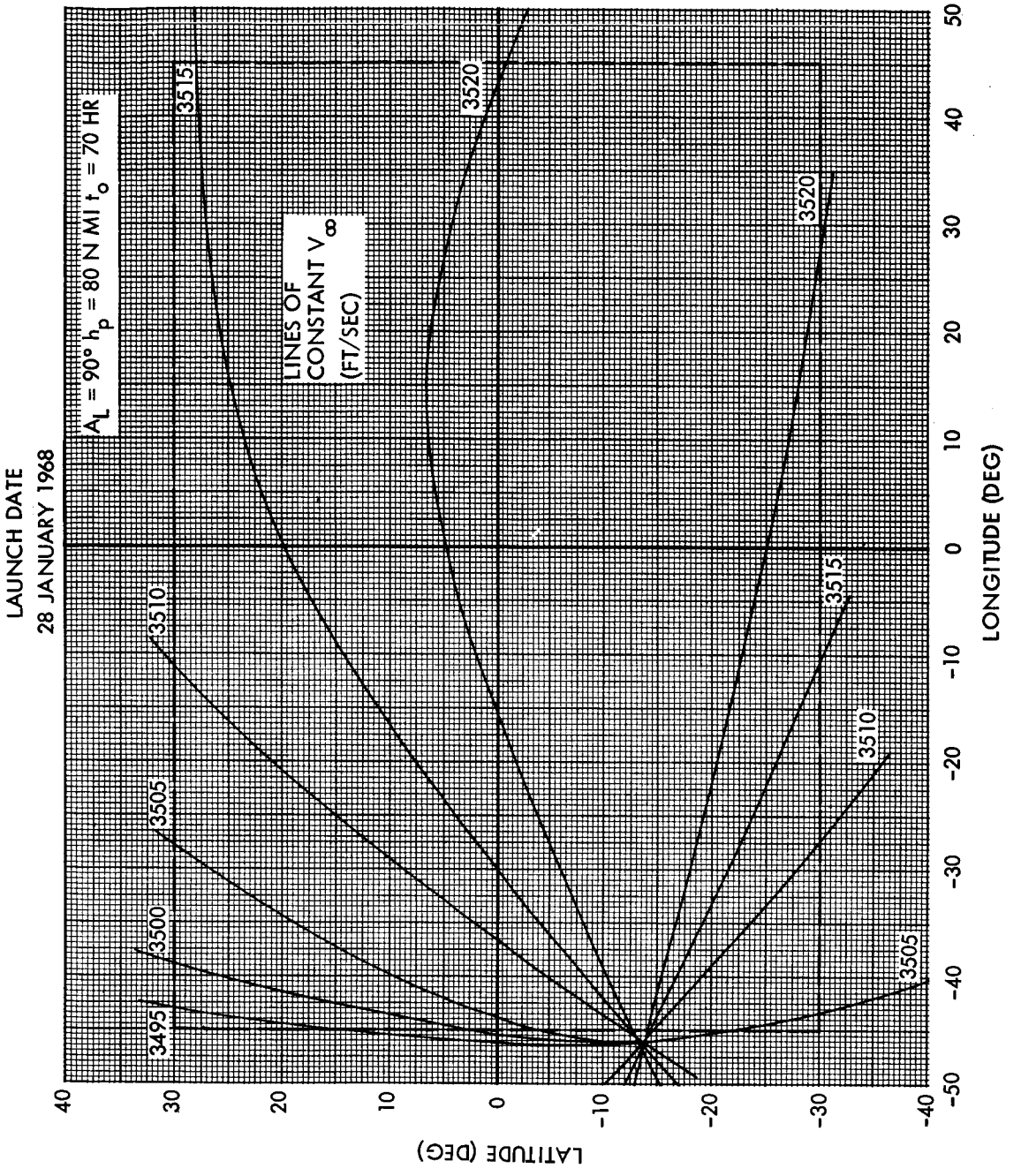

Figure 3.2-14. Effect of Lunar Site on V_∞ for the In-Plane Deboost (Type 5)

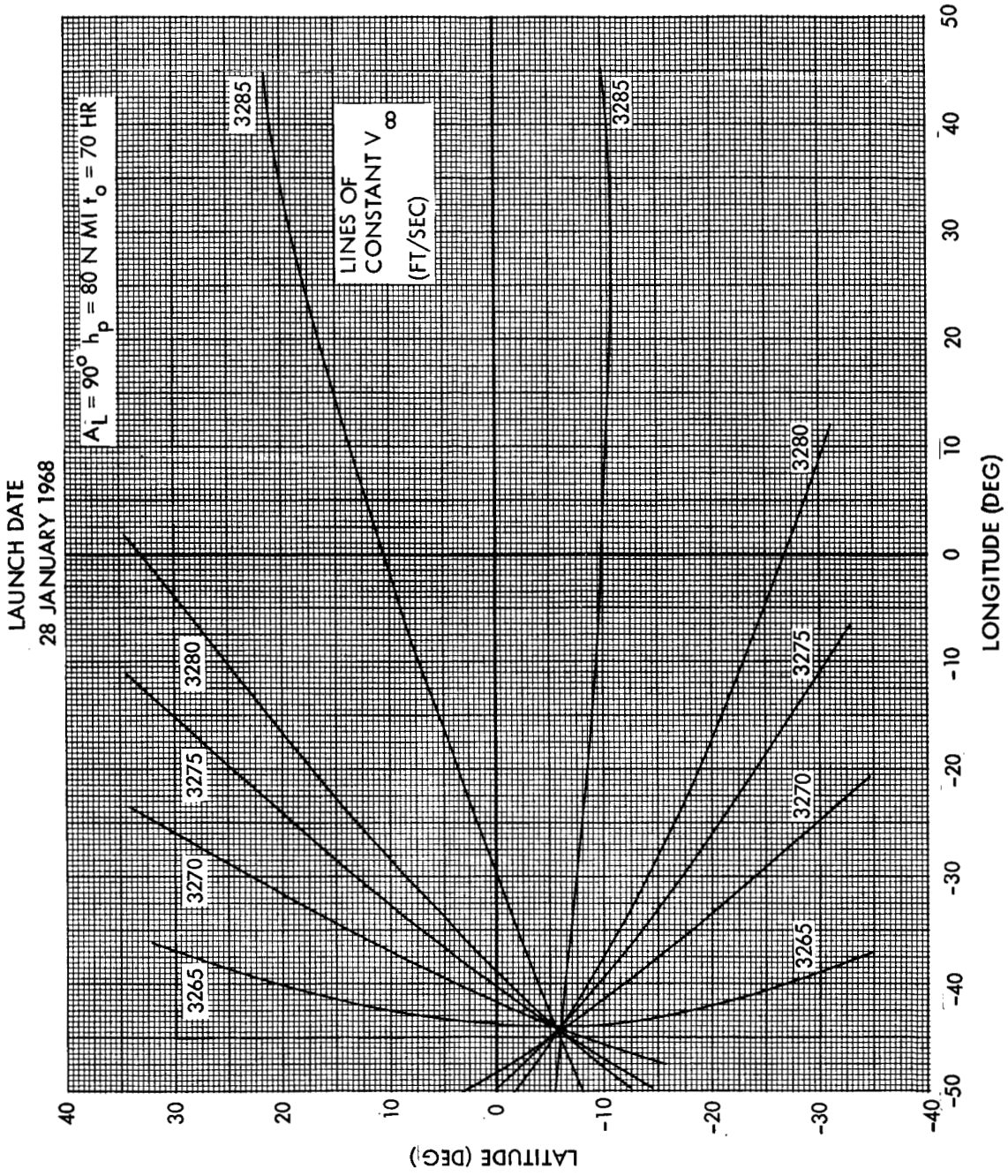

Figure 3.2-15. Effect of Lunar Site on V_∞ for In-Plane Deboost (Type 6)

edge of the region at +45 degrees longitude and near the lunar equator. Thus, a conservative selection of a site on the equator at 45 degrees longitude would result in the higher v_∞ magnitude assuring that no penalty would be encountered at any other site. The relationship of the v_∞ magnitude to pericynthion velocity is such that the difference in values experienced at infinity is reduced to approximately one-half this value at pericynthion. It should be noted that although most sites will determine the inclination of the hyperbola for in-plane overflights, this is not true for the site which corresponds to the selenographic position of the $\overline{v}_\infty$ vector. This site represents a singular point in that any inclination will result in an overflight. It would appear in these figures, that the location of the $\overline{v}_\infty$ vector lies at a single point, however an expanded view of the true location, as it varies with inclination was shown in Figures 3.2-12 and 3.2-13.

The launch day will have a rather important effect on the $\overline{v}_\infty$ vector in that for fixed trip times the velocity magnitude will vary at the lunar distance and the position depends primarily on the lunar declination and the inclination of the outbound trajectory to the moon's plane. A limited study has been done which can be used to make some general statements regarding these parameters. If the trip time is held at 60 hours, and the lunar site chosen at 45 degrees longitude on the moon's equator, the results based on alternate days in the month are as follows. The magnitude of v_∞, as shown in Figure 3.2-16, varies by about 600 ft/sec from a minimum value of 3950 ft/sec, which occurs when the lunar distance is near minimum. The position of the $\overline{v}_\infty$ vector is also highly influenced by the launch date. The latitude varies from -13 degrees to somewhat over +13 degrees, depending on the lunar geometry and outbound trajectory inclination to the moon's plane. The locus of the $\overline{v}_\infty$ vector locations is shown in Figure 3.2-17. Referring to Figure 3.2-1, note that the latitude position moves as the declination of the moon. This motion and the variation in the longitude can be attributed largely to the lunar libration, perhaps up to 8 degrees. The balance must then be geometrical effects.

It should be apparent that the non-periodic variation of lunar distance and declination with each other involves a separate analysis for each day as

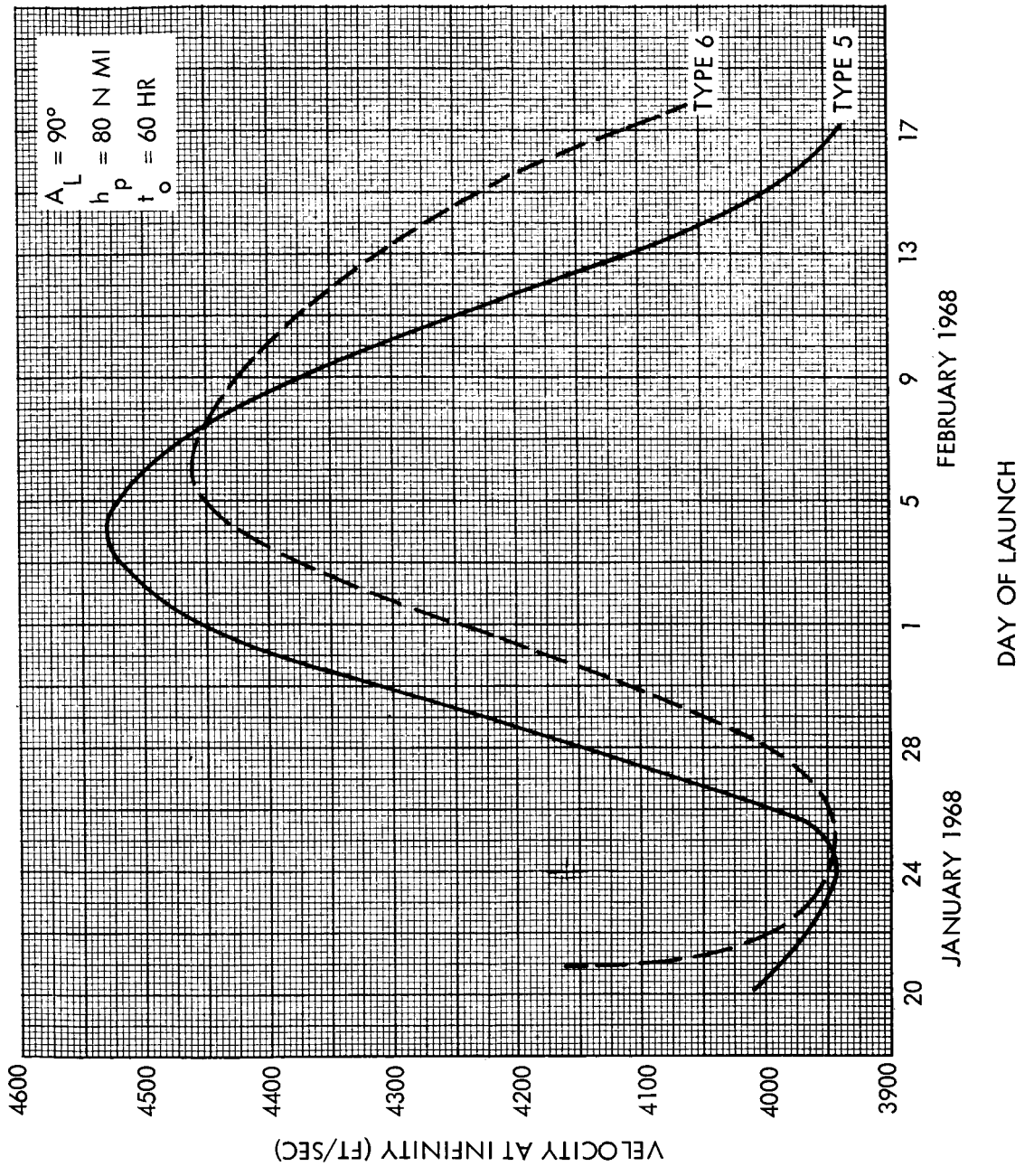

Figure 3.2-16. Variation of V_∞ During a Lunar Month

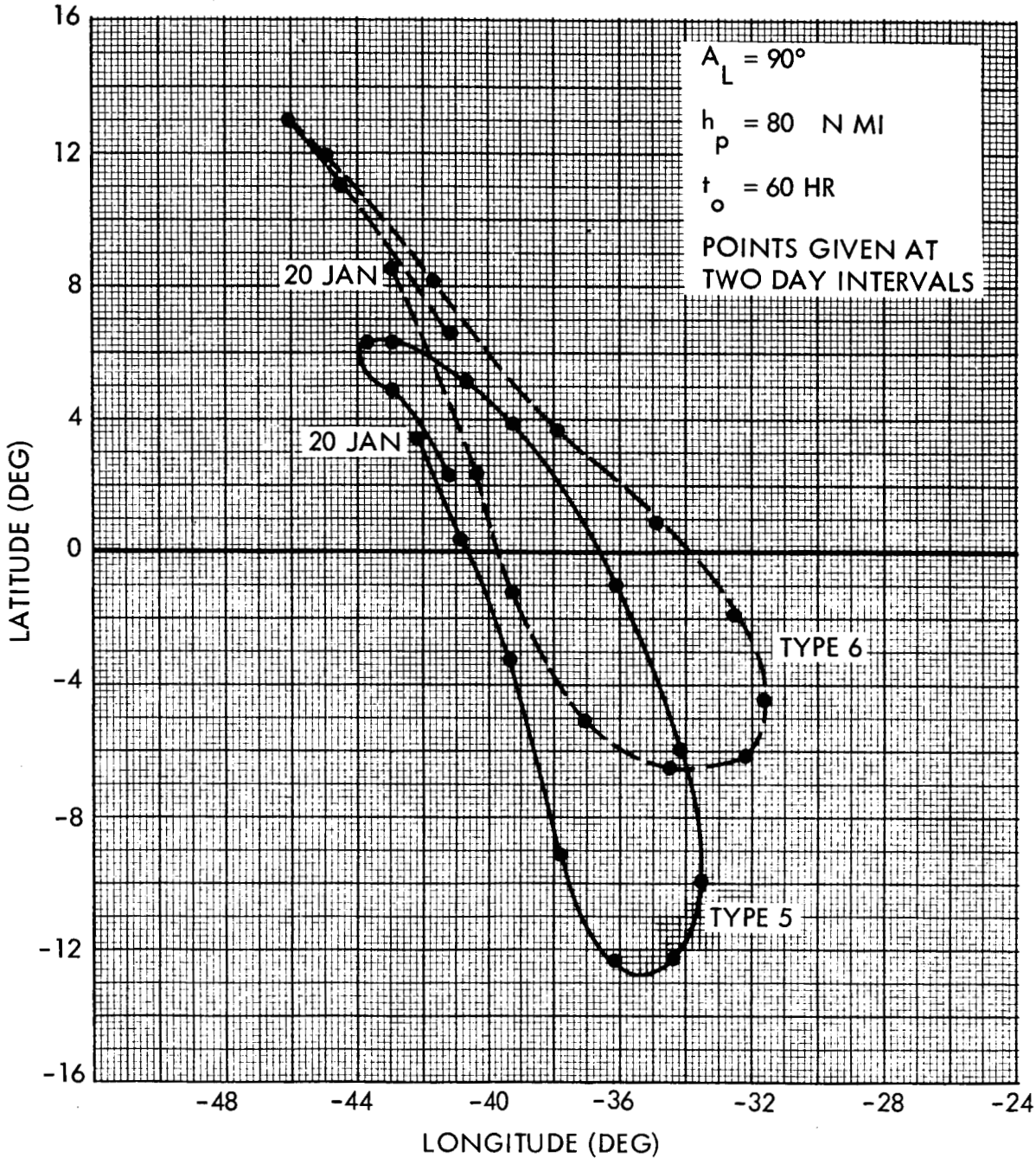

Figure 3.2-17. Locus of V_∞ Locations for a Lunar Month

it becomes impossible to eliminate or separate the variables in determining an adequate $\overline{v}_{\infty}$ vector.

The analysis described above indicates that the following parameters have a considerable influence on $\overline{v}_{\infty}$ of the lunar approach hyperbola:

a) Launch day (i.e., lunar distance and declination)

b) Type of trajectory (i.e., type 5 or 6 or their equivalents)

c) Flight time

The following variables are deemed to have, by comparison, a second order effect:

d) Launch Azimuth

e) Lunar landing site (i.e., selenographic inclination of the hyperbola)

The following variables have negligible effect:

f) Pericynthion altitude

g) Parking orbit duration (i.e., ± 1 revolution from nominal)

3.3 Effects of Transearth Parameters on the $\overline{v}_{\infty}$ Vector

The possible elimination of parameters as variables in this phase of the mission has been studied for a transearth injection date of February 1, 1968. The first phase of this analysis has been performed to determine if the location of a particular site on the lunar surface, which is contained within the orbit plane of the parking orbit at the time of transearth injection, has any sizable effect on the position and magnitude of the velocity vector an infinite distance from the moon. The hyperbolic plane is assumed to be inclined such that no plane change is required at transearth injection. This is equivalent to determining the effect of the inclination of the transearth hyperbola on the $\overline{v}_{\infty}$ vector. The parking orbit altitude was assumed to be 80 nautical miles, and the earth landing site was taken to be at San Antonio, Texas.

Figures 3.3-1 through 3.3-3 show contours of the magnitude and position (selenographic latitude and longitude) of $\overline{v}_{\infty}$, with variation in

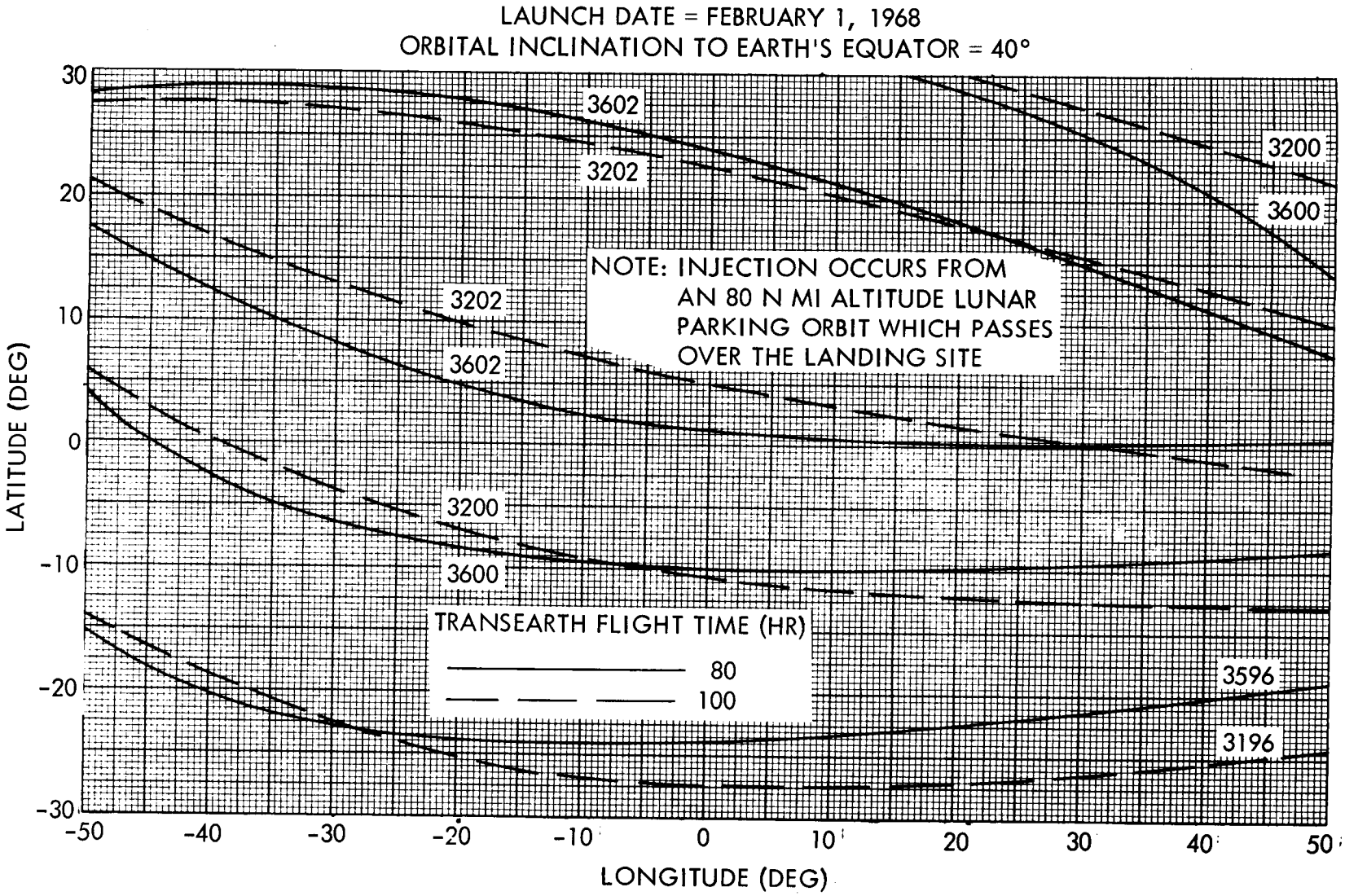

Figure 3.3-1. Variation in Transearth Hyperbolic Excess Velocity from the Moon with Lunar Landing Site

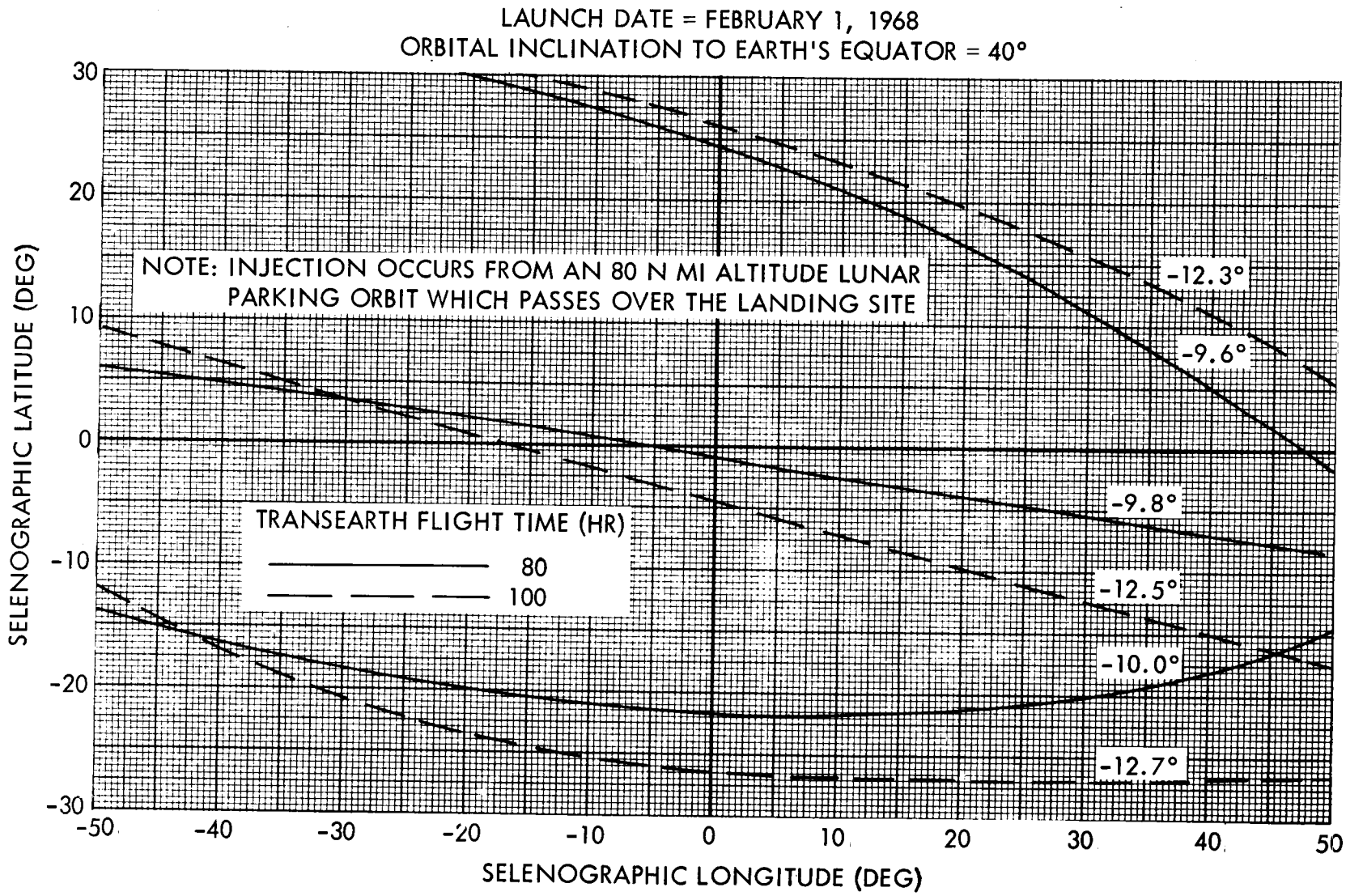

Figure 3.3-2. Variation in Selenographic Latitude of Velocity Vector at Infinity with Lunar Landing Site

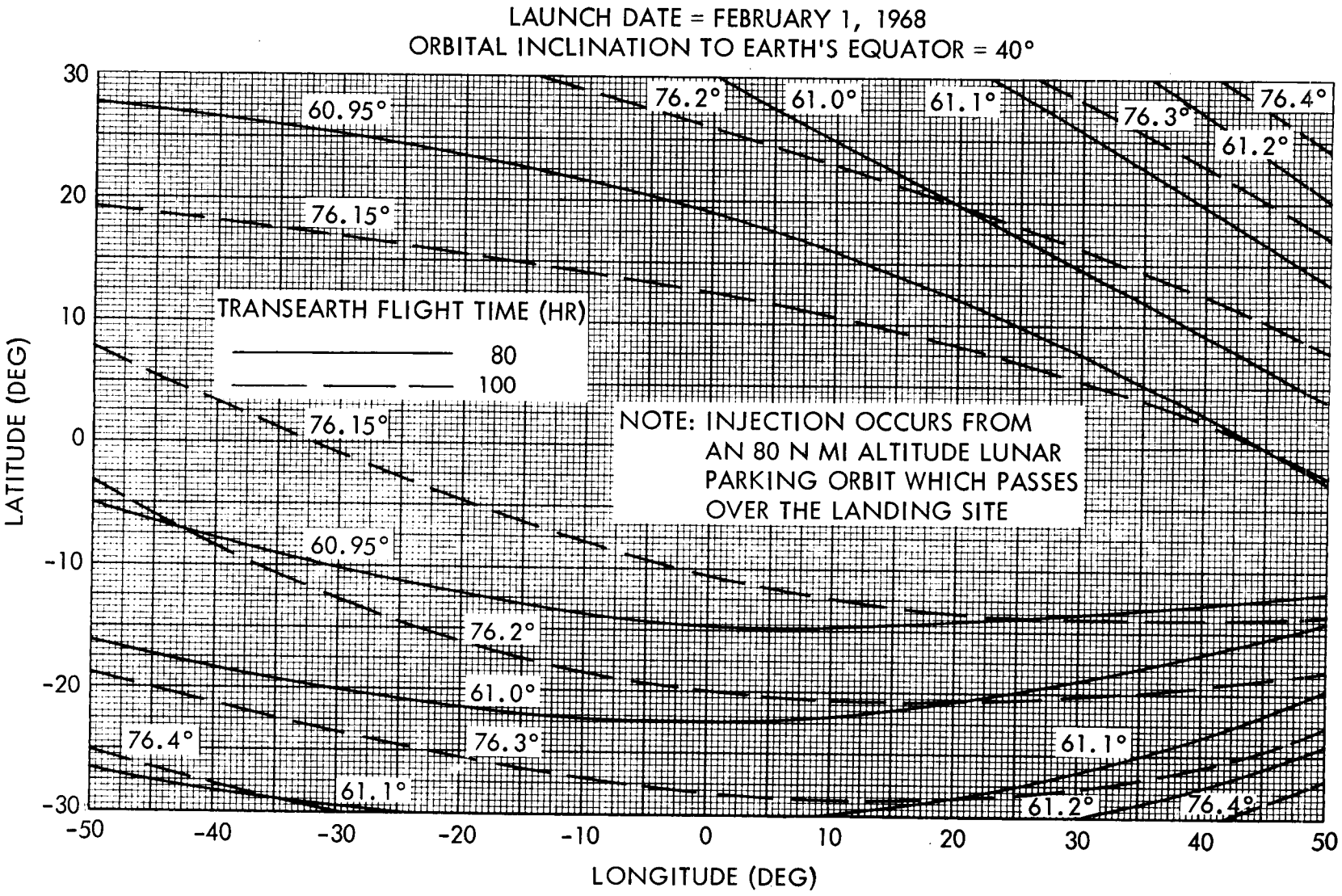

Figure 3.3-3. Variation in Selenographic Longitude of Velocity Vector at Infinity with Lunar Landing Site

the lunar site which is contained within the parking orbit plane at the time of transearth injection. The approach inclination at the earth was 40^{o} with respect to the earth's equator. Contours for transearth flight times of 80 and 100 hours are shown on each figure.

The magnitude, latitude, and longitude of the $\overline{v}_{\infty}$ vector varies less than 15 ft/sec, 1 deg, and 0.5 deg, respectively, within the considered range of lunar sites. For this study these differences are small enough to allow the lunar landing site to remain a constant while generating the $\overline{v}_{\infty}$ vector. Also, by choosing a site near the lunar equator these maximum variations can be reduced still further.

Figures 3.3-4 through 3.3-6 are similar plots, except they are for a transearth orbit inclination relative to the earth's equator of 30^{o} and earth return flight times of 60 and 80 hours. These also demonstrate about the same variation in the $\overline{v}_{\infty}$ vectors. These small variations signify that the location of the lunar landing site can be eliminated as a variable in regards to the $\overline{v}_{\infty}$ vector for transearth trajectories, but that the return inclination must remain as a parameter unless fixed by other considerations. It should be pointed out that the magnitude of these variations will remain essentially the same throughout the lunar orbital period. Only the slope and position of the contour lines will change.

Note also that the maximum variations in velocity, latitude, and longitude of the $\overline{v}_{\infty}$ vector occurs for lunar sites at the more easterly longitudes. This results from the lunar orbit inclination changing more rapidly as the longitude of the lunar base approaches the longitude of the $\overline{v}_{\infty}$ vector. The velocity vector at the moon's sphere of action, but in an earth-centered inertial coordinate system, must be essentially constant for a given set of end conditions no matter what the lunar orbit inclination. Thus as the lunar orbit inclination changes, the vehicle's velocity relative to the moon must also change, such that the vector addition of the vehicle's velocity relative to the moon and the moon's velocity relative to the earth gives essentially the same vehicle velocity vector relative to the earth.

Figure 3.3-7 helps in showing why the orbit inclination does change more rapidly as the site approaches the longitude of the $\overline{v}_{\infty}$ vector. The

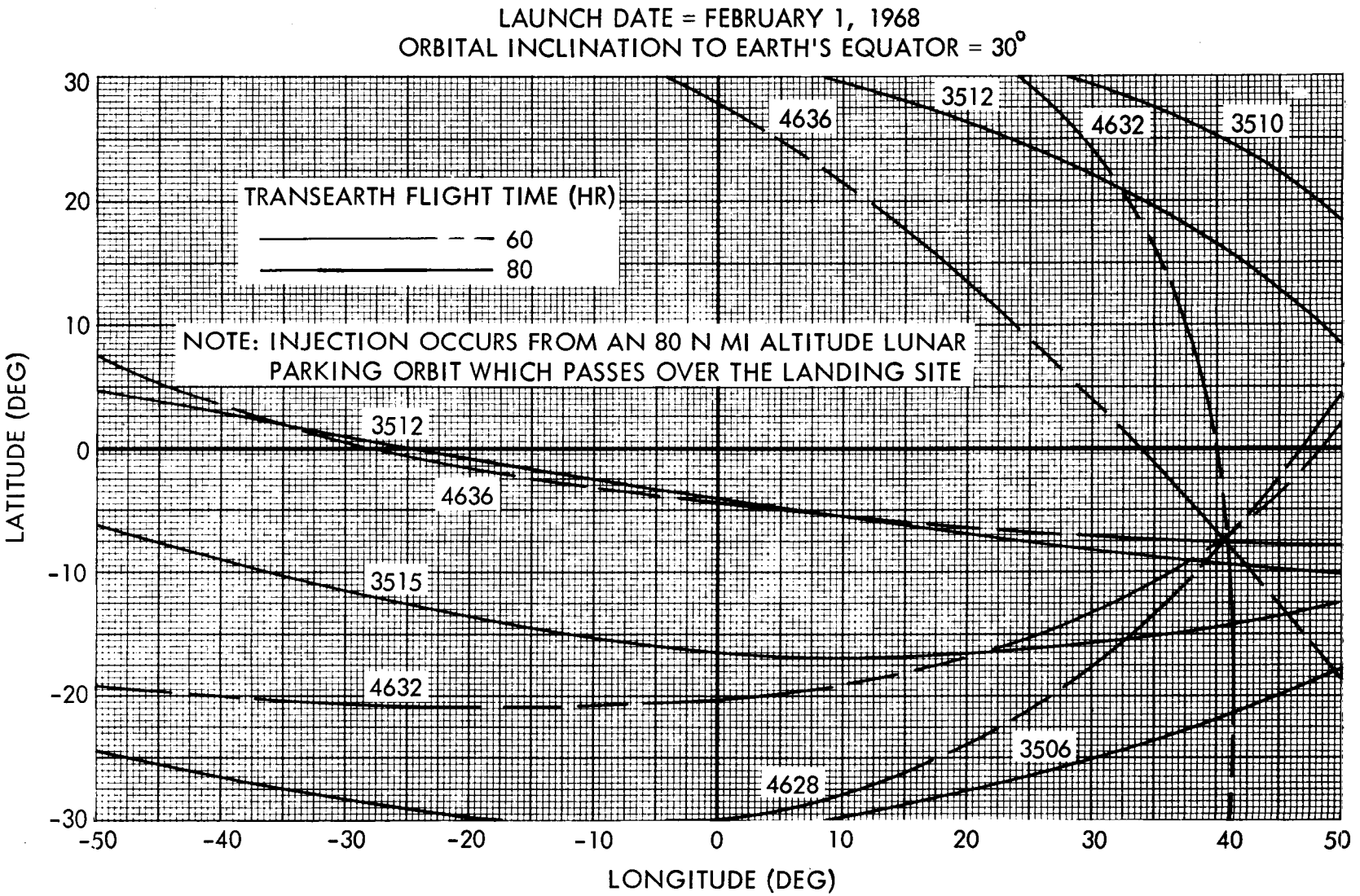

Figure 3.3-4. Variation in Transearth Hyperbolic Excess Velocity from the Moon with Lunar Landing Site

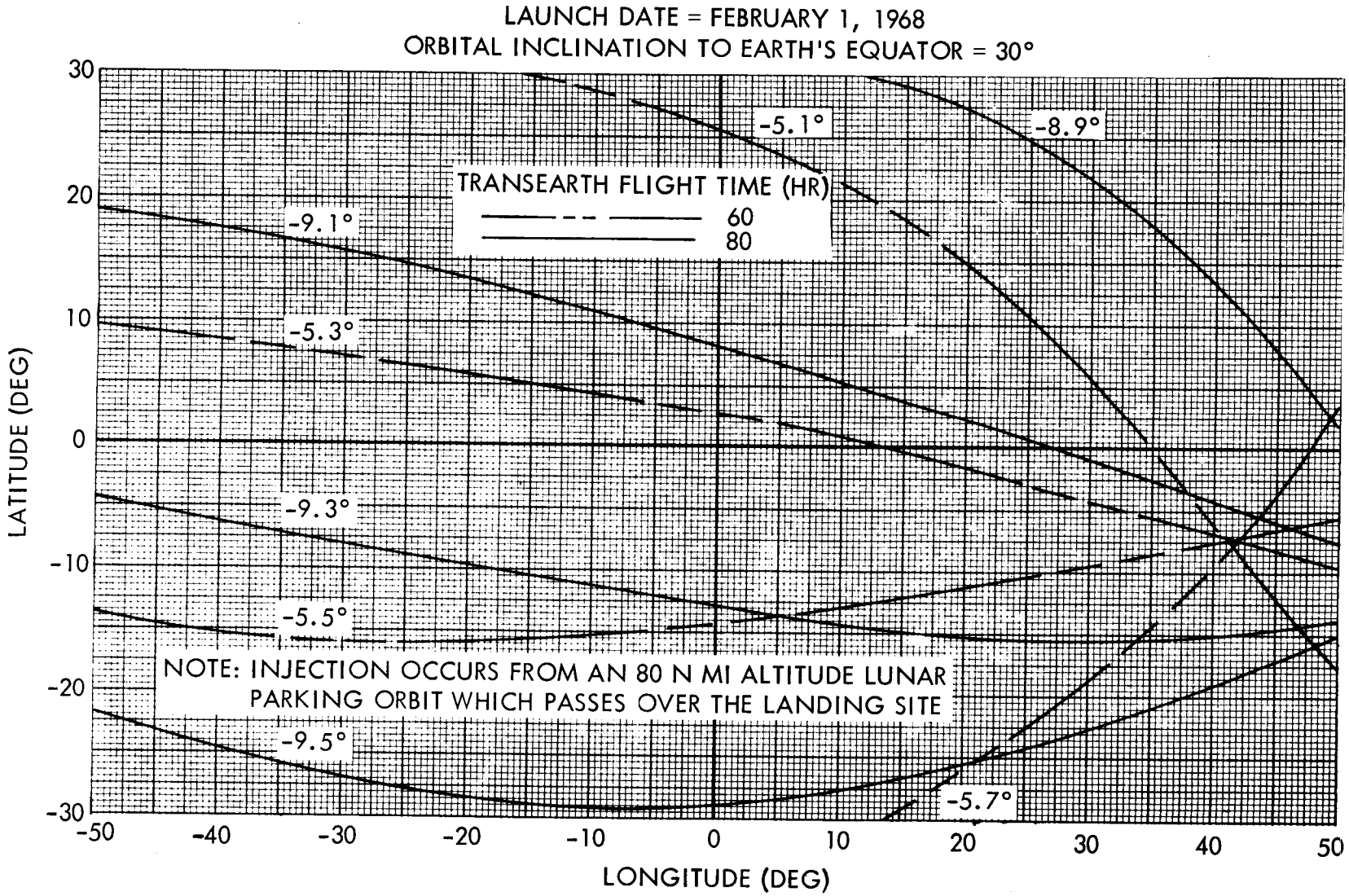

Figure 3.3-5. Variation in Selenographic Latitude of Velocity at Infinity with Lunar Landing Site

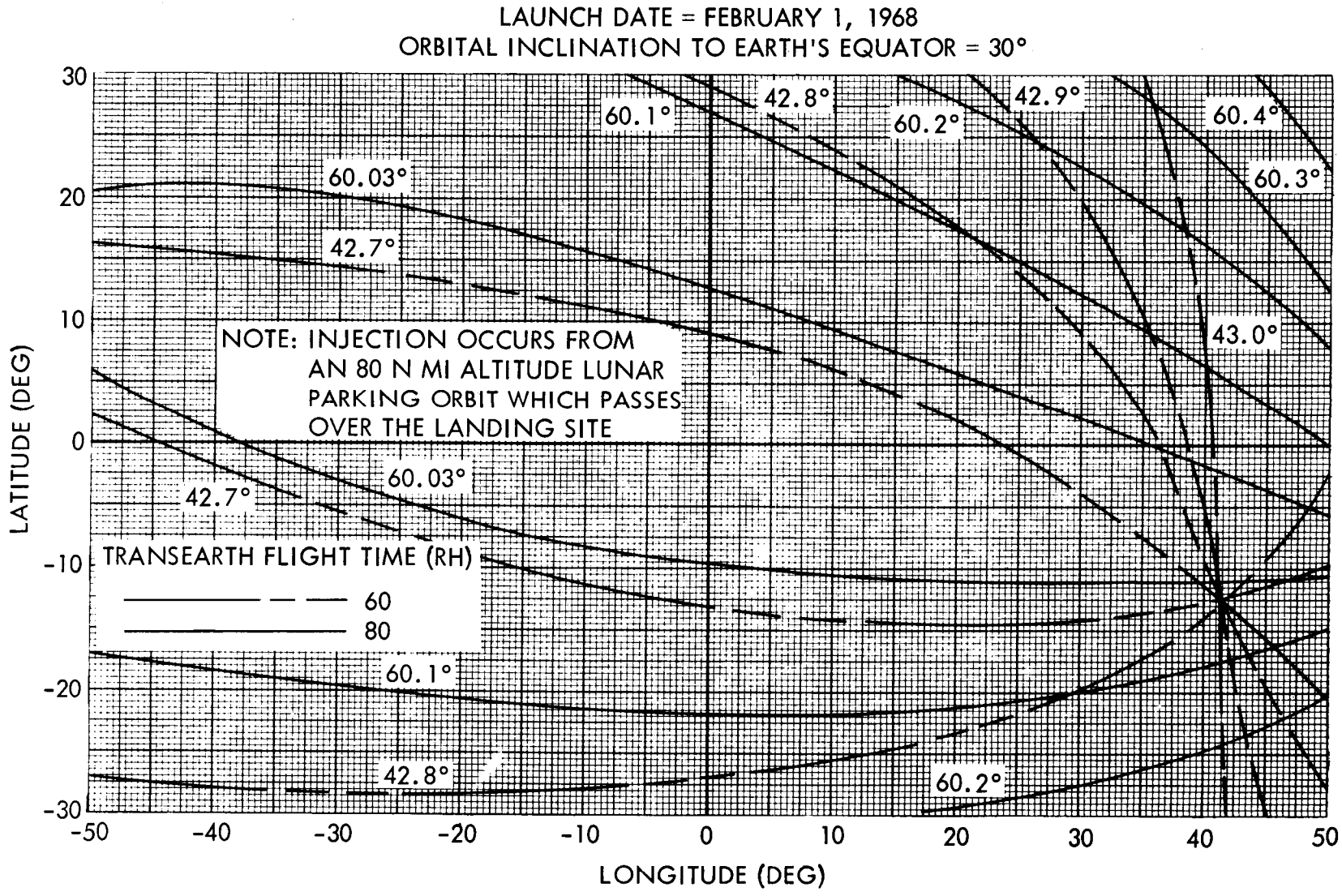

Figure 3.3-6. Variation in Selenographic Longitude of Velocity Vector at Infinity with Lunar Landing Site

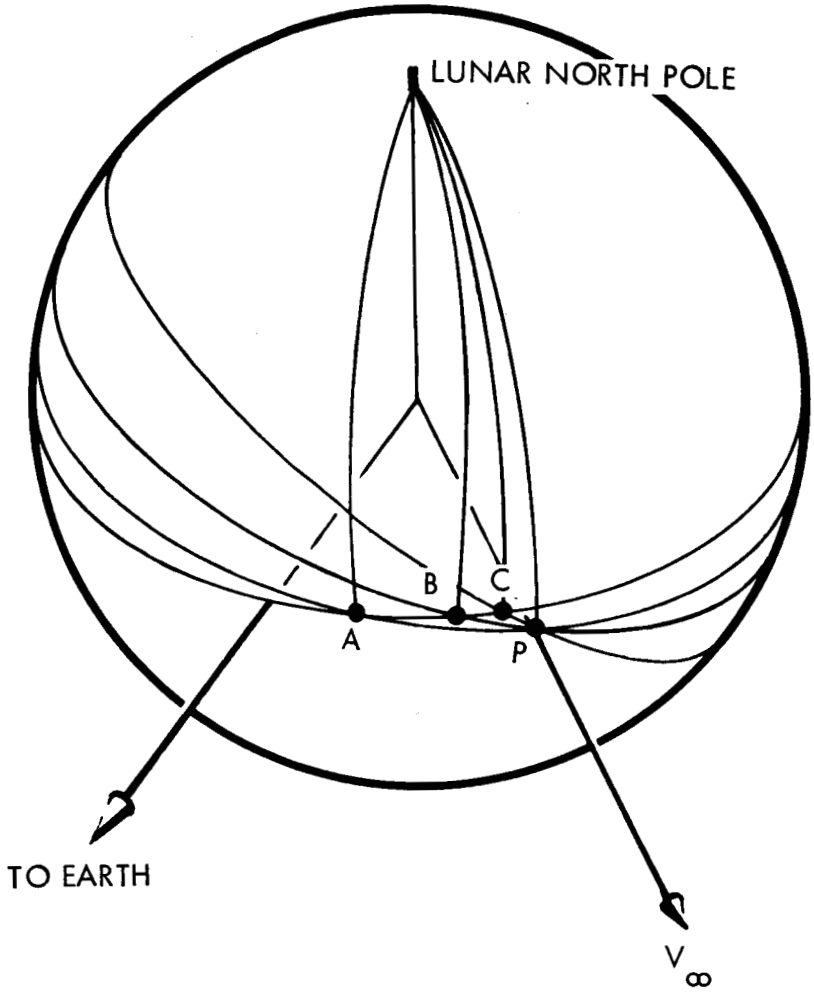

Figure 3.3-7. Variation in Orbit Inclination as the Landing Site Approaches the $\overline{V}_\infty$ Vector

velocity vector for transearth trajectories at an infinite distance from the moon will always be in the moon's eastern hemisphere for the type of trajectories considered. And for a given set of end conditions on return to earth, it has already been shown that the position of the $\overline{v}_\infty$ vector varies only minutely about a point (point P for instance). Thus regardless of the lunar site, the orbital plane must always contain this $\overline{v}_\infty$ vector. Therefore, as the base moves from point A to point C, the orbit plane simply rotates about the $\overline{v}_\infty$ vector. It can be seen that the inclination does decrease (in the sense that retrograde orbits are defined to have inclinations greater than 90°) as the site approaches the longitude of the $\overline{v}_\infty$ vector, reaching a minimum of 90° at the longitude of the $\overline{v}_\infty$ vector, and then increasing again for retrograde orbits as the site proceeds farther eastward past the longitude containing the $\overline{v}_\infty$ vector.

As may be expected, the effect of lunar site on reentry maneuver angle is small. The maximum variation in this angle for a given return flight time and orbital inclination to the earth's equator was less than 2 degrees for the range of lunar landing sites considered.

The lunar parking orbit altitude has already been shown to have only negligible effects on the $\overline{v}_\infty$ vector relative to the moon for translunar trajectories. Since transearth trajectories are essentially symmetric with translunar trajectories, the effect of lunar parking orbit altitude on the $\overline{v}_\infty$ vector will be correspondingly small for transearth trajectories.

A cursory analysis was also performed to determine the effects of the transearth geocentric orbit inclination and earth landing site on the $\overline{v}_\infty$ vector. Orbit inclination of 40 and 32 degrees and earth landing sites at San Antonio, Texas and Woomera, Australia were used. Every other day for a complete lunar month was chosen and a transearth flight time of 80 hours was assumed. Figure 3.3-8, which presents this information, indicates that the transearth orbit inclination has only a small (but significant) effect on the position of the $\overline{v}_\infty$ vector. The maximum difference in the position of this vector for the period of time shown is approximately 2.5 degrees, which seems too large for elimination of the transearth orbit inclination as a variable without further consideration. It can also readily

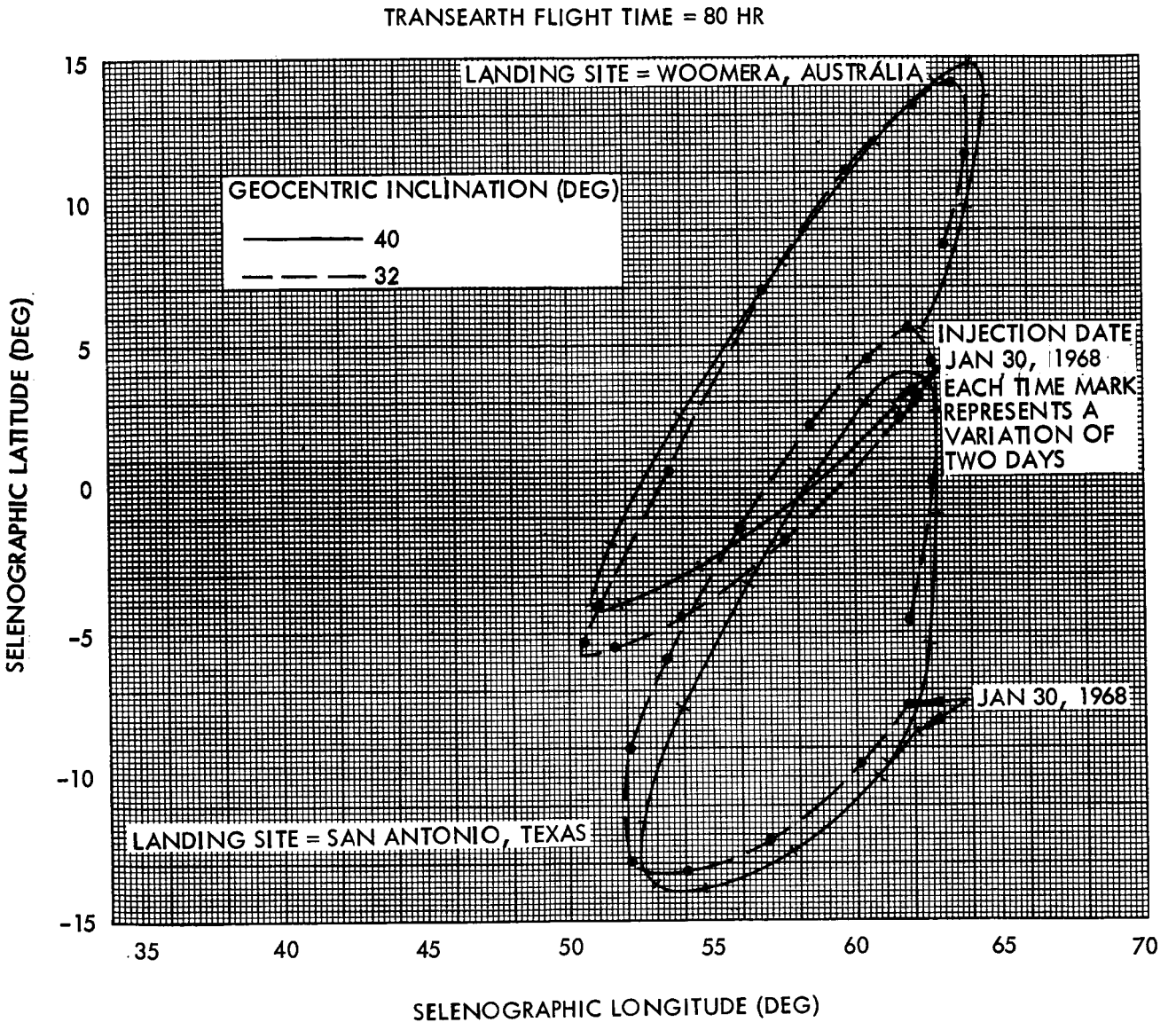

Figure 3.3-8. Variation in Position of Transearth Hyperbolic Excess Velocity Vector (Relative to the Moon) with Transearth Injection Date

be seen that the difference in the position of the $\overline{v}_\infty$ vector for the two earth landing sites is fairly large, and thus will also require that possibly both earth landing sites be used in a parametric study.

Figure 3.3-9 illustrates the effects of transearth flight time and injection date on the position of the $\overline{v}_\infty$ vector. As noted, the band of latitudes for the time shown is essentially the same for the range of flight times considered and varies at most by 5 degrees. The band of longitudes, however, is considerably shifted for a change in flight time. As one would expect, the shorter flight times move the longitude of the $\overline{v}_\infty$ vector towards the zero meridian.

Presented in Figures 3.3-10 and 3.3-11 are the variations in the reentry maneuver angle and in the $\overline{v}_\infty$ vector relative to the variation in the transearth injection date. The curves are not continuous since there is only one injection opportunity for an 80-hour flight time approximately every 25 hours. Also shown on Figure 3.3-11 are the days when return to one of the two landing sites is considered impossible because the reentry maneuver angle requirement exceeds the upper limit of 100 degrees. Thus, it will not always be possible to return to the site requiring the least amount of injection velocity at the moon. Also, it seems possible that for the longer flight times there may be some days throughout the year when the earth-moon geometry is such that the reentry angle would be exceeded for both landing sites.

The magnitude and position of the $\overline{v}_\infty$ vector for transearth trajectories for use in the lunar operations analysis are shown in Figures 3.3-12 through 3.3-14. It should be pointed out that only the solid curves are continuous. Values do not exist between the solid curves. Thus, for any specific departure time of day at the moon, a return can be made by selecting any of two or possibly three $\overline{v}_\infty$ vectors (within the range of flight times being considered) which have flight times separated by approximately 24 hours. In this manner, flight time is used to allow the earth landing site to rotate into successive proper positions. Conversely, with a fixed flight time, intervals of approximately 25 hours must elapse between each successive permissible lunar departure.

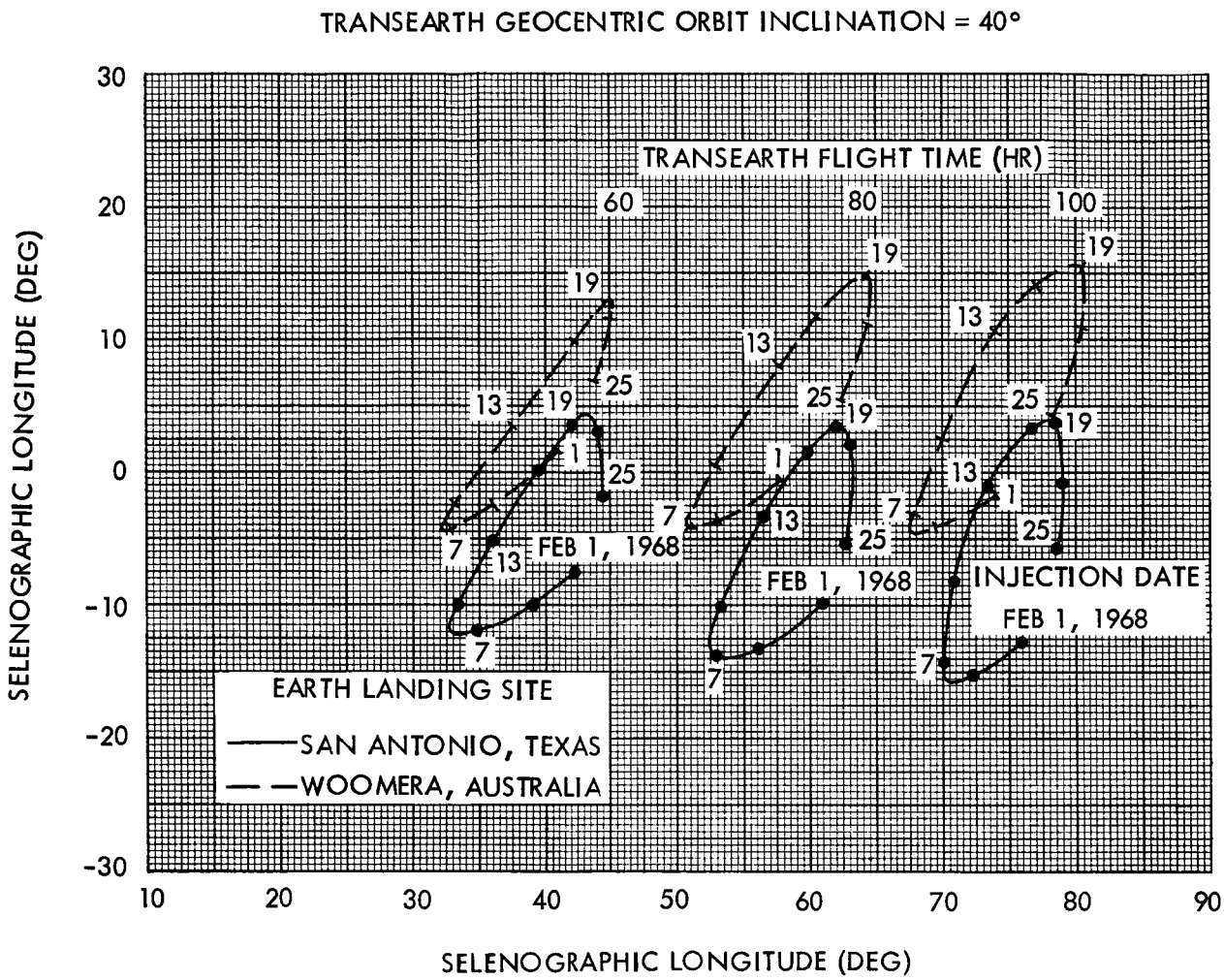

Figure 3.3-9. Effect of Transearth Flight Time and Injection Date on Position of Transearth Hyperbolic Excess Velocity Vector

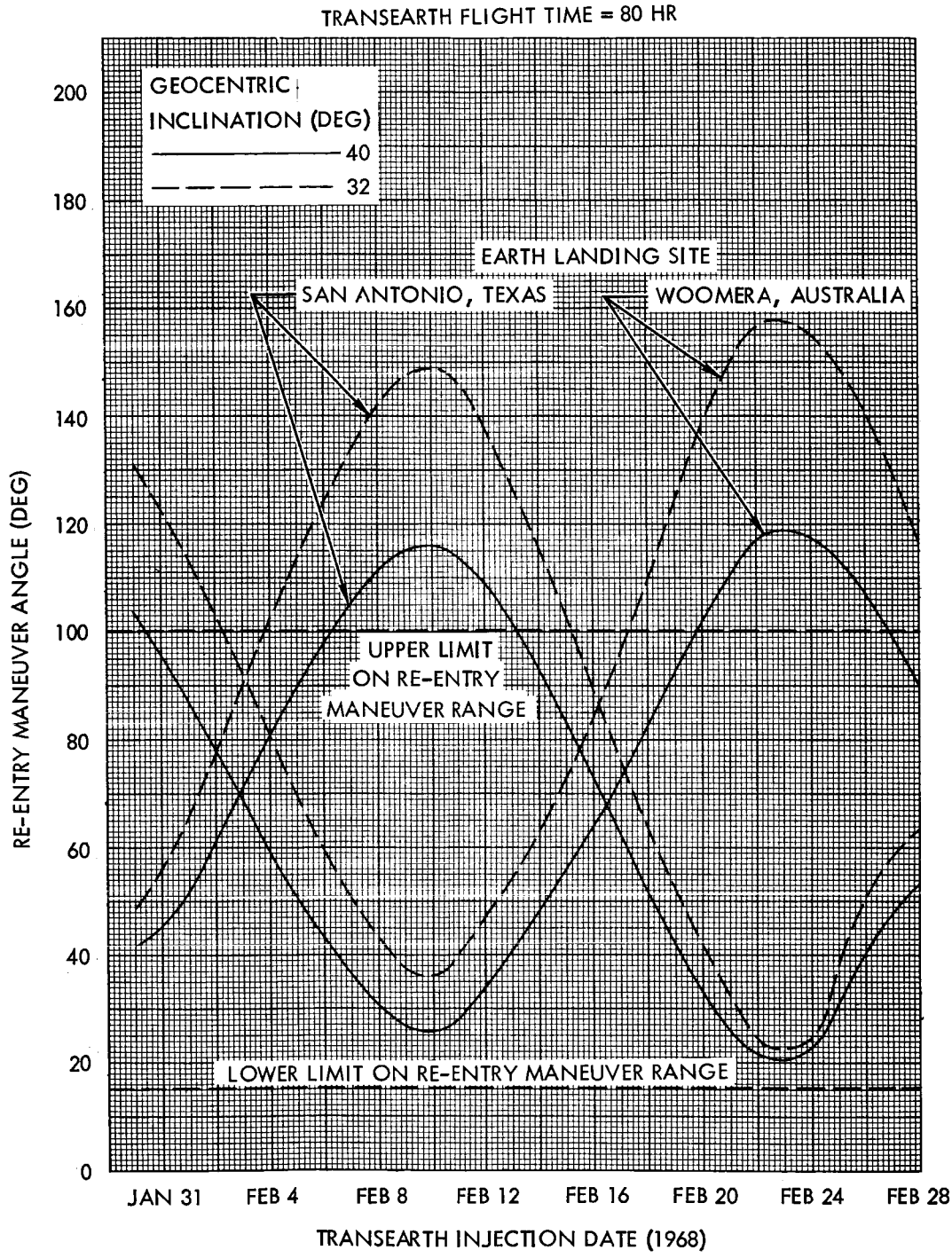

Figure 3.3-10. Variation in Reentry Maneuver Angle with Transearth Injection Date

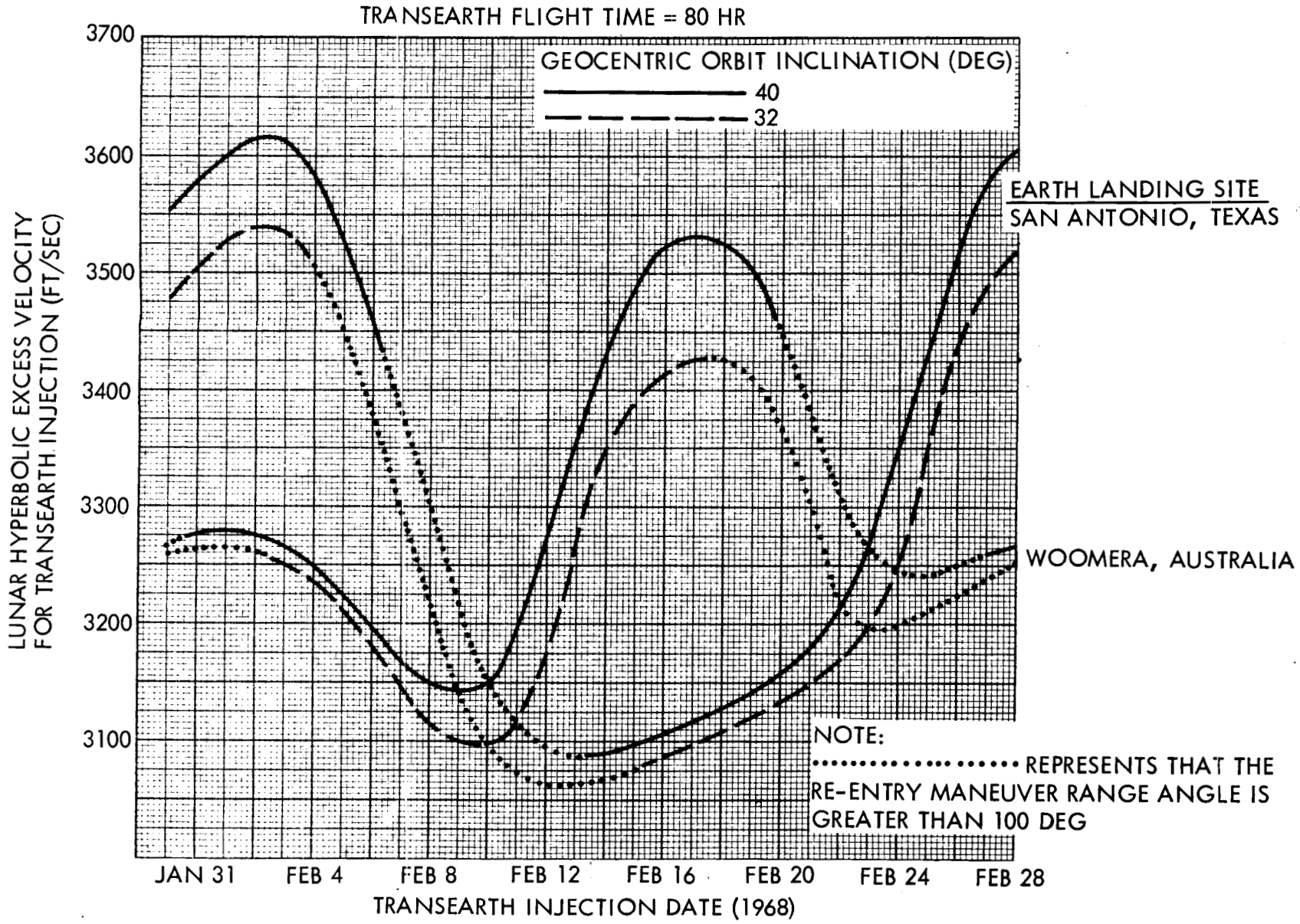

Figure 3.3-11. Variation in Hyperbolic Excess Velocity for Transearth Injection

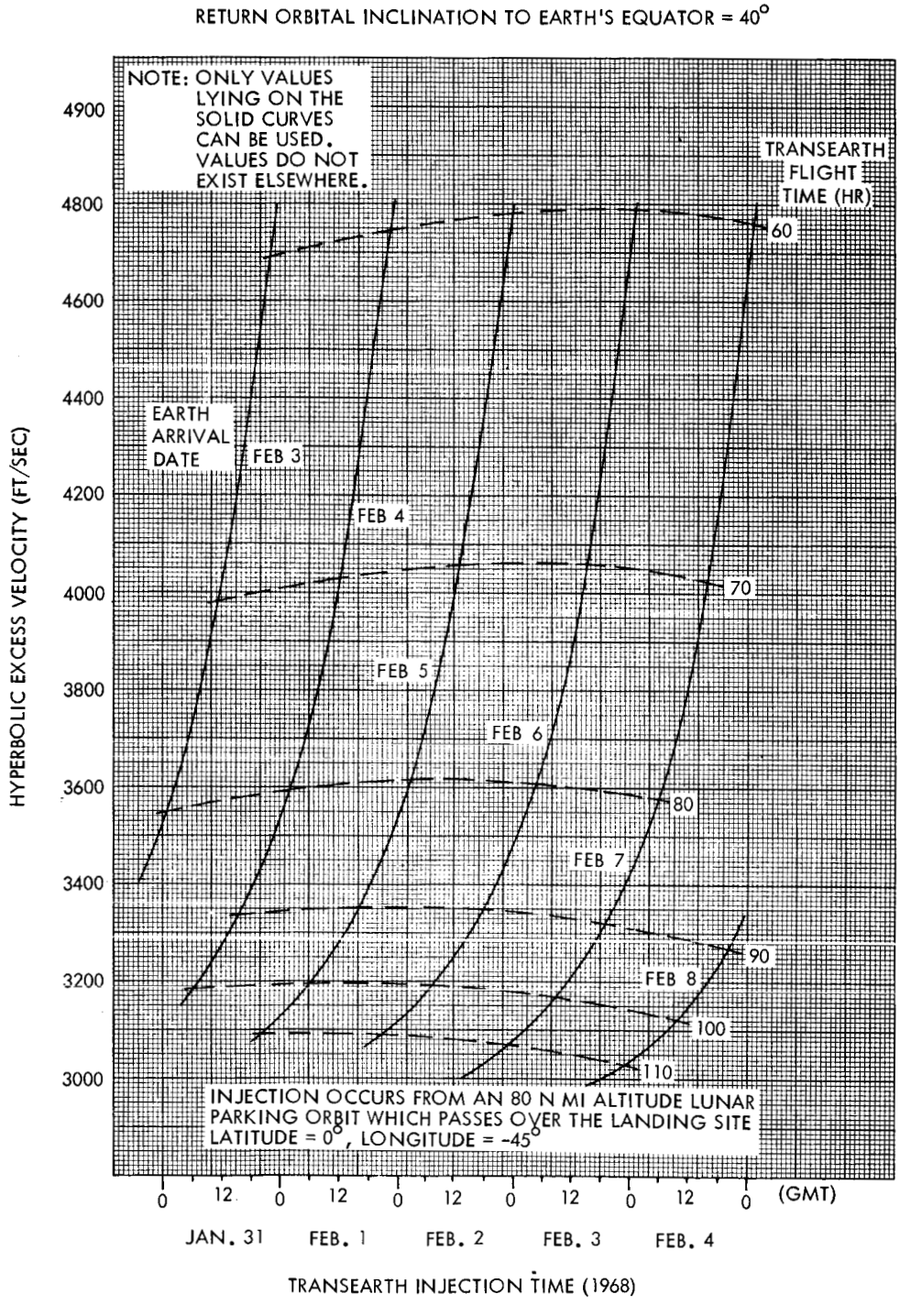

Figure 3.3-12. Hyperbolic Excess Velocity for Transearth Injection

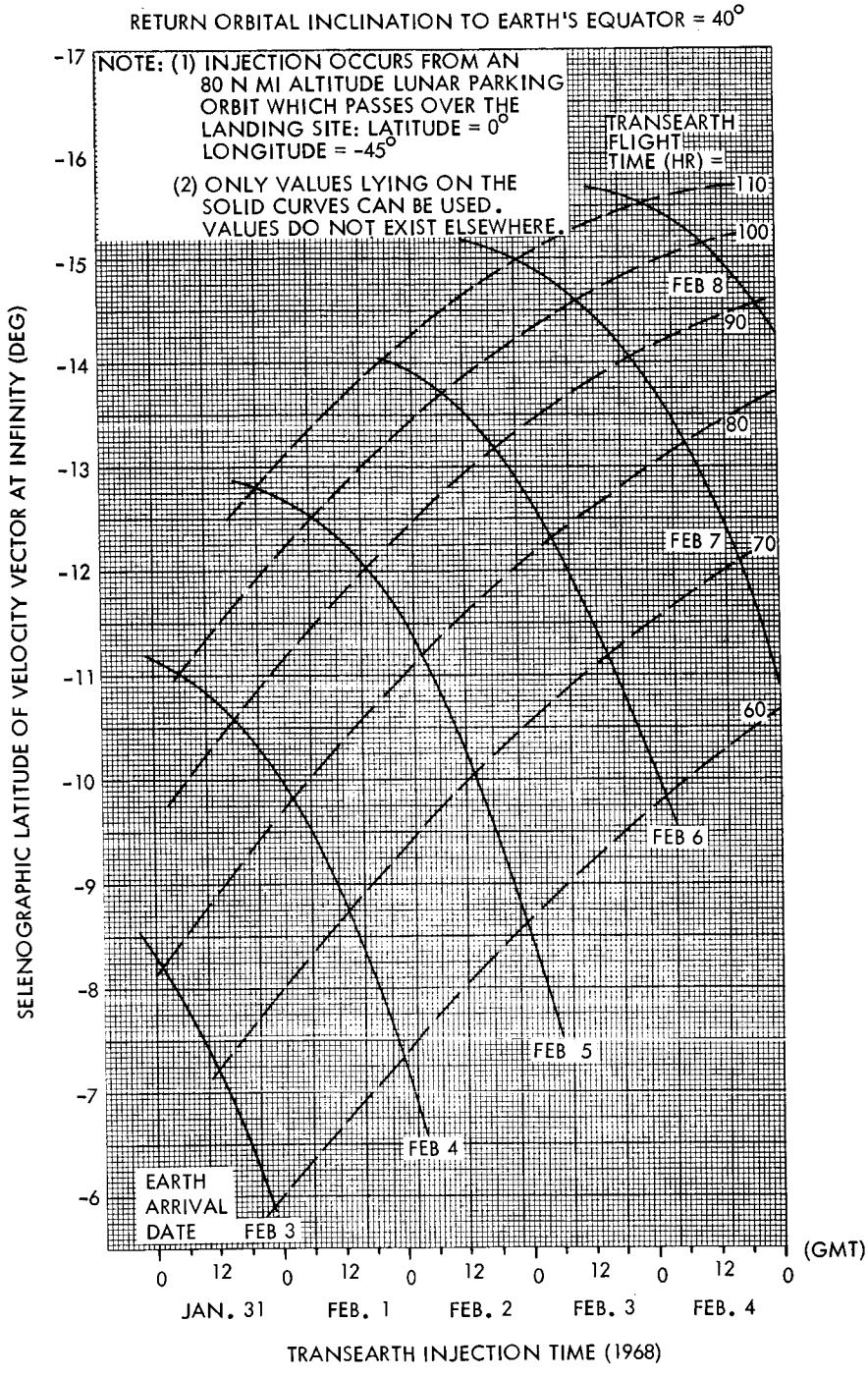

Figure 3.3-13. Selenographic Latitude of Velocity Vector at Infinity for Transearth Injection

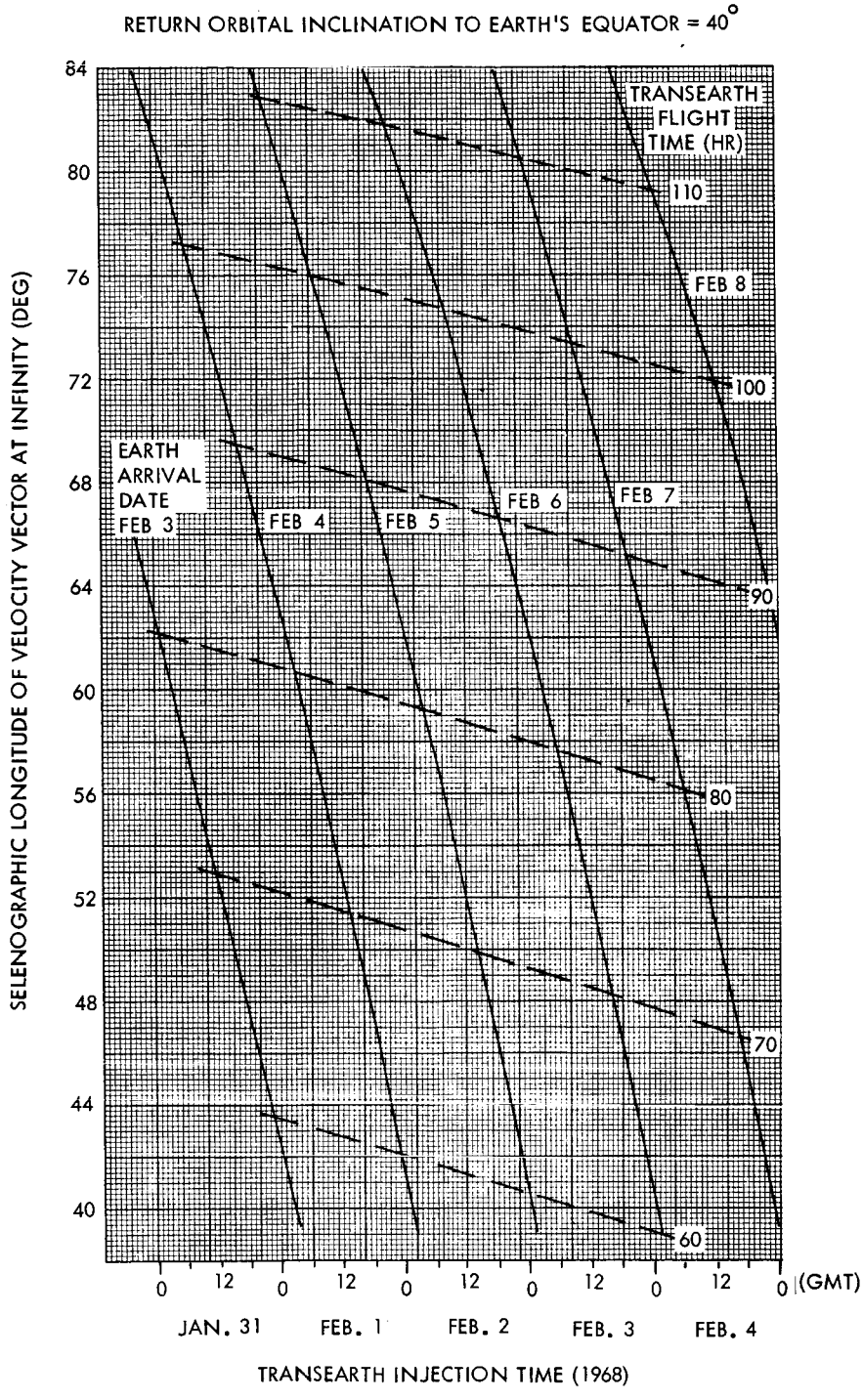

Figure 3.3-14. Selenographic Longitude of Velocity Vector at Infinity for Transearth Injection

Figure 3.3-15 helps in explaining the latter. For a given transearth flight time the in-plane angle traversed from the moon's sphere of action to the reentry point will essentially remain constant. Every sideral day results in the earth landing site having the same right ascension. However, during this time the moon has moved from point A to point B. In order to return to the same phase as the previous day for a launch opportunity, the earth must rotate an additional angle Δn. This argument carries over, approximately, to the actual three dimensional trajectory..

This interval of time between successive transearth injection opportunities is approximately equal to the synodic period of the earth landing site with respect to the moon. The combination of the changing position of the moon and the constrained transearth trajectory seem to be the main reason for the slight difference between successive transearth injection opportunities (for constant flight times) and the above mentioned synodic period.

Therefore, by allowing both the departure time and the flight time to vary, returns can be initiated approximately every two hours (the circular lunar orbit period). At the beginning of a launch opportunity interval, the flight time required is high and decreases with each following two-hour increment until the lower limit is reached. However, as soon as the flight time required has decreased by 24 hours, the cycle can be repeated with earth landing occurring one day later.

On the basis of the analysis of the parametric behavior of $\overline{V}_\infty$ with respect to the transearth trajectory variables, it may be concluded that the following parameters have a significant influence on the transearth hyperbola:

a) Day of return injection (i.e., distance and declination)

b) Flight time

c) Earth landing site

d) Trajectory inclination with respect to the earth's equator

The following variables are deemed to have, by comparison, a negligible effect:

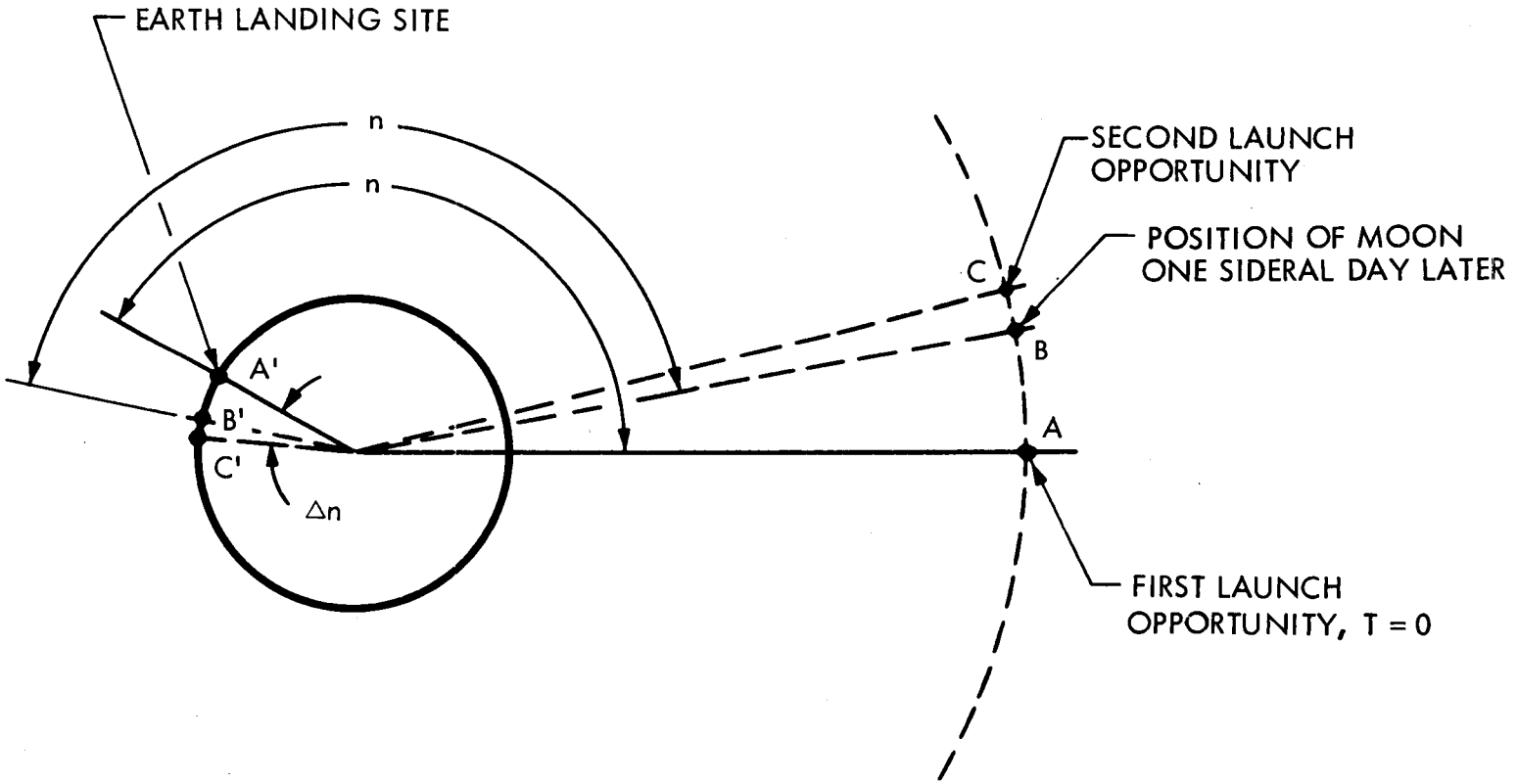

Figure 3.3-15. Phasing for Launch Opportunities for Constant Flight Time

e) Lunar landing site (i.e., selenographic inclination of the hyperbola)

f) Pericynthion altitude

3.4 Service Module Propellant Requirements

The analyses in the foregoing sections have indicated those mission parameters which need not be examined in the lunar operations phase over their full ranges of variation. This section of the report provides an exemplary analysis of the remaining parameters for one earth launch date January 28, 1968. The results are presented as contours of Service Module propellant requirements over the range of landing sites requested. The propellant requirement, for each landing site and set of mission parameters, is optimized with respect to the azimuth of approach to the landing site and the pericynthion altitudes of the hyperbolic approach and departure conics. In addition, those landing sites for which the stay time is restricted by the LEM ascent plane change limitation of 4 degrees, are indicated on the contours for one translunar flight time.

The computation of total Service Module propellant weight required for each combination of mission parameters is based on the characteristic velocity requirements of the deboost and transearth injection maneuvers. These characteristic velocity requirements are determined impulsively by vector subtractions of the velocities on the hyperbolic approach and departure conics and the circular orbit velocity at their points of intersection. The propellant weight requirement for each maneuver is computed by use of the rocket equation. Assuming a fixed weight injected to the moon the propellant requirement for the deboost maneuver is computed first, using the velocity impulse from the above subtraction and 300 ft/sec for translunar midcourse corrections. The LEM weight is then subtracted from the burnout weight at deboost to establish the initial weight for the transearth injection. A midcourse allowance of 300 ft/sec is added to the transearth injection velocity impulse for the propellant weight computation of the second Service Module maneuver. Thus, the total propellant requirement for each set of mission parameters includes the necessary allowances for midcourse corrections. The spacecraft data used in the computations are as follows:

Weight Injected to the Moon	86,000 lbm
LEM Weight	26,500 lbm
Service Module Specific Impulse	323 sec

A complete analysis of Service Module performance was made for two sets of Group 1 mission parameters with an earth landing site at San Antonio and a return inclination of 40 degrees. The first set of Group 1 parameters consist of the following:

a) Earth Launch Date - 28 January 1968

b) Earth Parking Orbit Coast - Type 6

c) Translunar Flight Time - 80 hours

A typical graph indicating the variation of minimum Service Module propellant requirement with lunar orbit stay time is presented in Figure 3.4-1, for the above set of Group 1 parameters. For this figure, the lunar landing site is at 30 degrees latitude and -45 degrees longitude. It can be seen that the propellant requirement on each earth landing date increases with lunar orbit stay time. This variation reflects the effect, discussed in the last section, of the decreasing transearth flight time at later injection opportunities. For the later earth landing dates, and therefore longer total mission times, the propellant requirement decreases at a constant return flight time. This variation indicates that the more easterly shift of the transearth $\overline{v}_\infty$ vector, at the longer lunar orbit stay times, produces a more favorable geometry of the vectors relative to the landing site. Figures 3.4-2 through 3.4-23 provide similar data for additional landing sites at latitudes of 30, 15, 0, -15, and -30 degrees.

It is worthwhile at this point to examine the locations of the $\overline{v}_\infty$ vectors for all of the injection opportunities associated with the above set of Group 1 parameters. The data presented in Section 3.3 show that the latitudes of the transearth $\overline{v}_\infty$ vectors fall in the southern hemisphere between a range of -6 and -16 degrees, and the longitudes vary between 40 and 85 degrees. The translunar $\overline{v}_\infty$ vector is located at -6.2 degrees latitude and -53.2 degrees longitude (Section 3.2). Thus, the difference in longitude between the translunar and transearth $\overline{v}_\infty$ vectors, including

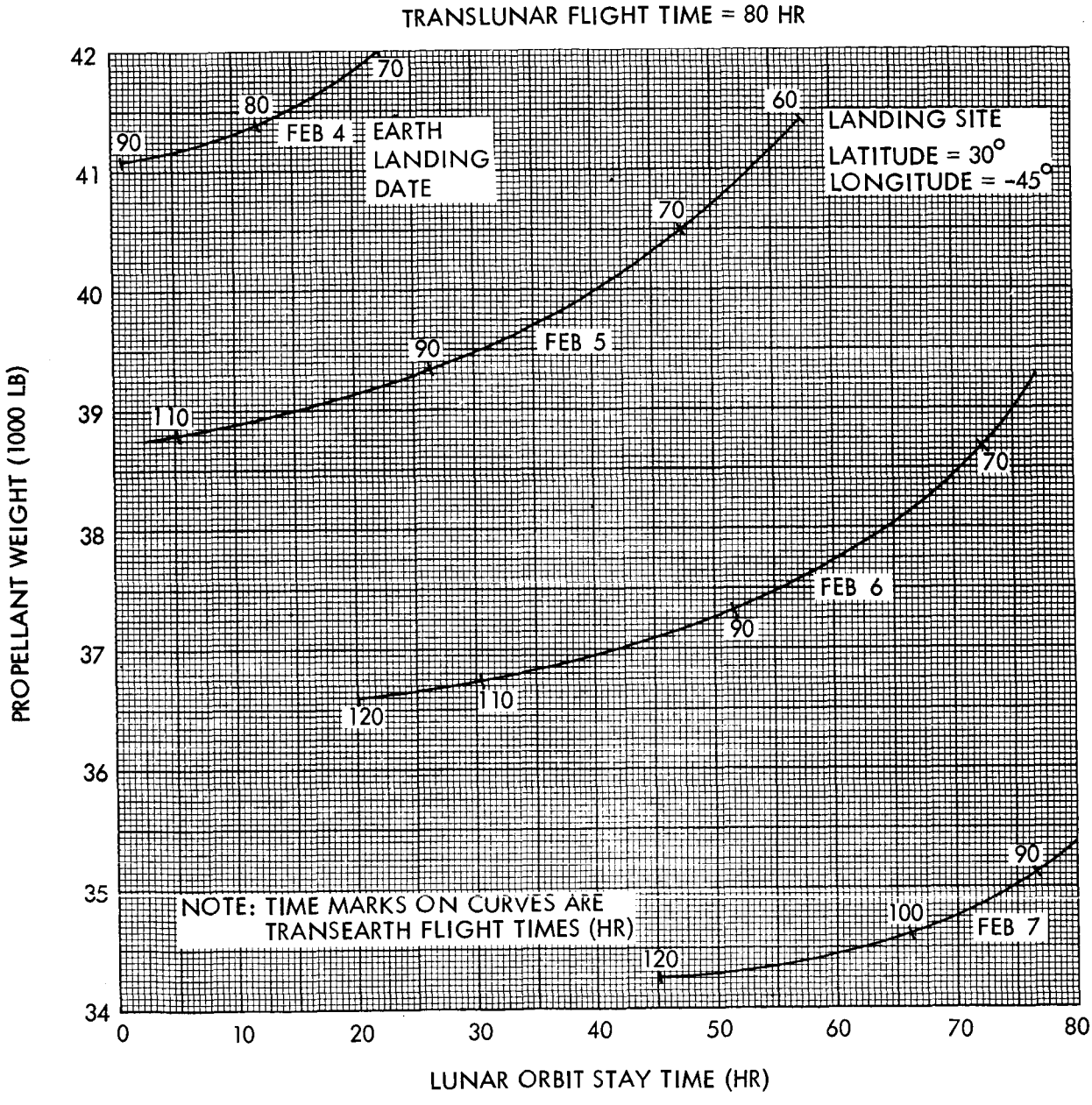

Figure 3.4-1. Propellant Weight Variations versus Lunar Orbit Stay Time and Total Mission Time

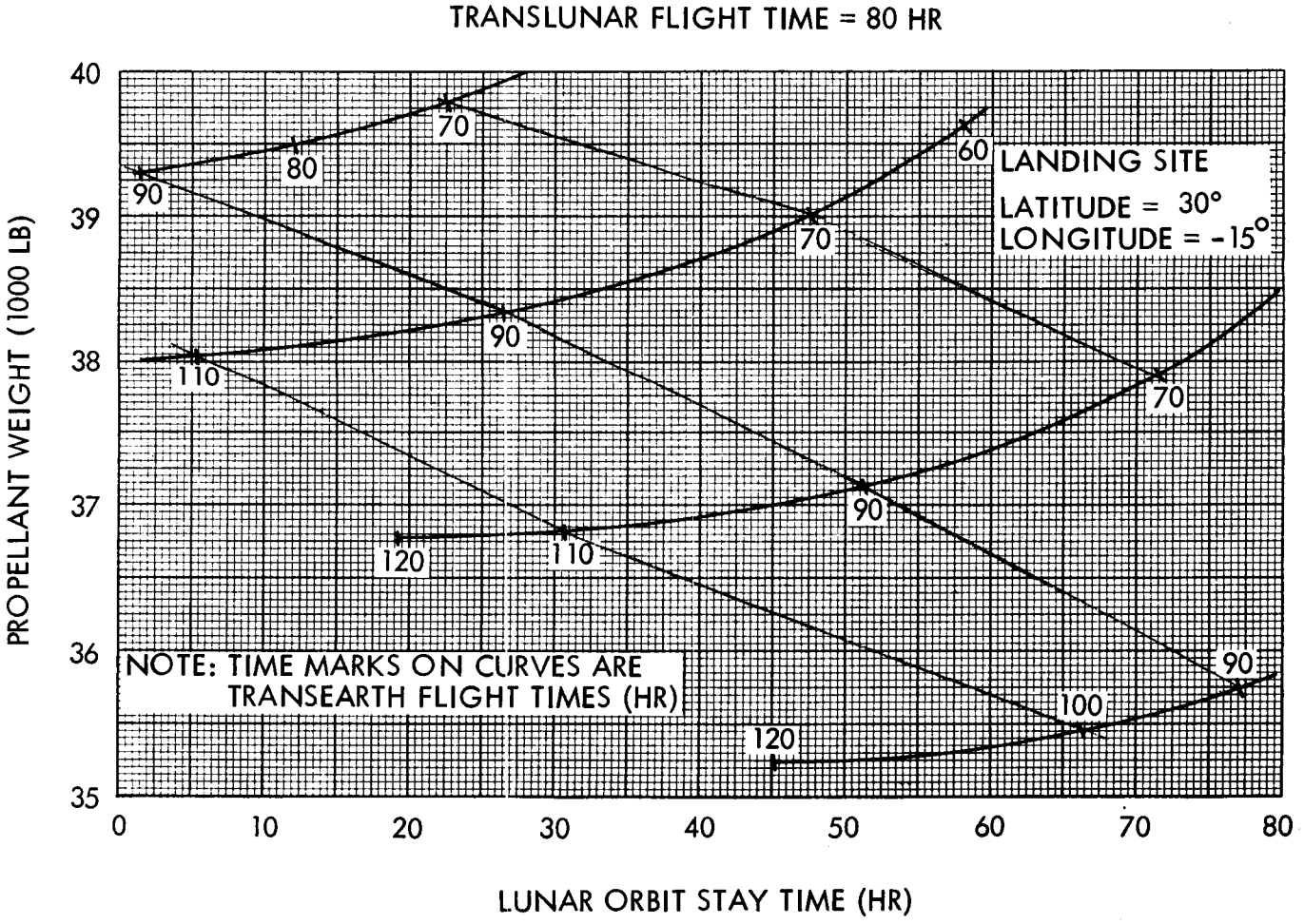

Figure 3.4-2. Propellant Weight Variations versus Lunar Orbit Stay Time and Total Mission Time

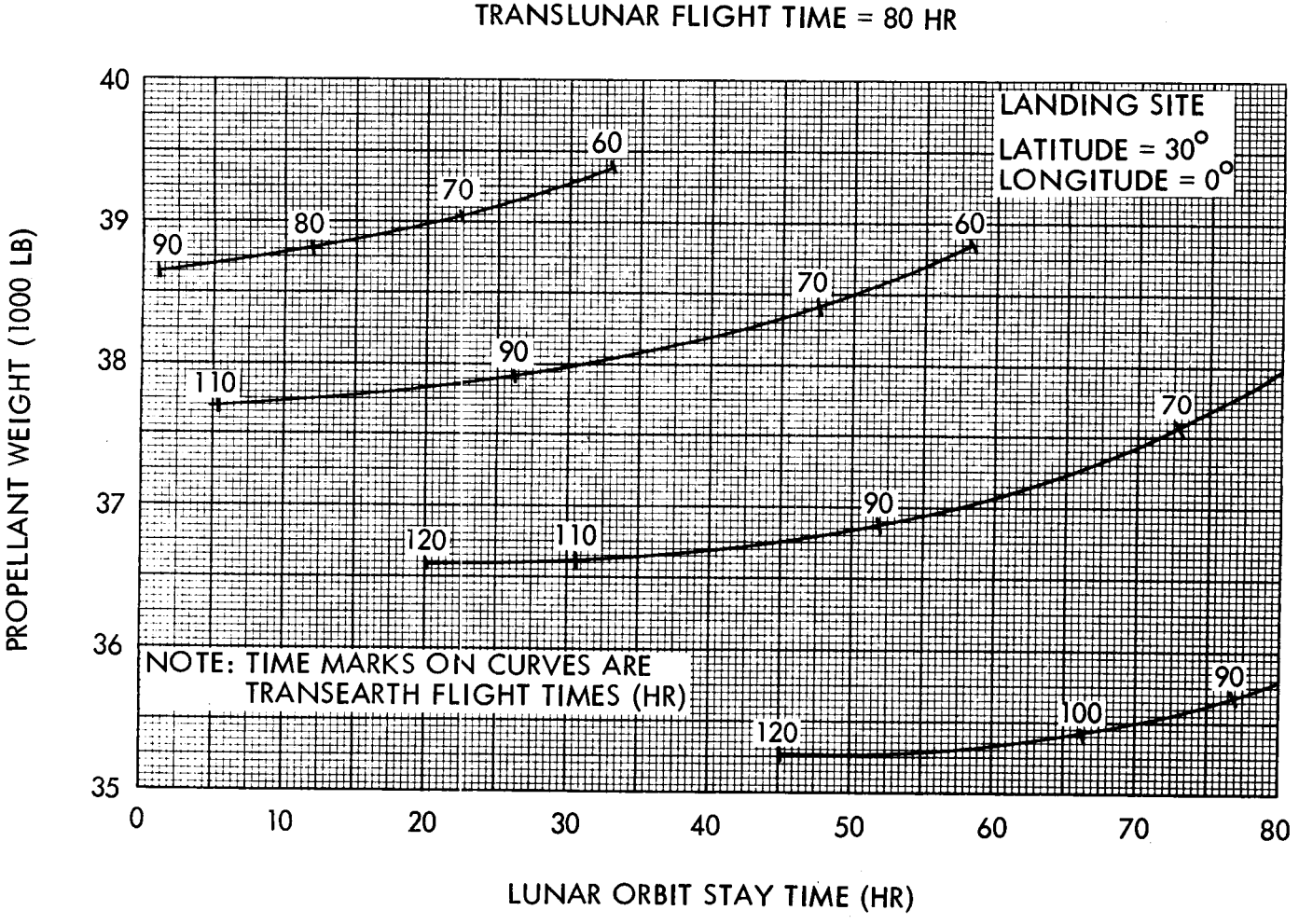

Figure 3.4-3. Propellant Weight Variations versus Lunar Orbit Stay Time and Total Mission Time

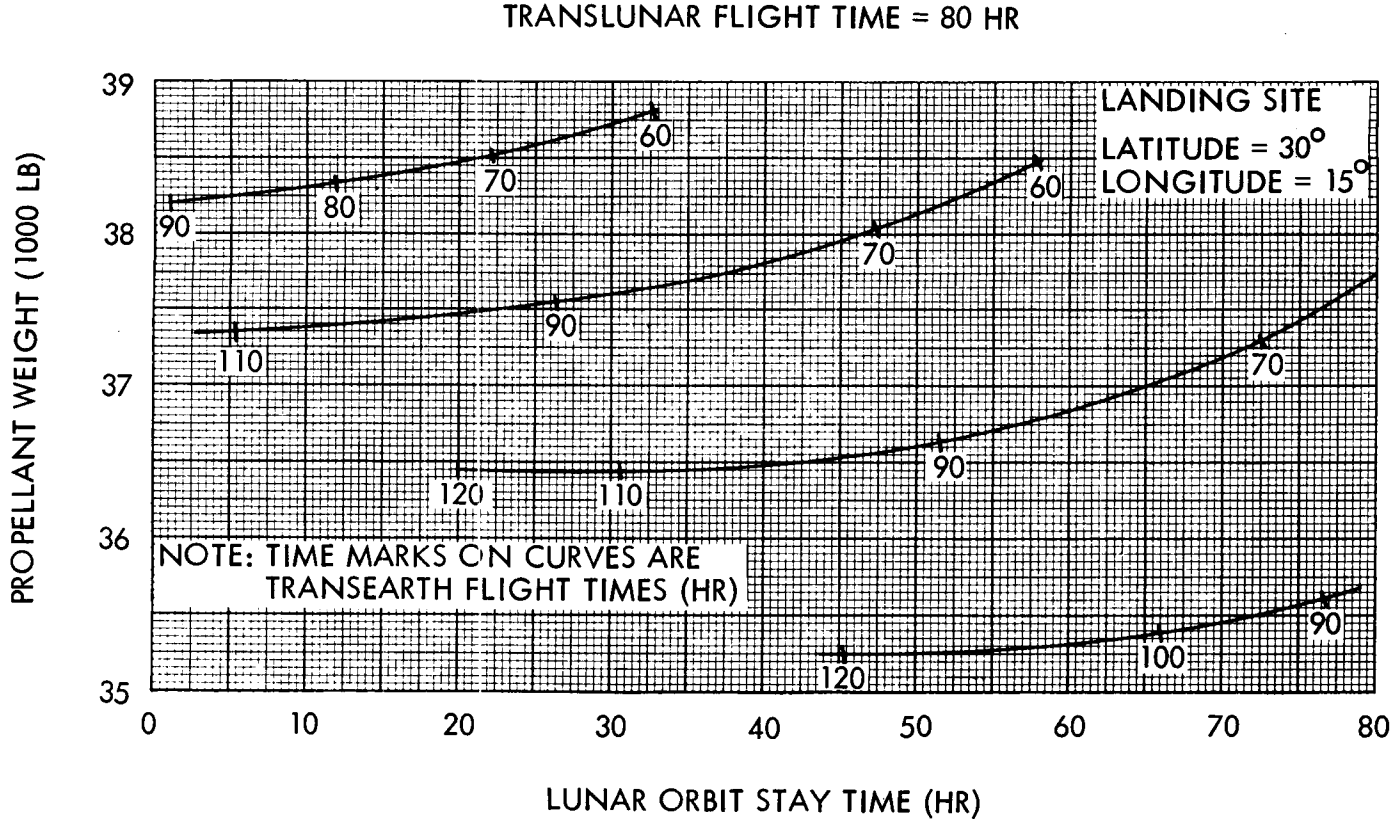

Figure 3.4-4. Propellant Weight Variations versus Lunar Orbit Stay Time and Total Mission Time

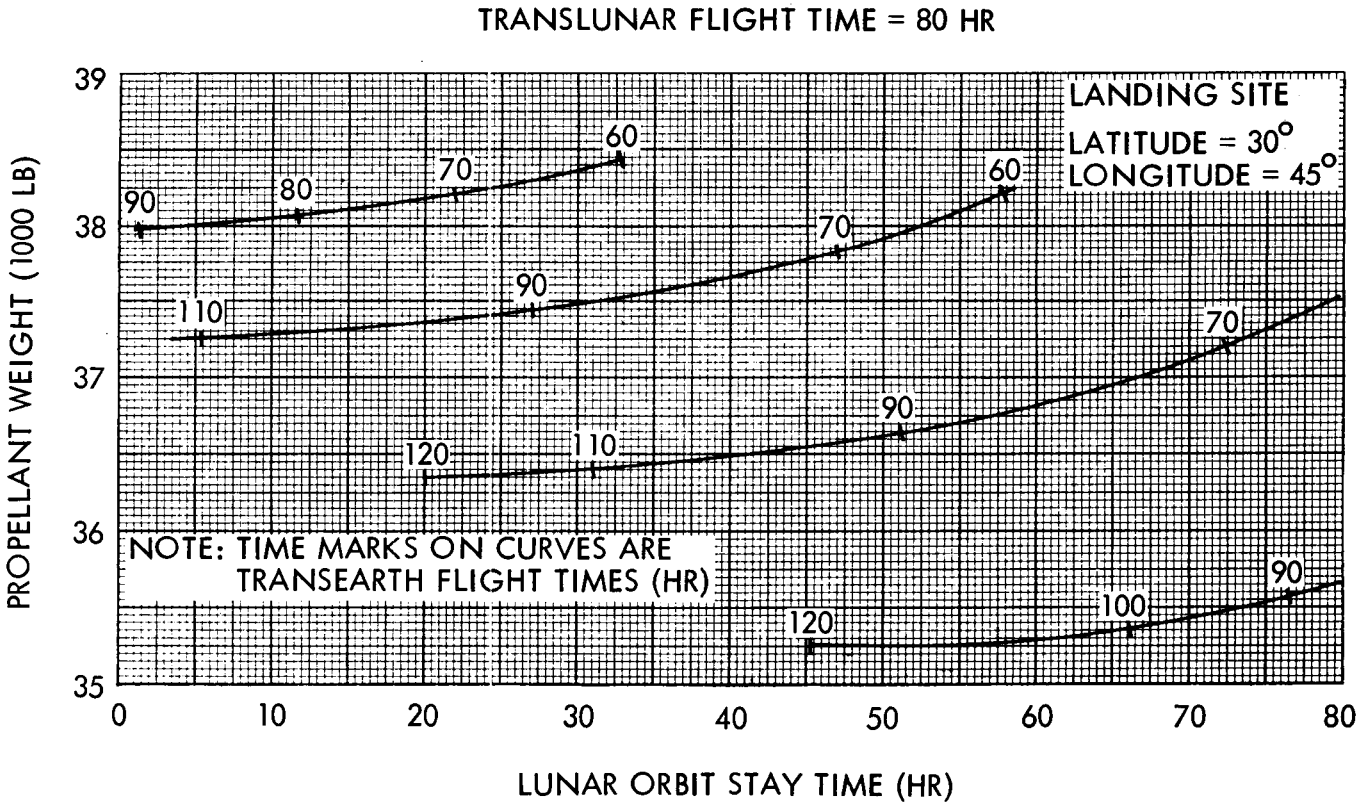

Figure 3.4-5. Propellant Weight Variations versus Lunar Orbit Stay Time and Total Mission Time

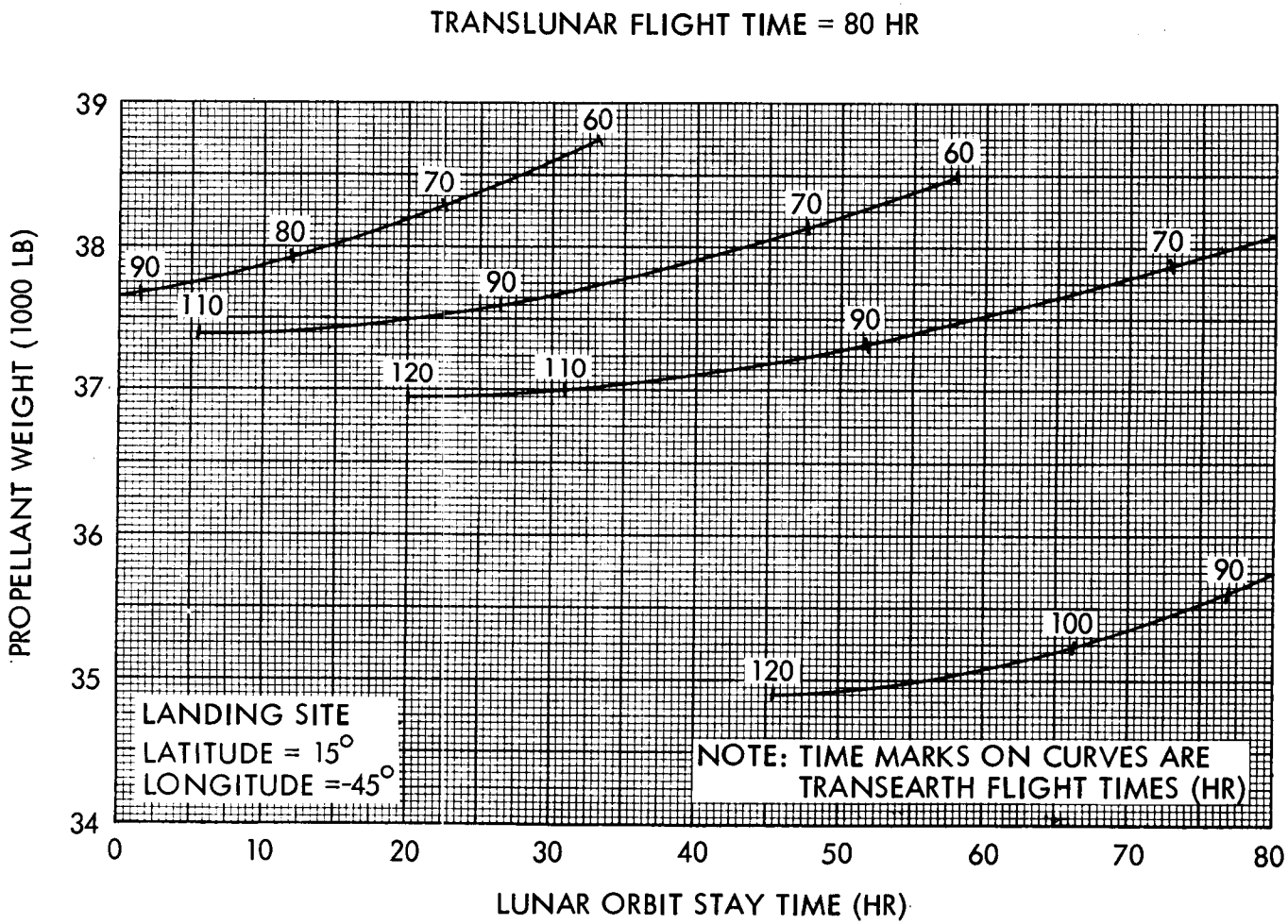

Figure 3.4-6. Propellant Weight Variations versus Lunar Orbit Stay Time and Total Mission Time

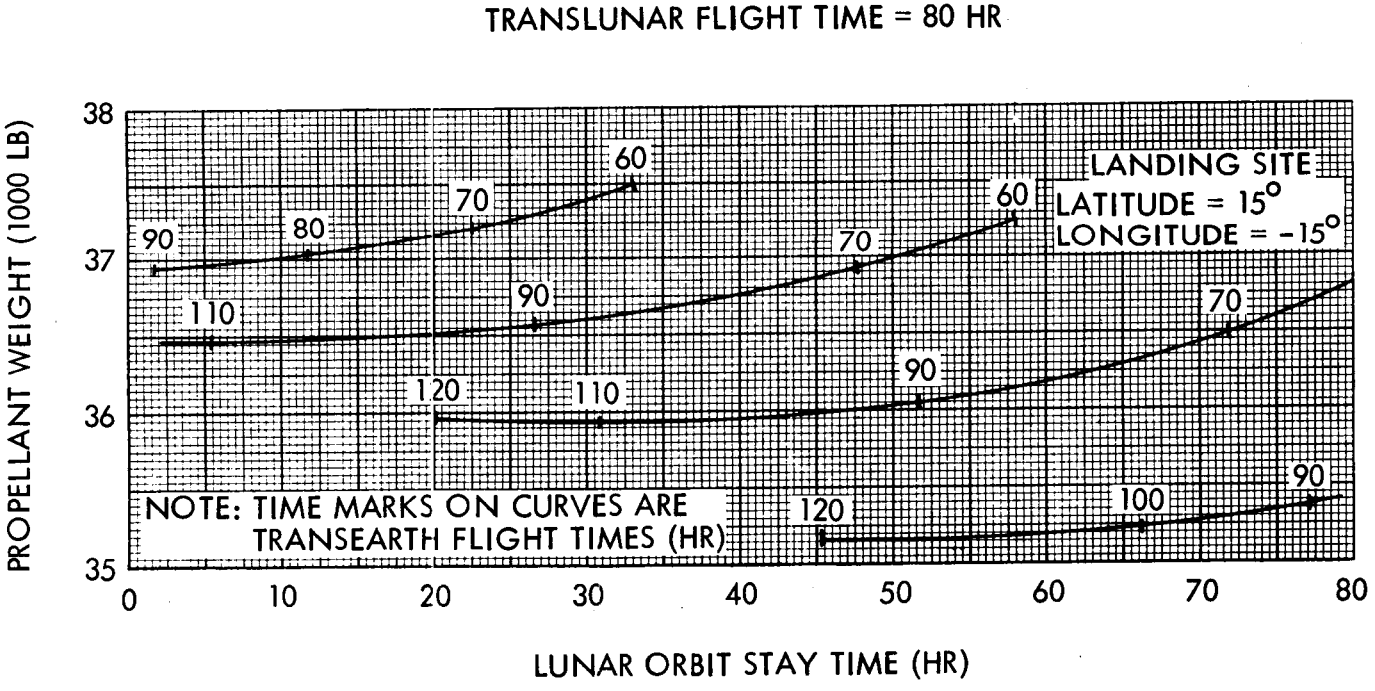

Figure 3.4-7. Propellant Weight Variations versus Lunar Orbit Stay Time and Total Mission Time

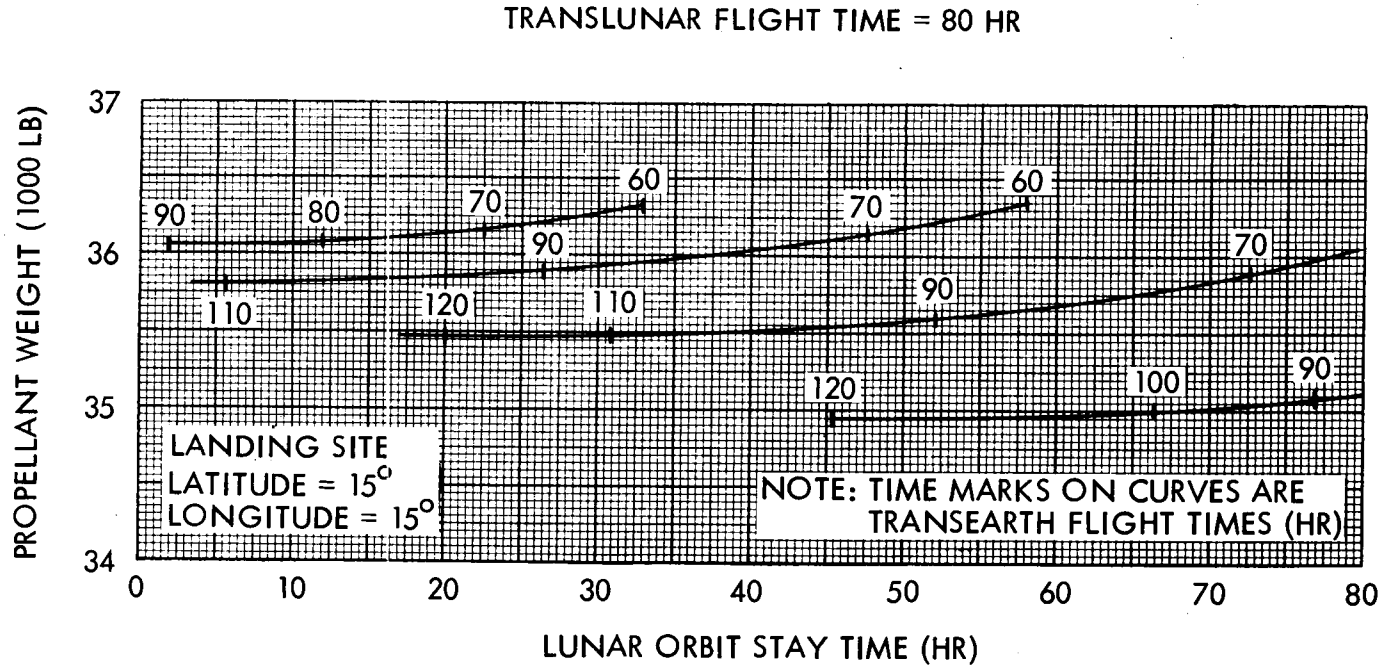

Figure 3:4-8. Propellant Weight Variations versus Lunar Orbit Stay Time and Total Mission Time

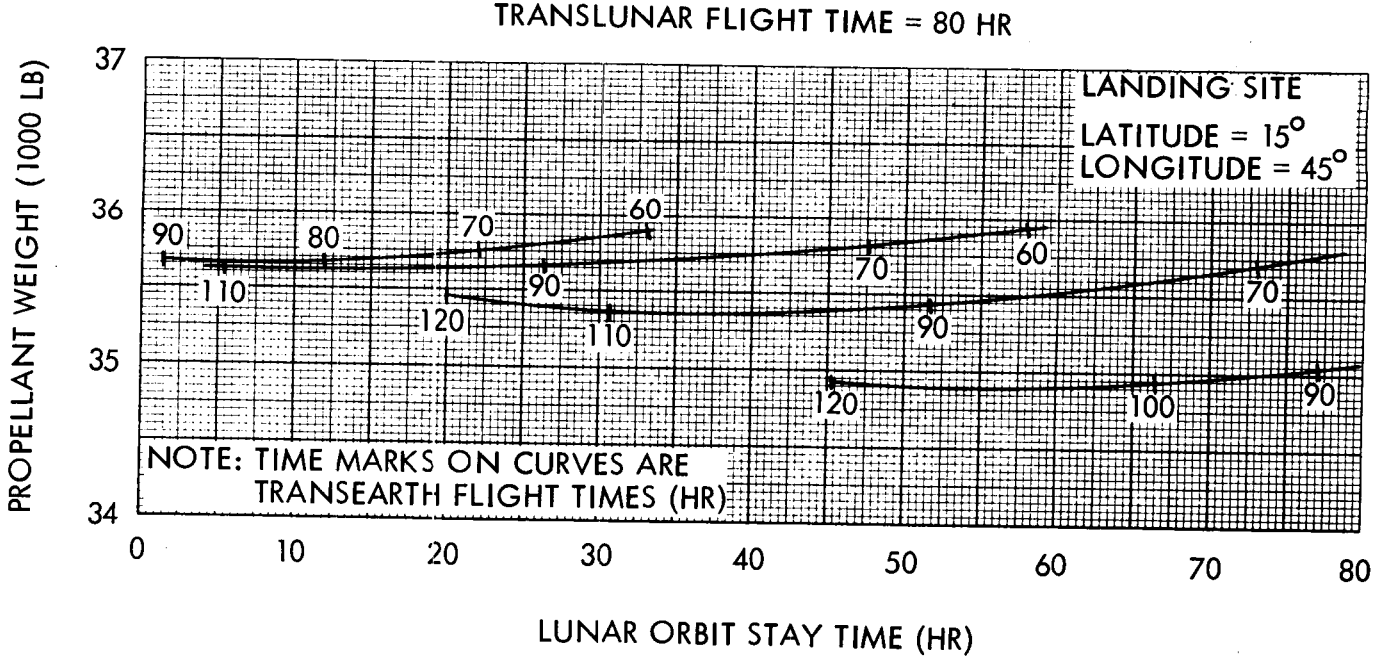

Figure 3.4 9. Propellant Weight Variations versus Lunar Orbit Stay Time and Total Mission Time

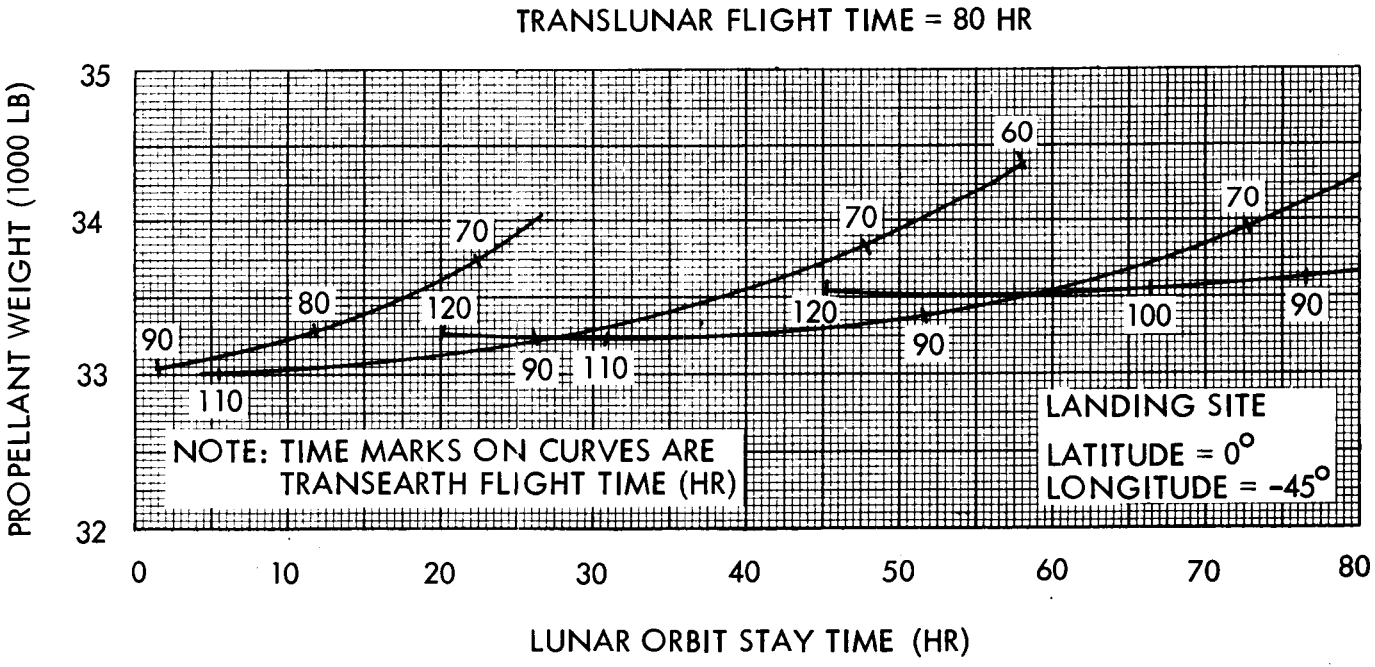

Figure 3.4-10. Propellant Weight Variations versus Lunar Orbit Stay Time and Total Mission Time

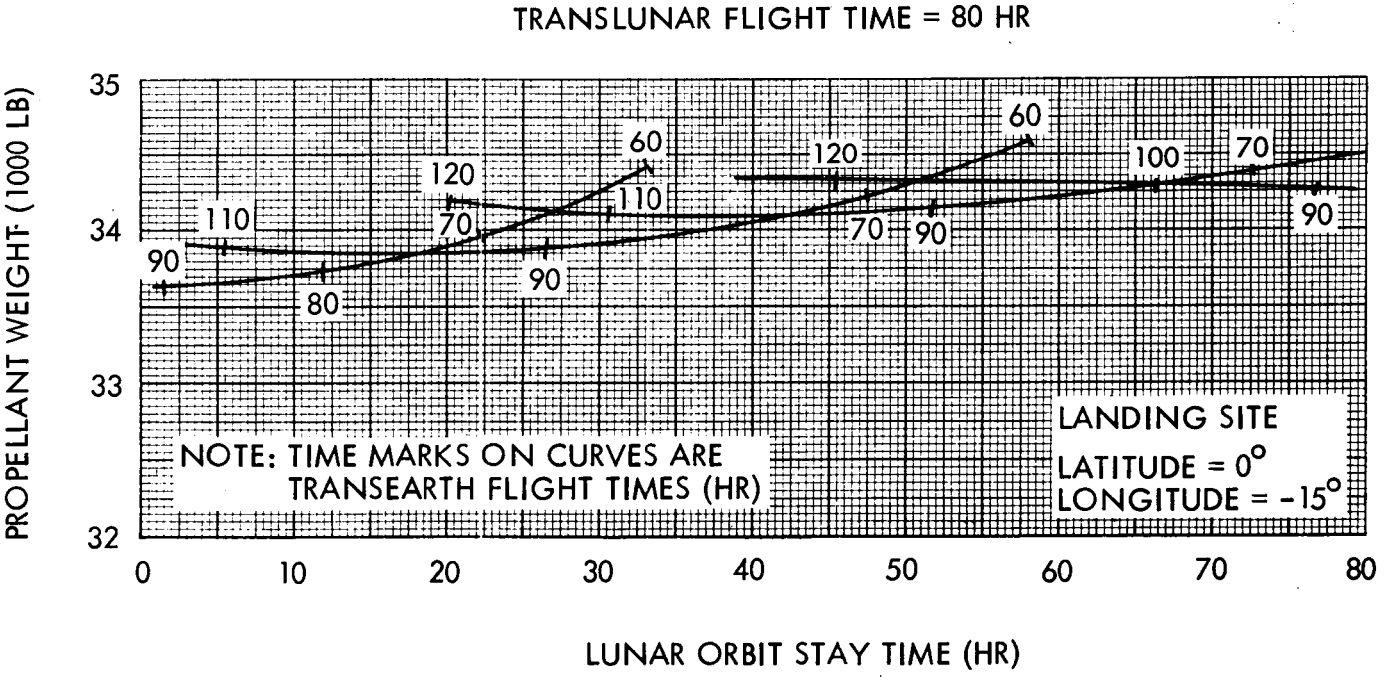

Figure 3.4-11. Propellant Weight Variations versus Lunar Orbit Stay Time and Total Mission Time

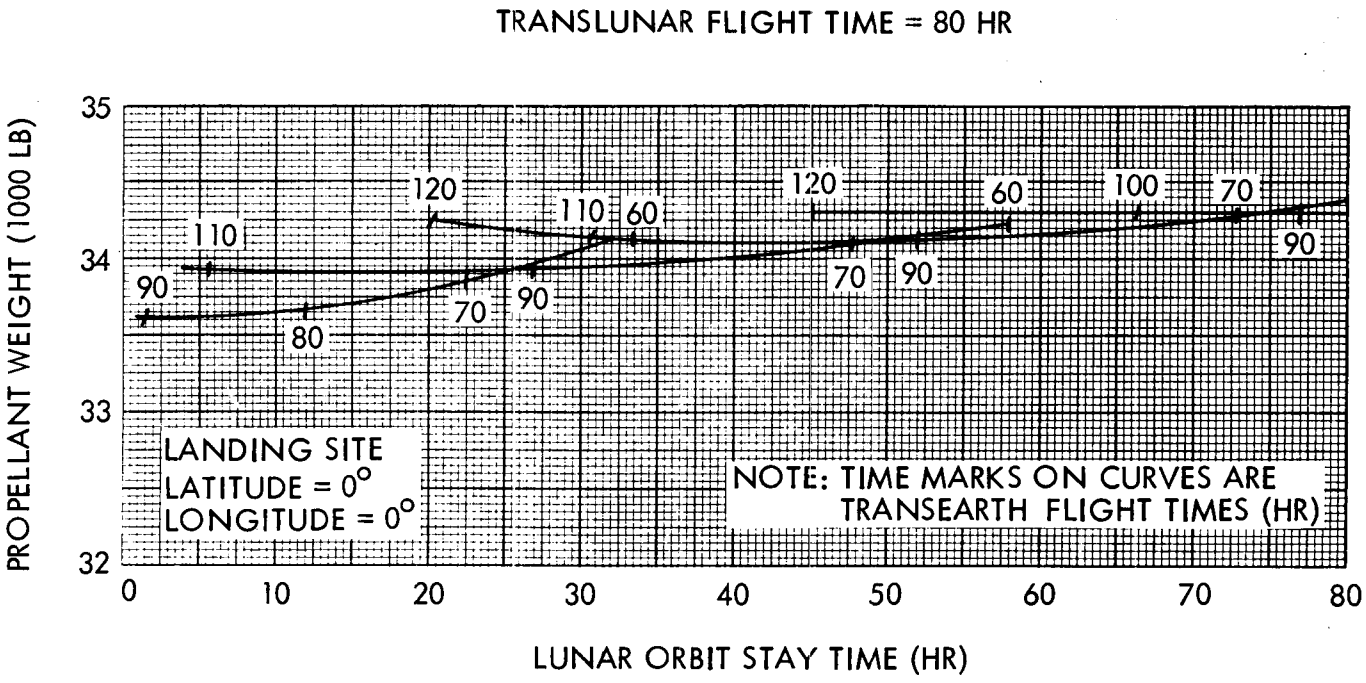

Figure 3.4-12. Propellant Weight Variations versus Lunar Orbit Stay Time and Total Mission Time

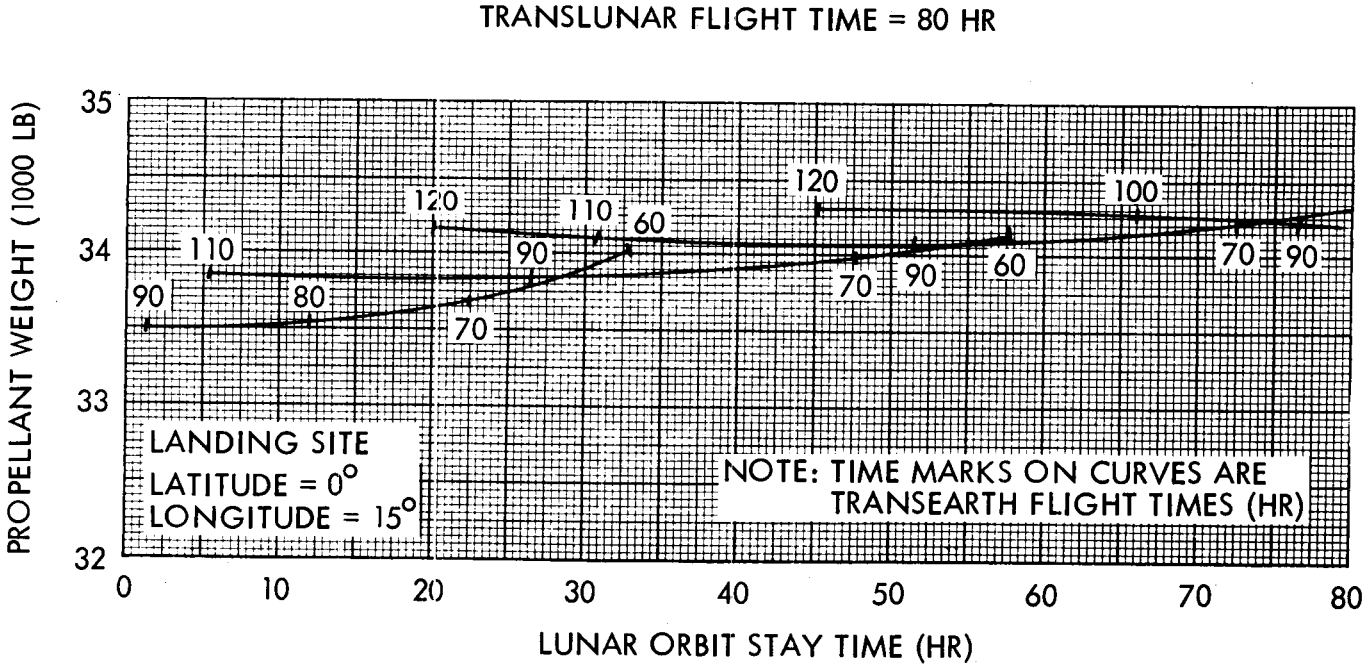

Figure 3.4-13. Propellant Weight Variations versus Lunar Orbit Stay Time and Total Mission Time

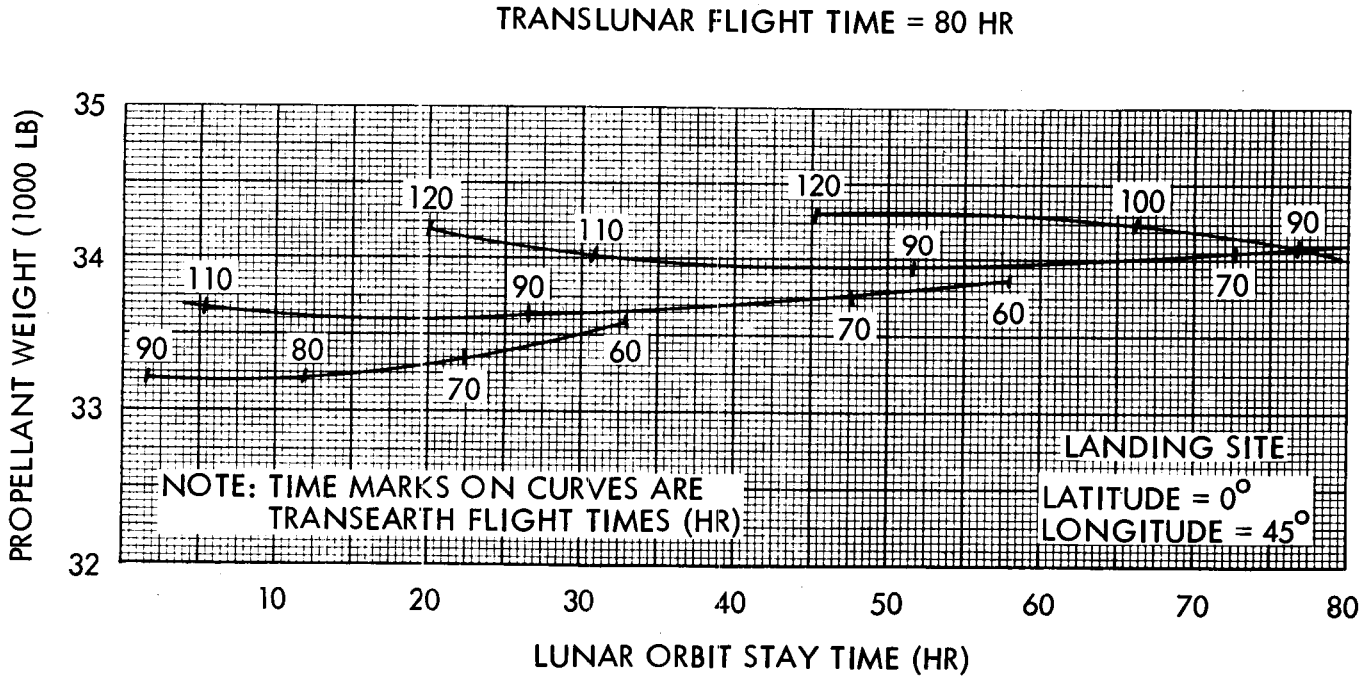

Figure 3.4-14. Propellant Weight Variations versus Lunar Orbit Stay Time and Total Mission Time

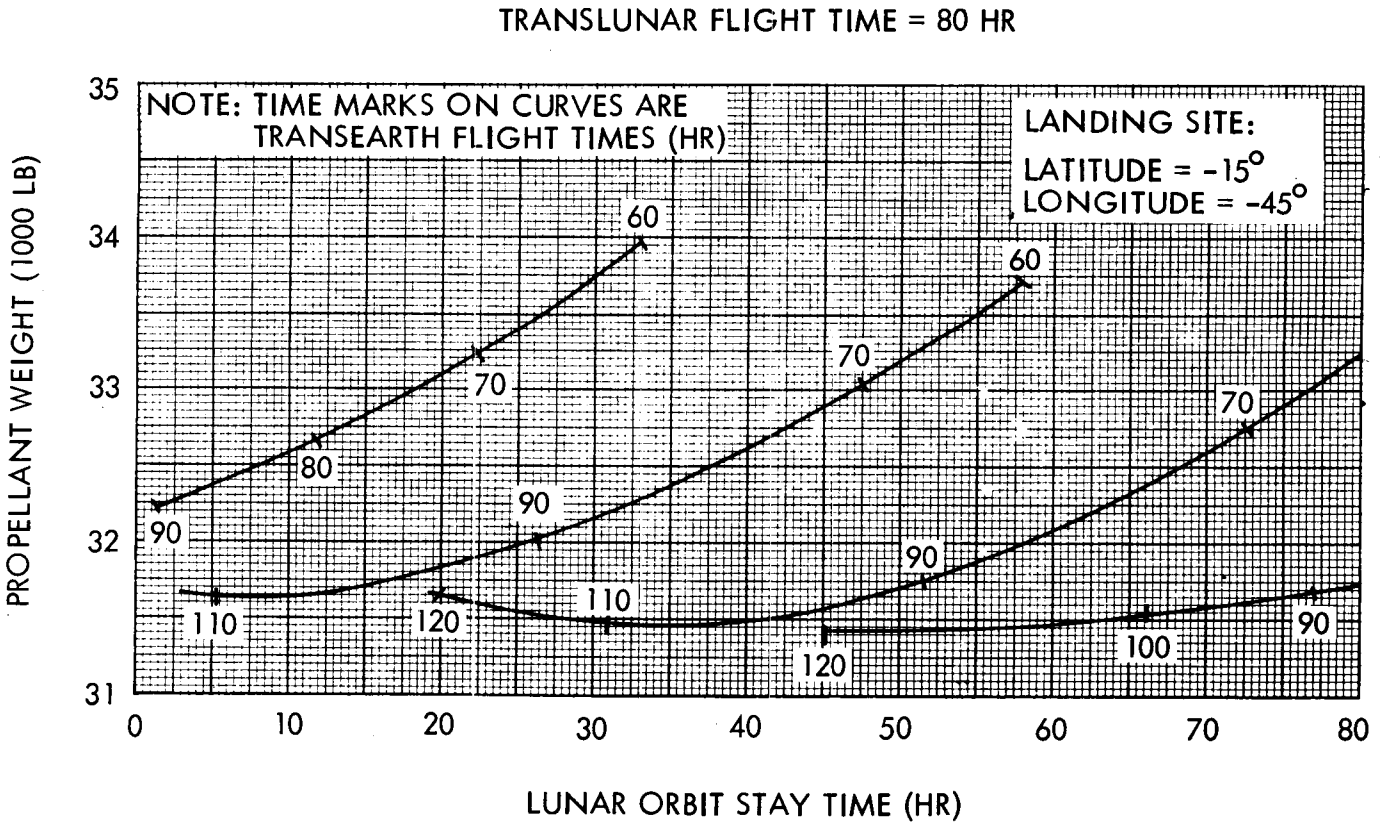

Figure 3.4-15. Propellant Weight Variations versus Lunar Orbit Stay Time and Total Mission Time

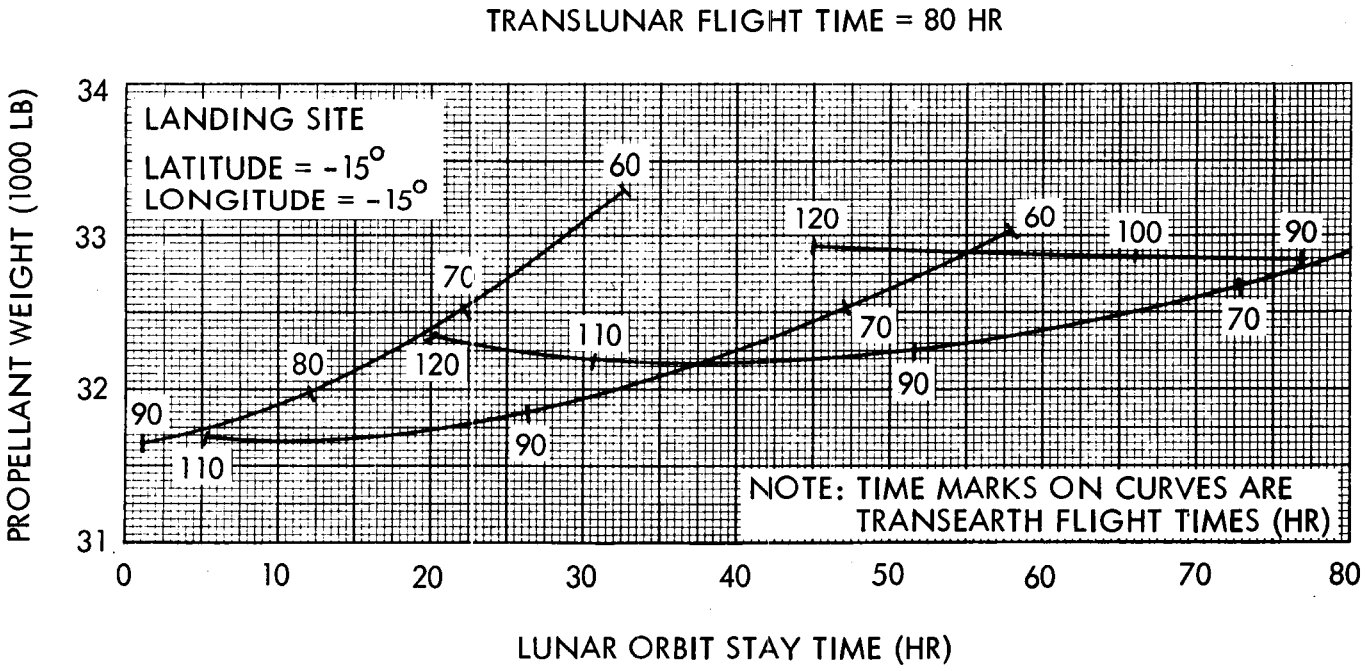

Figure 3.4-16. Propellant Weight Variations versus Lunar Orbit Stay Time and Total Mission Time

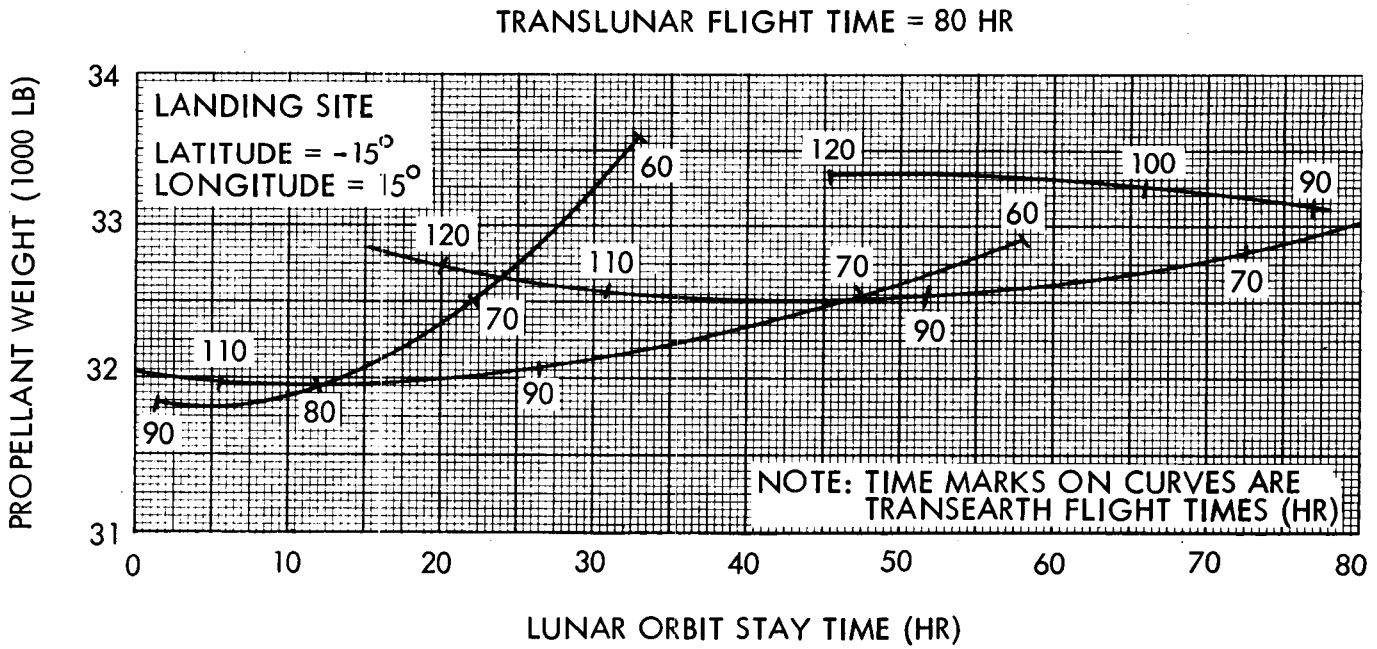

Figure 3.4-17. Propellant Weight Variations versus Lunar Orbit Stay Time and Total Mission Time

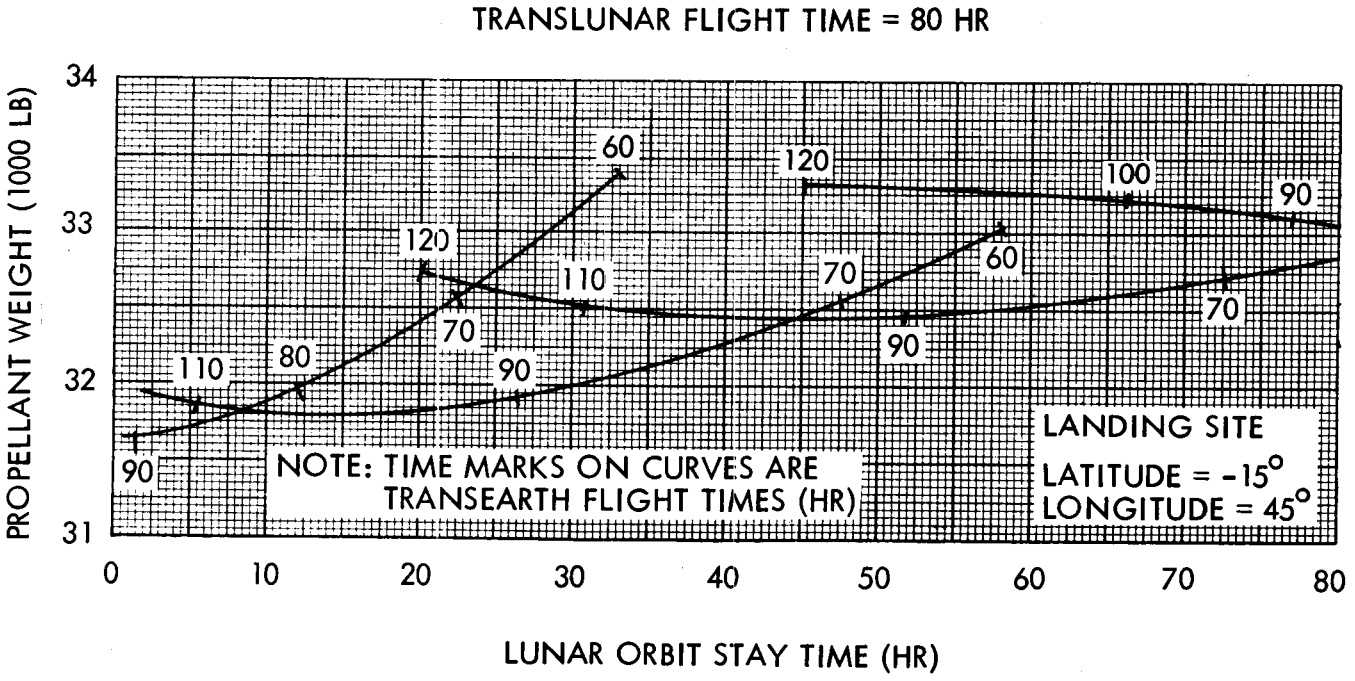

Figure 3.4-18. Propellant Weight Variations versus Lunar Orbit Stay Time and Total Mission Time

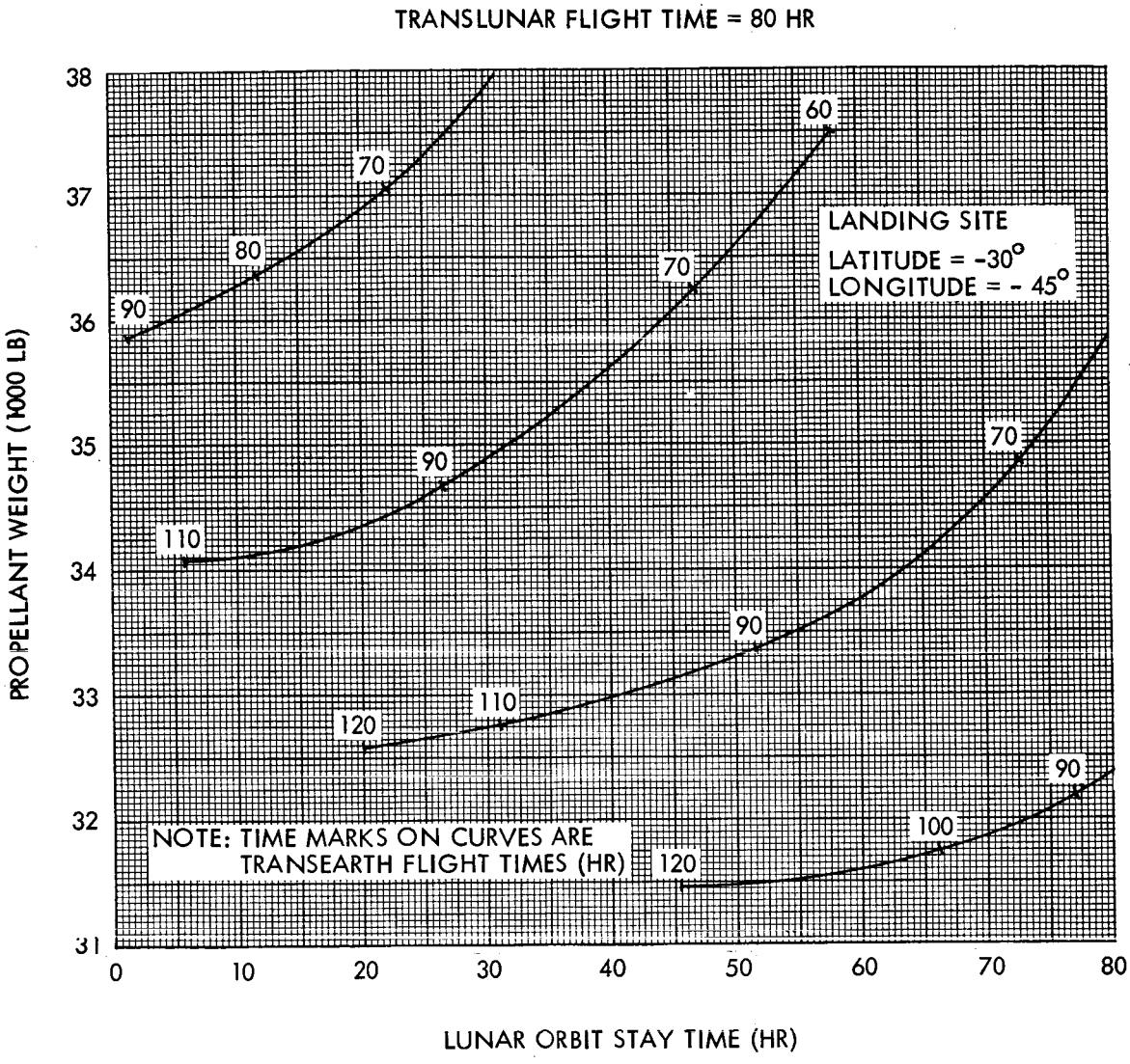

Figure 3.4-19. Propellant Weight Variations versus Lunar Orbit Stay Time and Total Mission Time

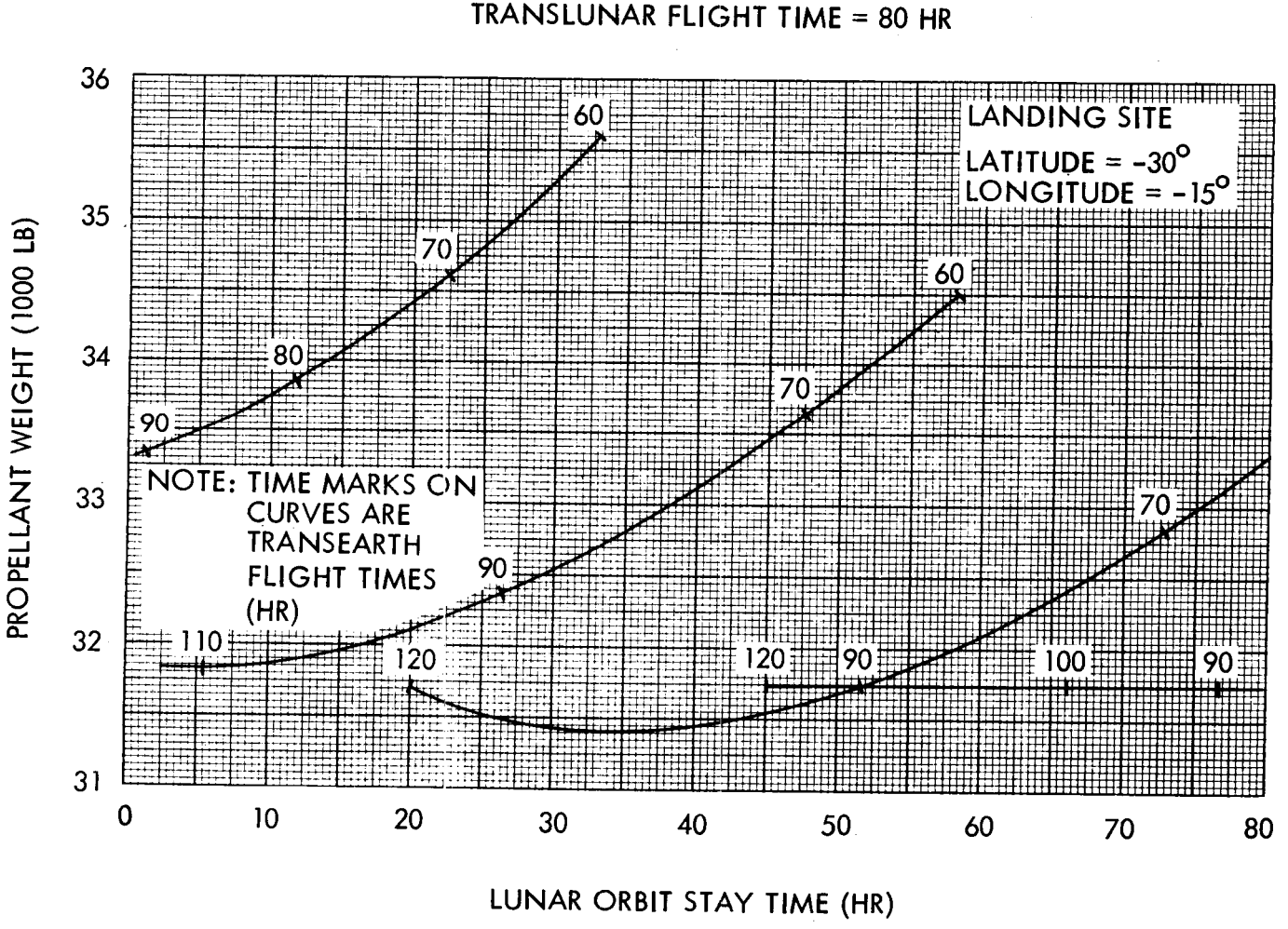

Figure 3.4-20. Propellant Weight Variations versus Lunar Orbit Stay Time and Total Mission Time

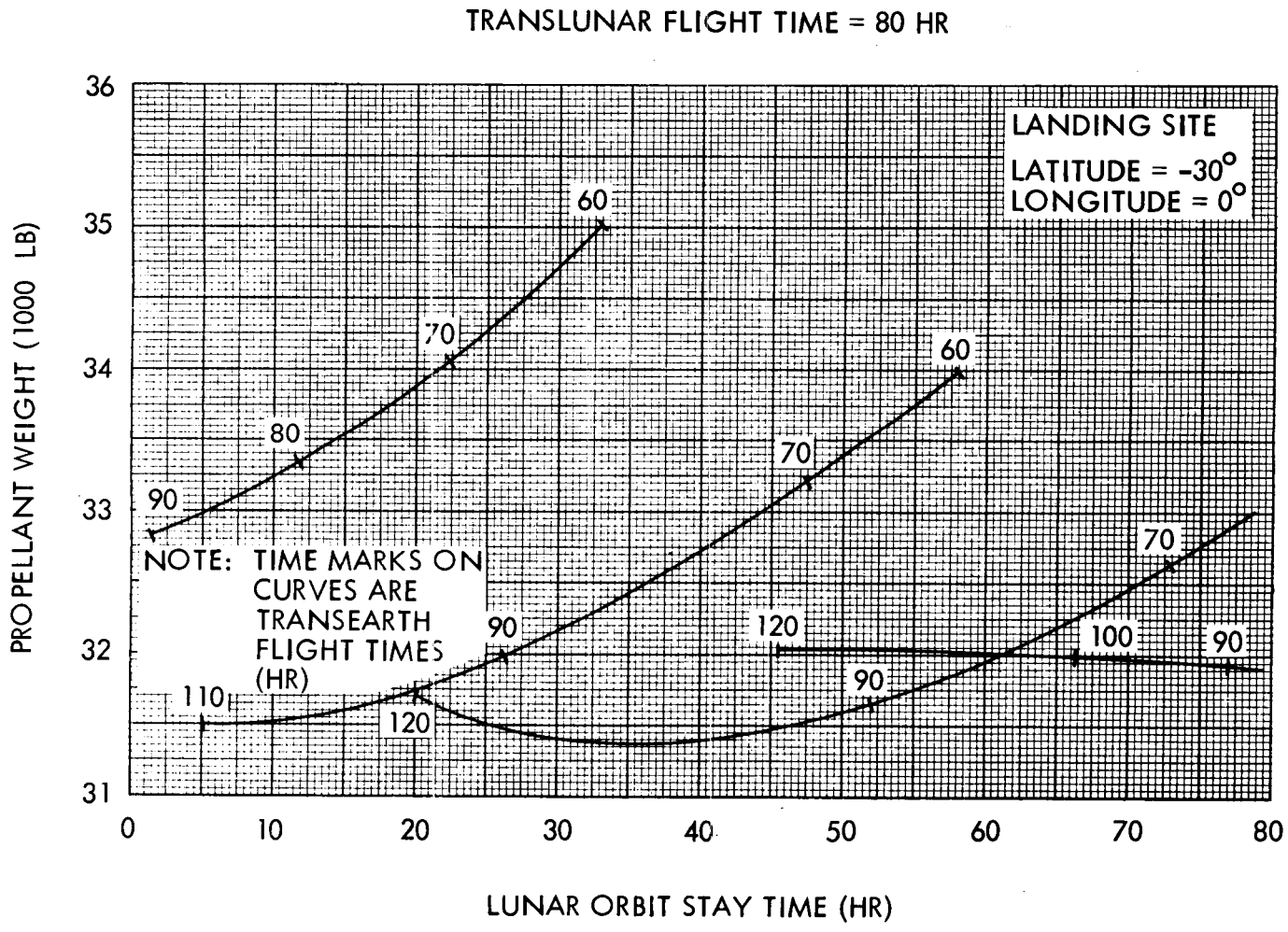

Figure 3.4-21. Propellant Weight Variations versus Lunar Orbit Stay Time and Total Mission Time

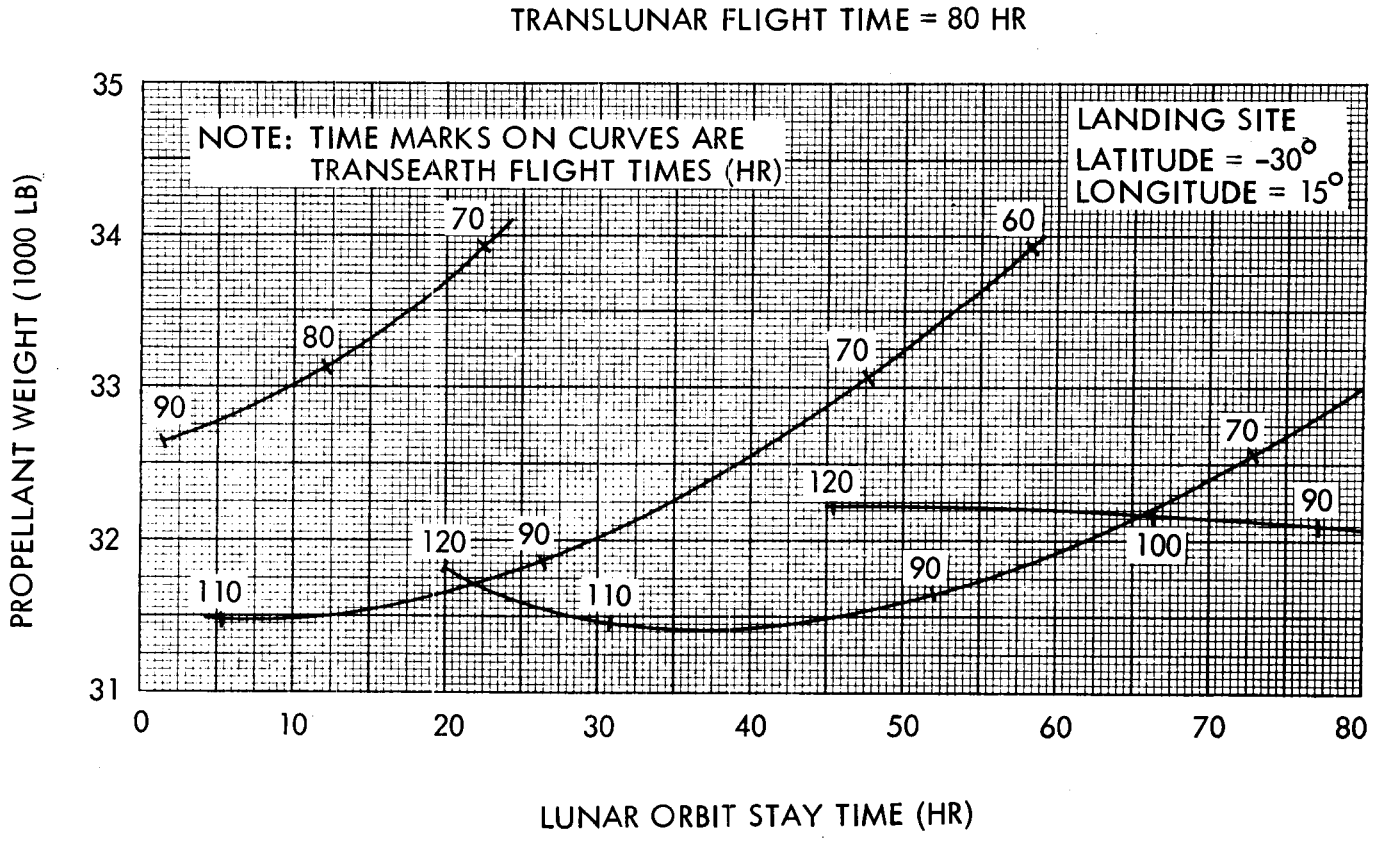

Figure 3.4-22. Propellant Weight Variations versus Lunar Orbit Stay Time and Total Mission Time

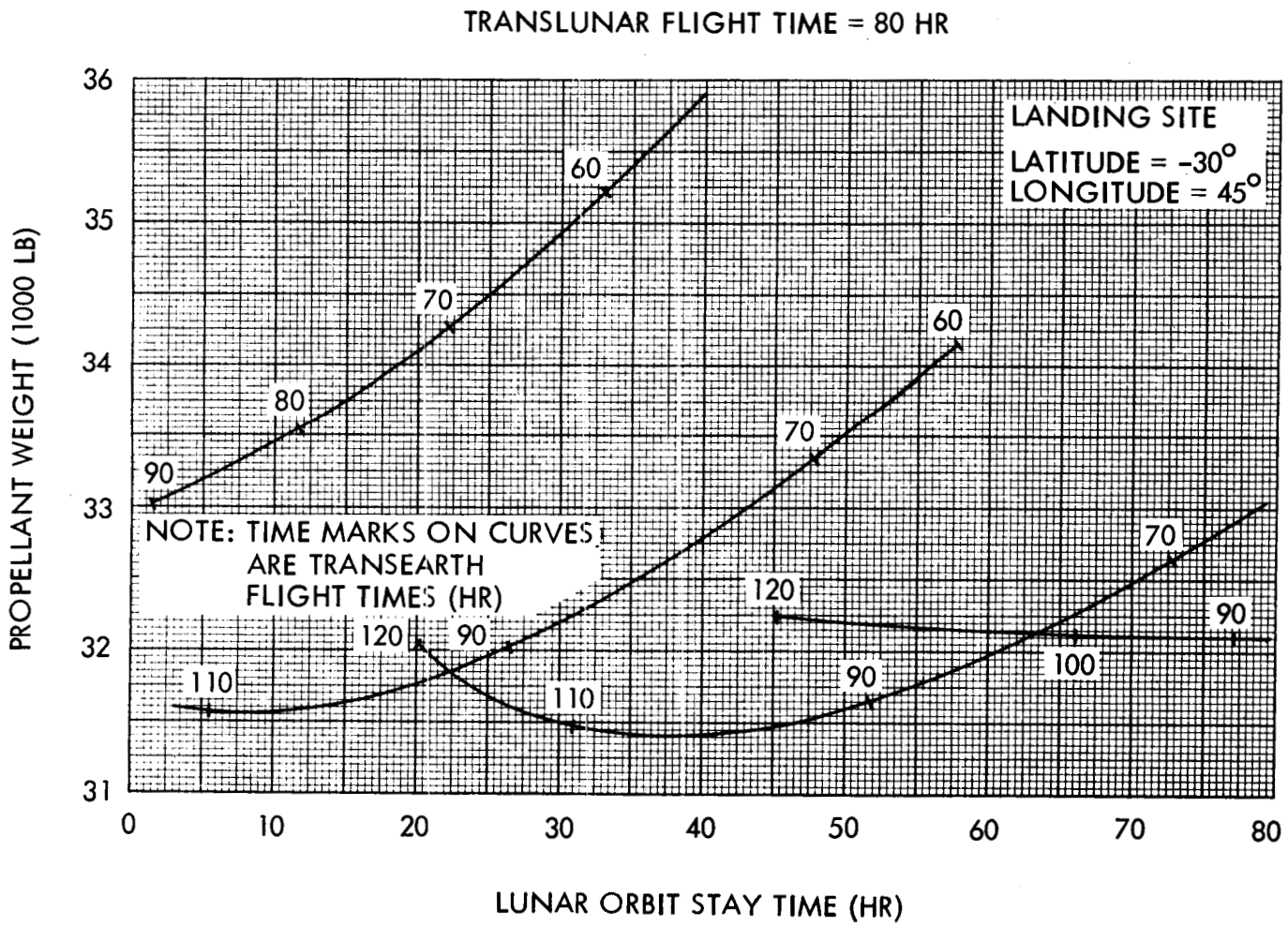

Figure 3.4-23. Propellant Weight Variations versus Lunar Orbit Stay Time and Total Mission Time

the effect of the moon's rotation, is always less than 180 degrees; and the latitudes of both vectors are in the southern hemisphere. The resulting geometry is such that the locus of landing sites, for which the propellant requirement is minimum, is always in the southern hemisphere at longitudes between -45 and 45 degrees.

This fact is illustrated by examining the propellant requirements presented in Figures 3.4-1 through 3.4-23 at constant landing site longitudes. It can be seen that after the landing site latitude is moved through zero degrees in a southerly direction, the propellant requirement approaches a minimum and then increases. Several other facts of interest can be noted in examining these figures. First, the sensitivity of propellant requirement to both transearth flight time and total mission time is greatly reduced as the loci of the optimum landing sites are approached. Second, the trend of decreasing propellant requirement with increased total mission time is reversed for landing sites near the optimum loci, although the variations are small.

In addition to the foregoing observations, it should be noted that a unique set of lunar operations geometry, which is determined by the optimization procedure, exists for each transearth injection opportunity represented in Figures 3.4-1 through 3.4-23. Thus each transearth injection opportunity has particular inclinations for the hyperbolic approach conic, the orbit, and the hyperbolic departure conic. Thus, a preselected nominal stay time will determine the inclinations for which the mission must be targeted. These curves do not represent the variation in propellant weight for delays in transearth injection from the targeted nominal.

Propellant weight contours are generated by cross-plotting the propellant requirements at the various landing sites, for fixed combinations of lunar orbit stay time and earth landing date (total mission time). Eight such contours were generated, using the following combinations of lunar orbit stay time and earth landing date:

Figure	Lunar Orbit Stay Time	Earth Landing Date
3.4-24	20 hours	Feb 4
3.4-25	20 hours	Feb 5
3.4-26	40 hours	Feb 5
3.4-27	58 hours	Feb 5
3.4-28	20 hours	Feb 6
3.4-29	40 hours	Feb 6
3.4-30	58 hours	Feb 6
3.4-31	58 hours	Feb 7

The first propellant weight contour, Figure 3.4-24, is representative of the shortest total mission time possible for the selected set of Group 1 parameters, this being about 7 days. The locus of landing sites, requiring the minimum propellant weight (no plane changes) is represented by the heavy line in the southern hemisphere. A region of landing sites, rendered inaccessible by a maximum Service Module propellant capacity such as 39,500 pounds, is indicated by the cross-hatched area at the upper left. The dashed lines show those landing sites at which the lunar surface stay time limitation posed by the 4 degree plane change is equal to or less than the lunar orbit stay time. The lines of constant propellant weight tend to compress at landing site longitudes near those of the $\overline{v}_{\infty}$ vectors. It appears that this compression effect is less severe at the landing site longitudes near that of the transearth $\overline{v}_{\infty}$ vector. A greater range of landing site longitudes must, however, be investigated to establish this as a general trend.

The propellant weight contours presented in Figures 3.4-25 through 3.4-27 are representative of a total mission time of 8 days and lunar orbit stay times of 20, 40 and 58 hours. Comparing these three contours, the lines of constant propellant weight compress with increased lunar orbit stay time, showing the effect of the decreasing transearth flight time. The minimum propellant requirement for each contour is determined by the magnitudes of the associated $\overline{v}_{\infty}$ vectors and the locus of the minimum is determined by the locations of the $\overline{v}_{\infty}$ vectors. Thus, it is seen that the minimum propellant requirement increases at the longer lunar orbit stay

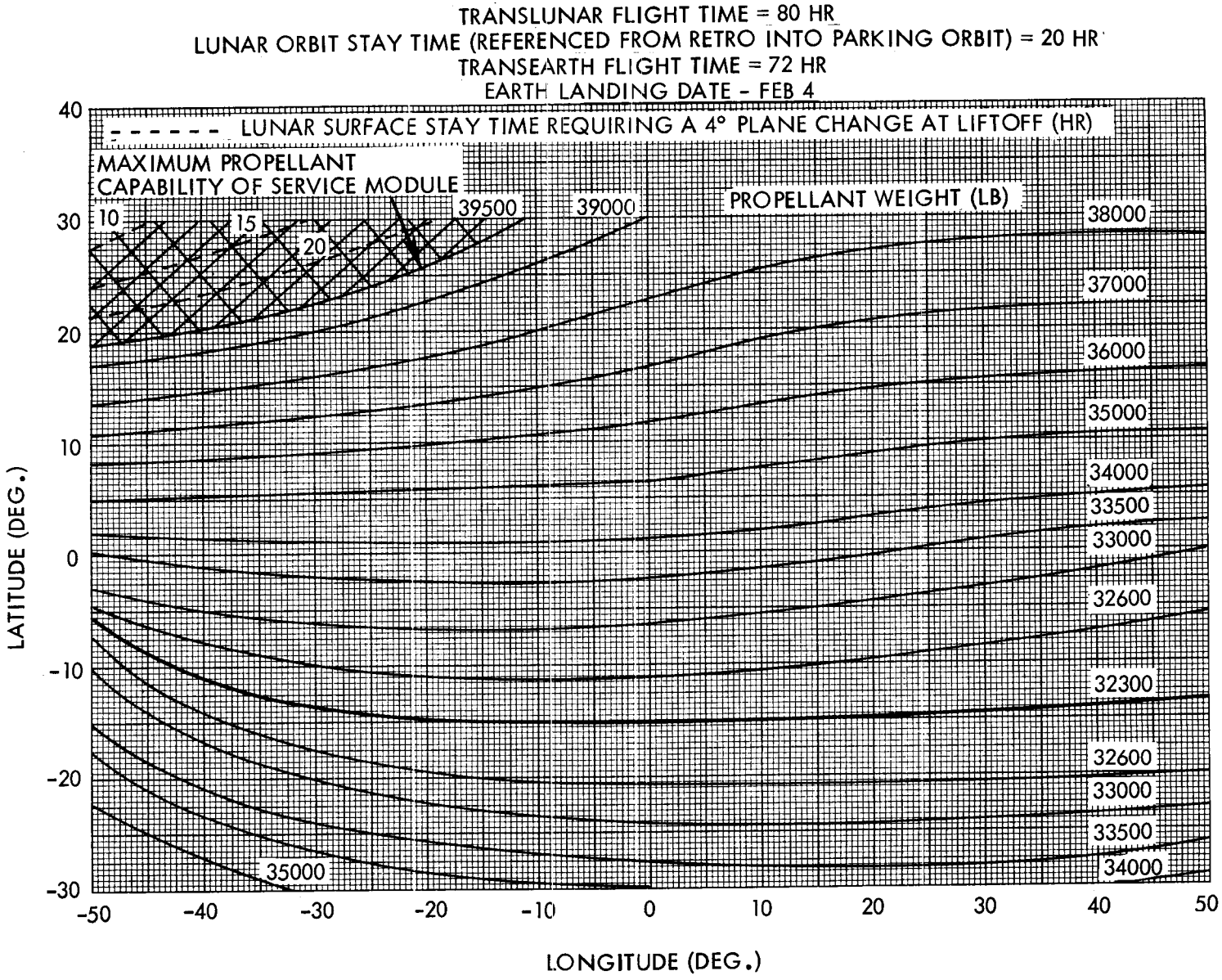

Figure 3.4-24. Propellant Weight Contour

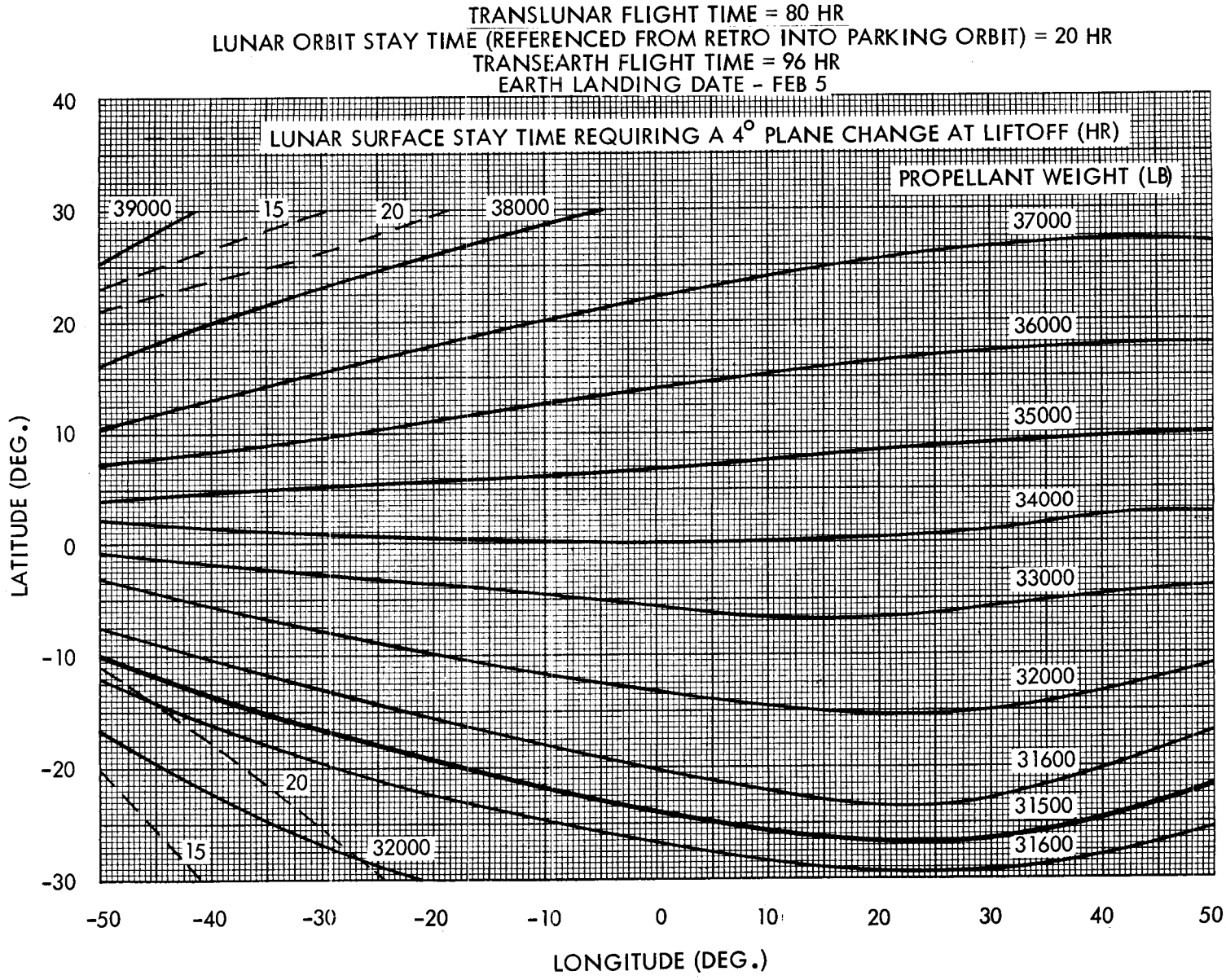

Figure 3.4-25. Propellant Weight Contour

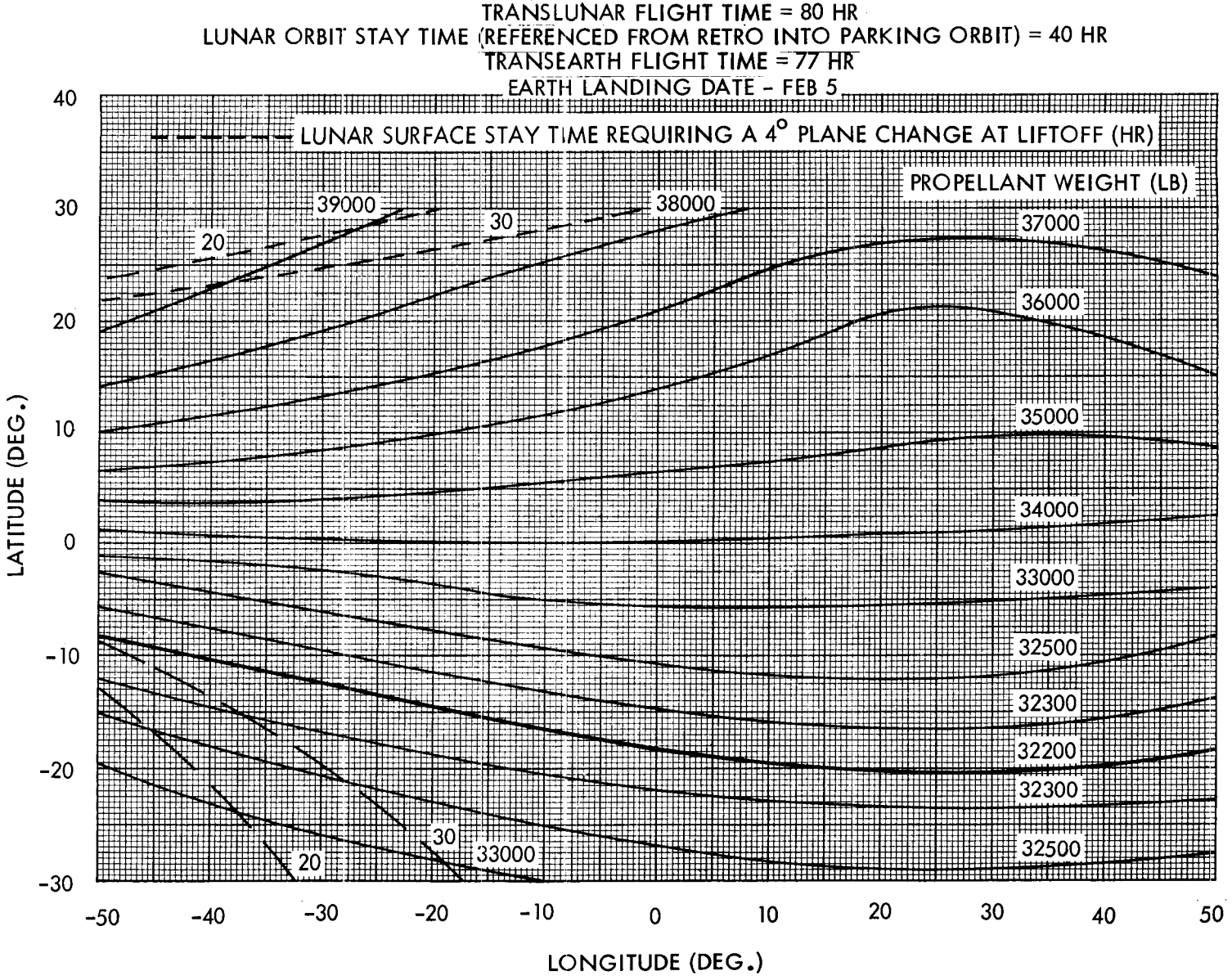

Figure 3.4-26. Propellant Weight Contour

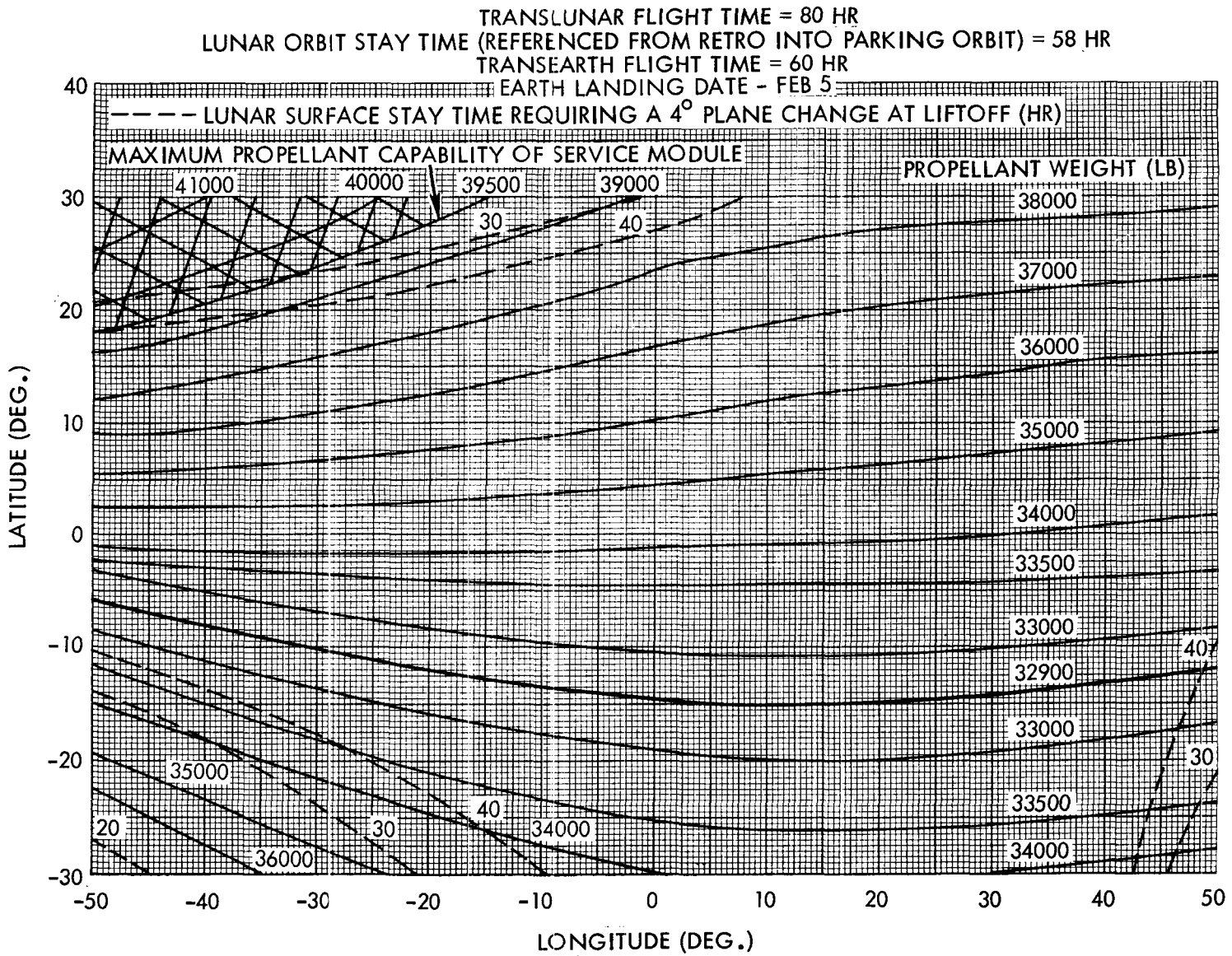

Figure 3.4-27. Propellant Weight Contour

times due to the shorter transearth flight time required, and the locus of the minimum shifts in a northerly direction.

Figures 3.4-28 through 3.4-30 provide propellant weight contours for a total mission time of 9 days and a lunar orbit stay time of 20, 40, and 58 hours. Figure 3.4-31 is representative of a total mission time of 10 days and a lunar orbit stay time of 58 hours. A comparison of the contours for the various total mission times yields the following:

a) The propellant requirement, at a constant lunar orbit stay time, decreases in general with increased total mission time due to the necessarily longer transearth flight times.

b) For the case where the two $\bar{V}_\infty$ vectors lie below the lunar equator the locus of the minimum propellant requirement, at a constant lunar orbit stay time, moves in a southerly direction with increased total mission time due to the longer transearth flight times.

c) The lunar surface stay time at a constant lunar orbit stay time becomes more restrictive with increased total mission times, indicating that the circular orbits are becoming more highly inclined.

The second set of Group 1 parameters selected for analysis is similar to the first with only the translunar flight time being changed to 60 hours. The combinations of lunar orbit stay time and earth landing date, for which contours were generated, are as follows:

Figure	Lunar Orbit Stay Time	Earth Landing Date
3.4-32	20 hours	Feb 4
3.4-33	40 hours	Feb 4
3.4-34	40 hours	Feb 5

All of the trends noted for the first set of Group 1 parameters were found in the 60 hour translunar flight time. The major effect of the shorter translunar flight time is to increase the area of landing sites inaccessible due to a maximum Service Module propellant capacity. One additional effect is clearly noted here; that being the geometric relief of propellant requirement at the high latitude landing sites, provided by the

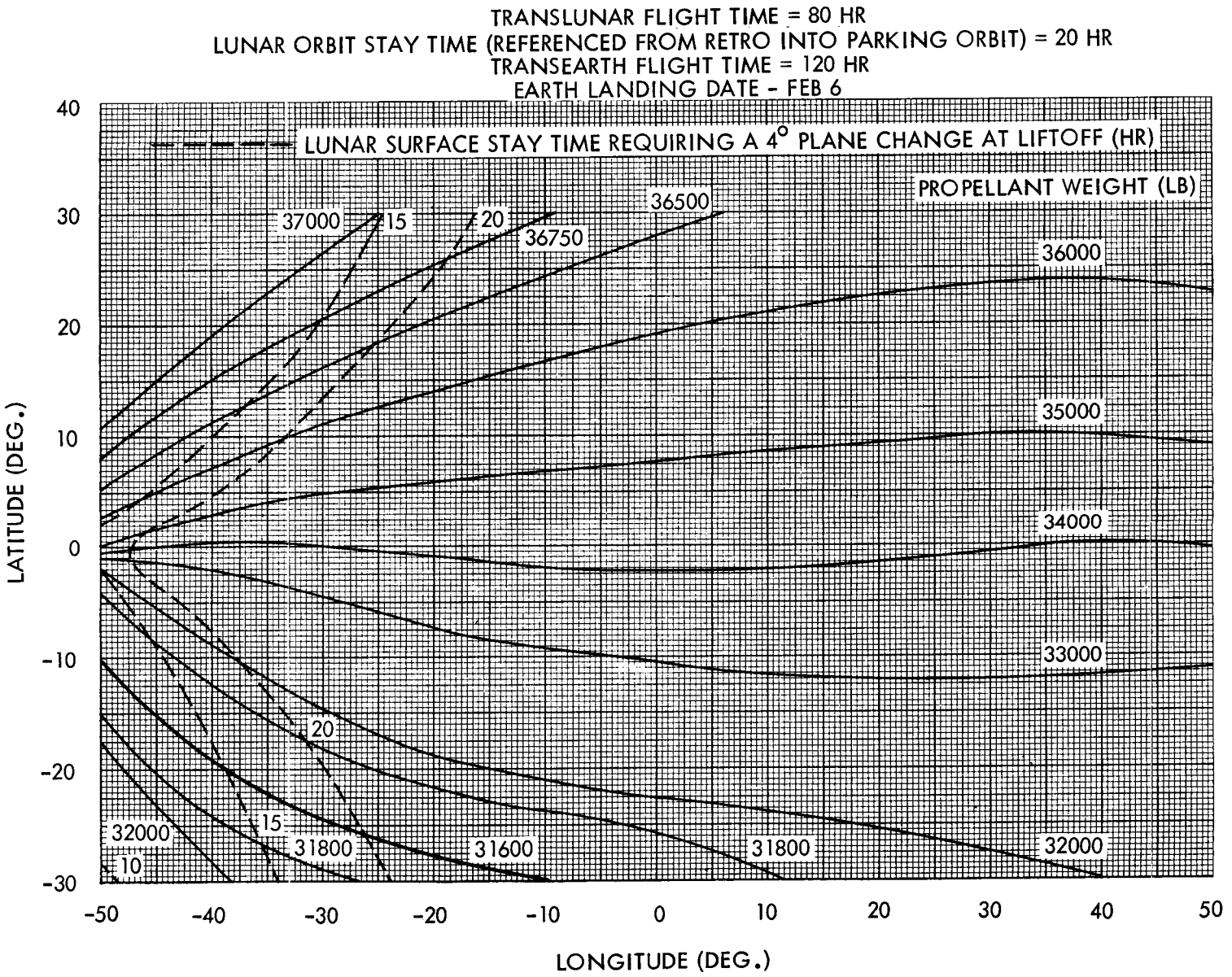

Figure 3.4-28. Propellant Weight Contour

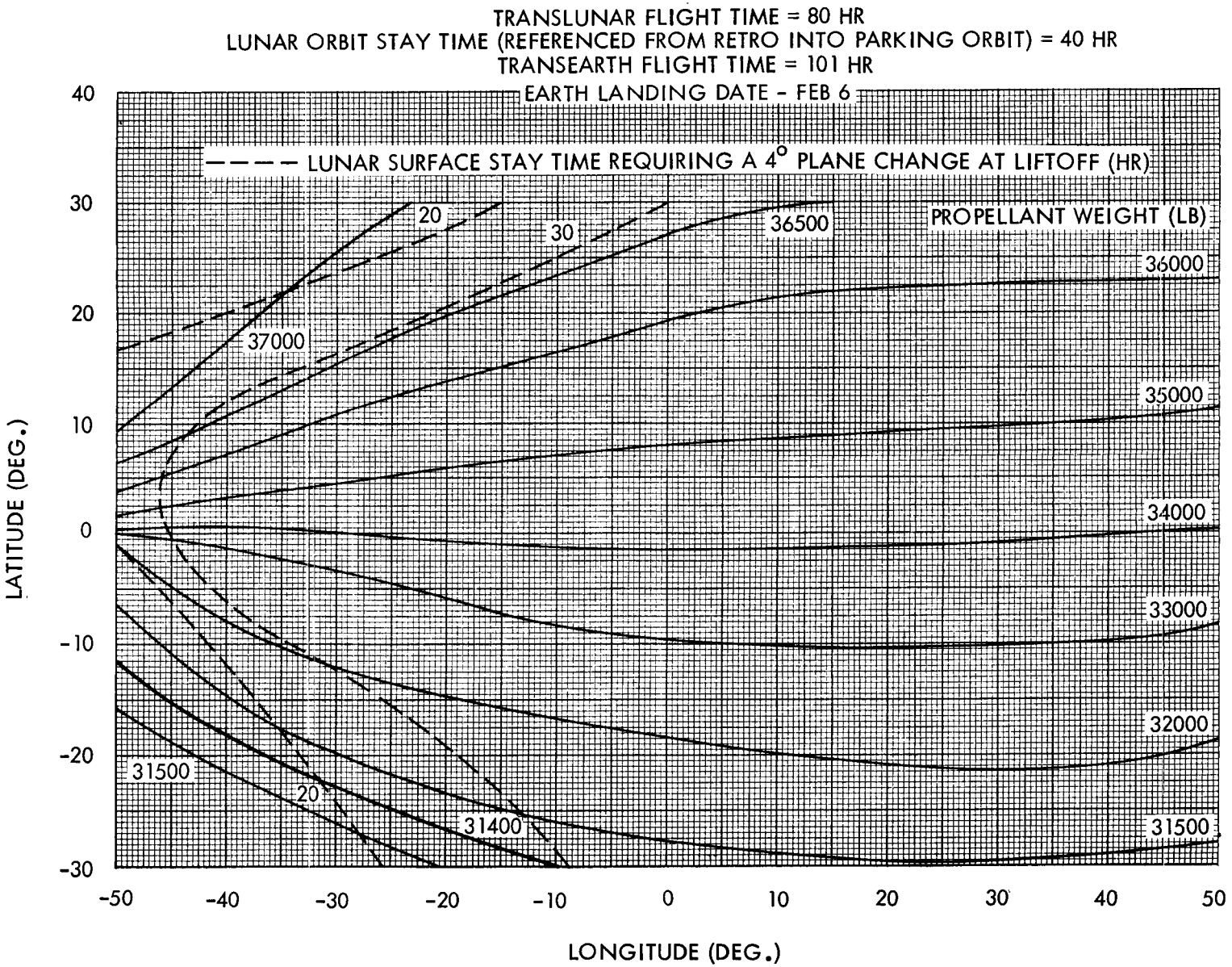

Figure 3.4-29. Propellant Weight Contour

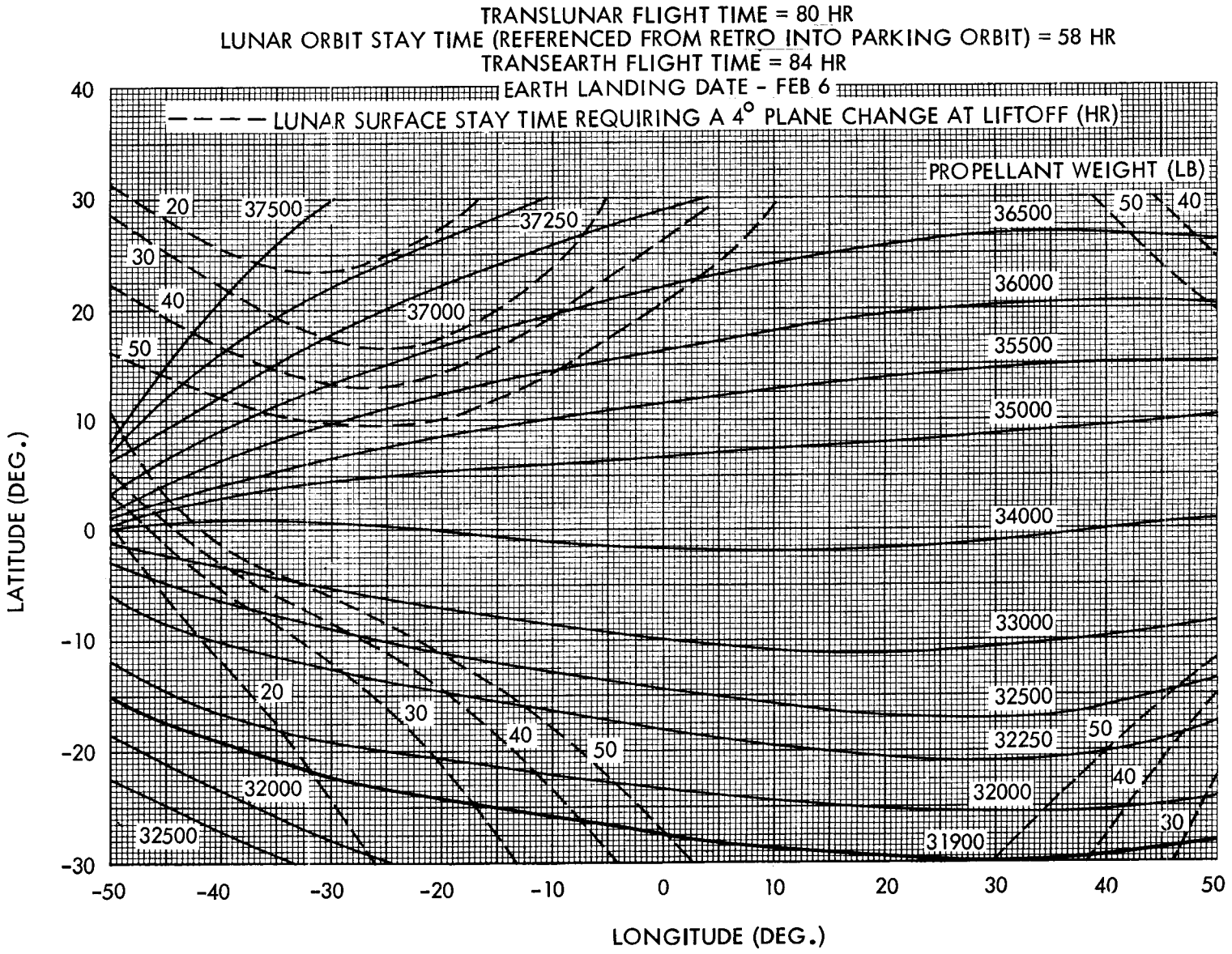

Figure 3.4-30. Propellant Weight Contour

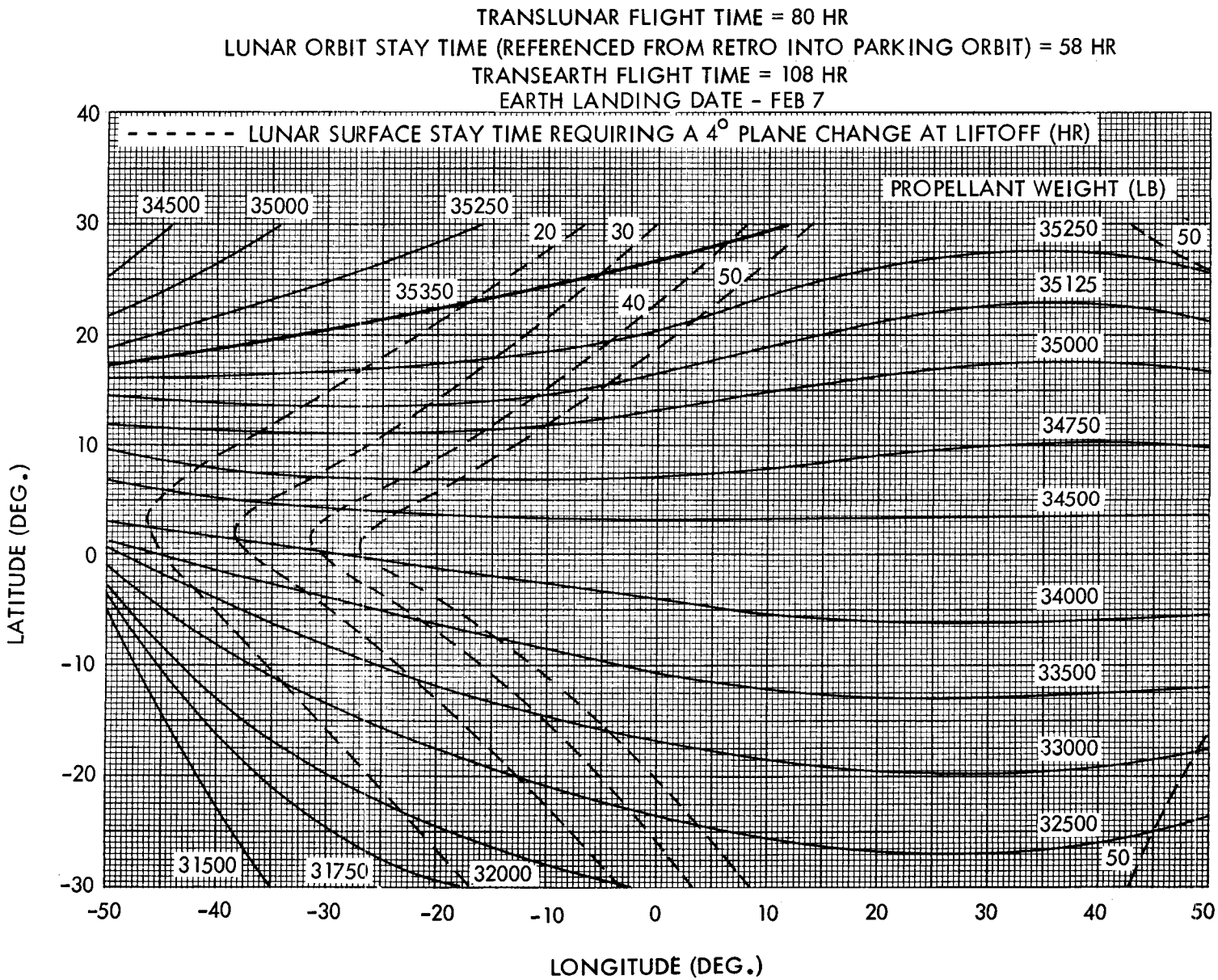

Figure 3.4-31. Propellant Weight Contour

more favorable positions of the $\overline{v}_{\infty}$ vectors relative to these landing sites at longer lunar orbit stay times. In comparing Figures 3.4-32 with 3.4-33, the minimum propellant weight is seen to increase for the longer lunar orbit stay time due to the shorter transearth flight time. The range of inaccessible landing sites at the high latitudes is, however, about the same for both lunar orbit stay times. This indicates that the compression effect of the shorter transearth flight time was offset by the relative geometry at the longer stay time.

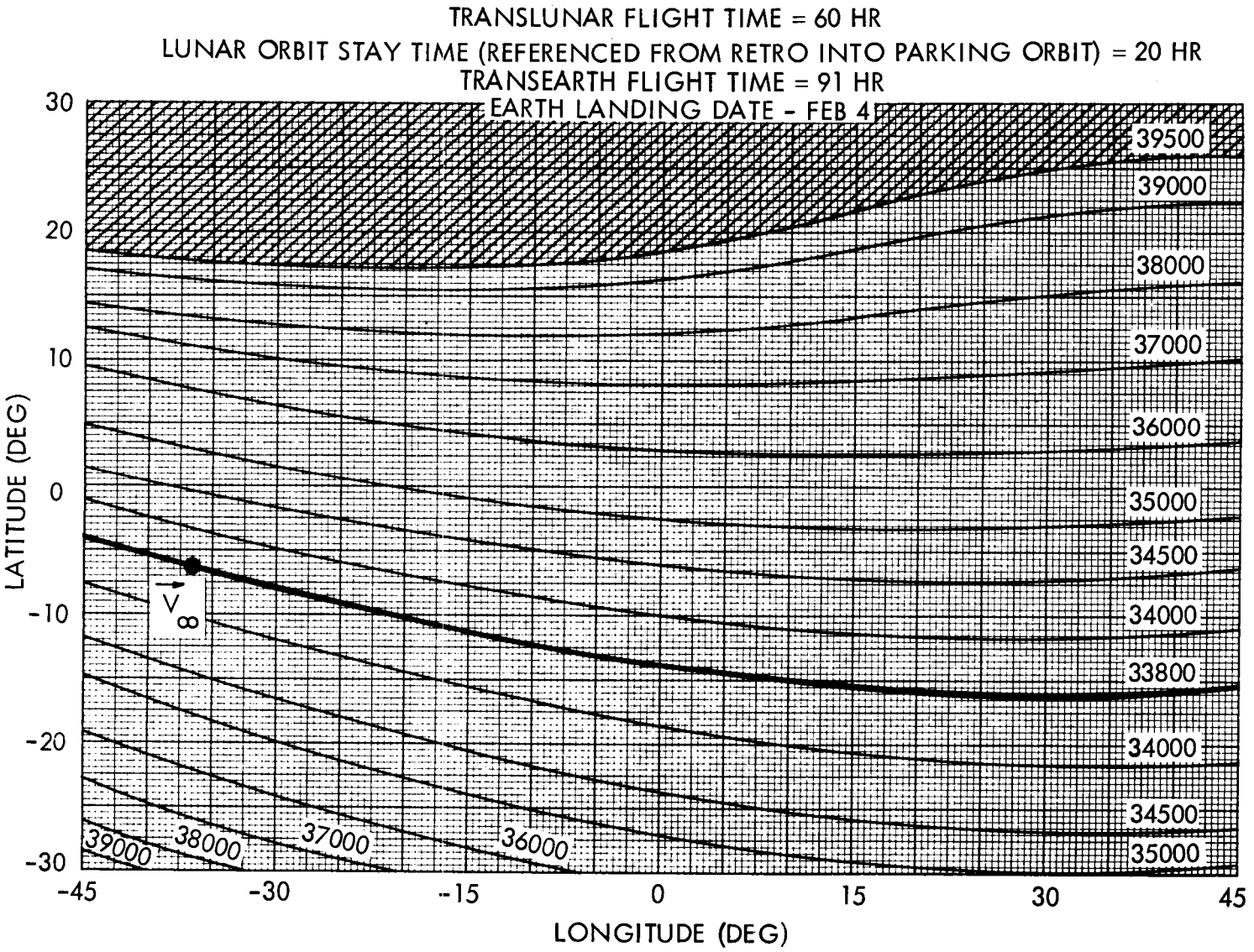

Figure 3.4-32. Propellant Weight Contour

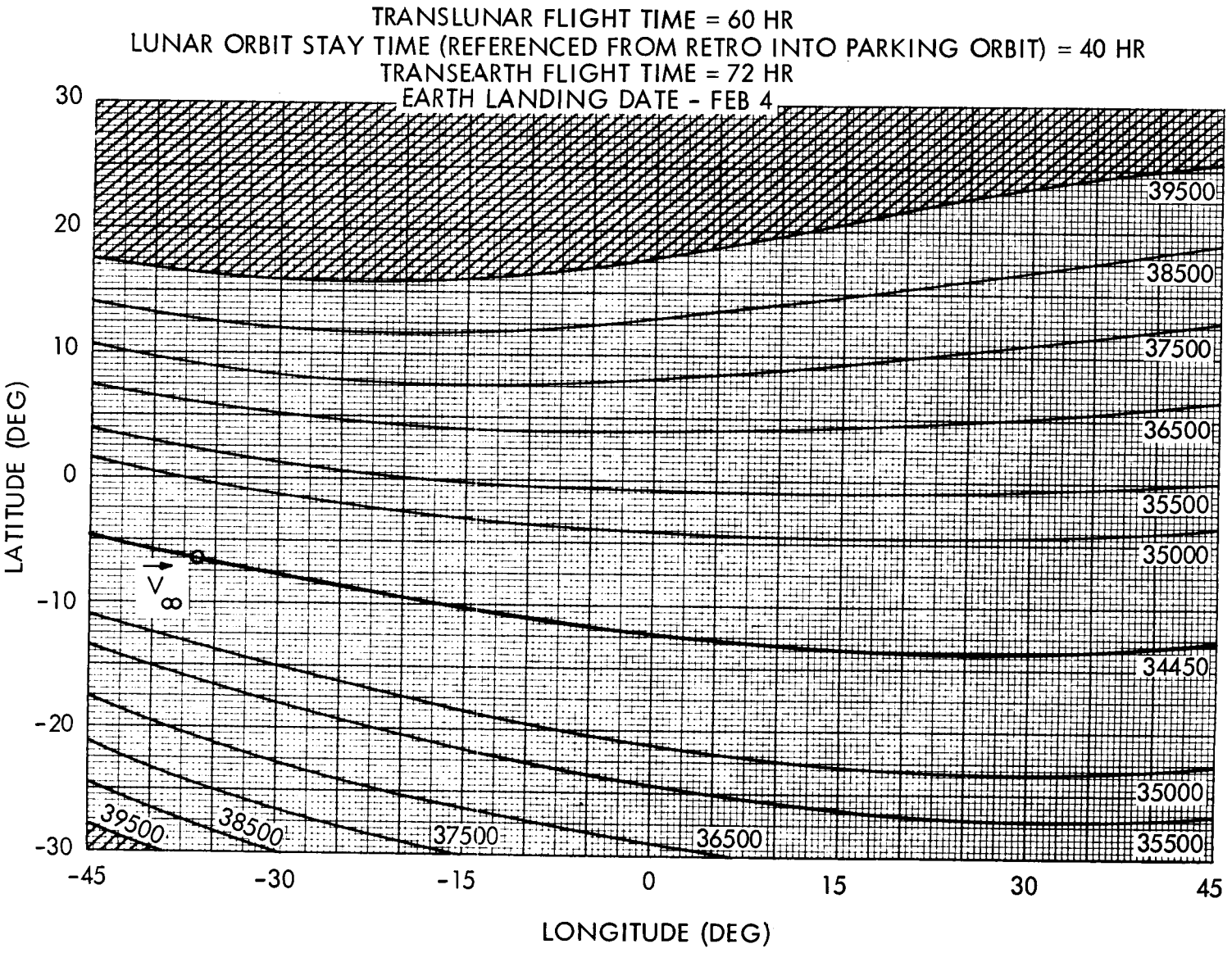

Figure 3.4-33. Propellant Weight Contour

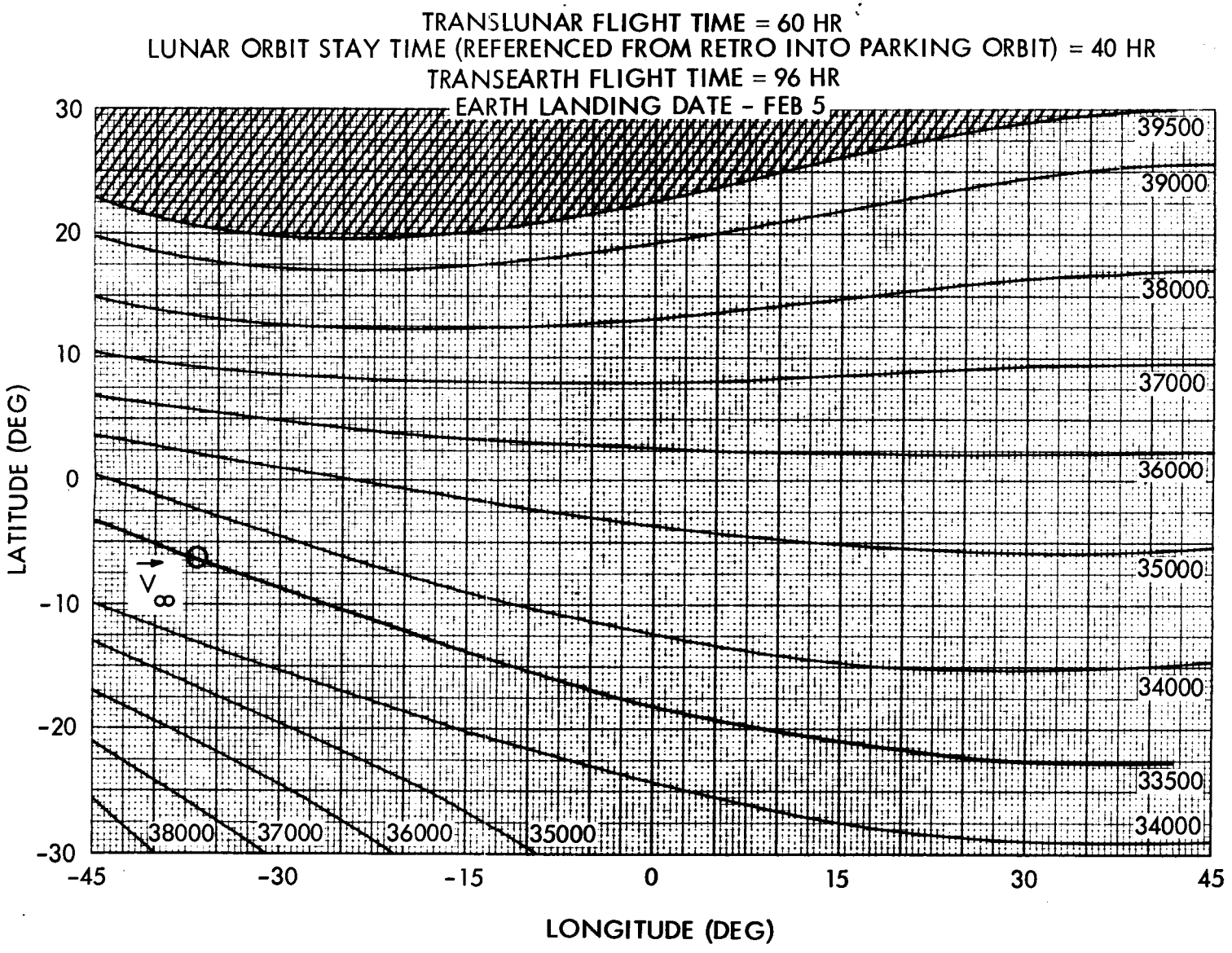

Figure 3.4-34. **Propellant Weight Contour**

4. CONCLUDING REMARKS

This interim report on the mission parameter study has concentrated on two of the more important questions that arise in connection with Apollo trajectory analysis. These are:

a) What procedure may be used to permit a parametric analysis of the large number of independent variables connected with the complete trajectory?

b) What approach should be taken to analyze the more complex lunar operations phase of the problem?

It has been decided that a feasible answer to the first question is to separate the complete Apollo trajectory into three relatively independent phases; i. e., the translunar phase, the lunar operations phase, and the transearth phase. This method becomes practicable with the acceptance of the moon's sphere of action concept of the earth-moon system. A further simplification of this model, that is the introduction of the idea that the inbound and outbound $\overline{v}_\infty$ vectors in the moon phase may be treated as free vectors, leads to the independency of the three phases. The connecting links are, of course, these $\overline{v}_\infty$ vectors.

The acceptance of this approach is dependent on whether or not these $\overline{v}_\infty$ vectors are indeed sufficiently independent of the lunar phase variables which determine the preferred shape and orientation of the incoming and outgoing hyperbolas. If they are, then the $\overline{v}_\infty$ vectors may be treated as the free vectors assumed above and may be used to analyze the characteristics of the lunar geometry without concern that adoption of some moon phase geometry might disturb the assumed translunar and transearth phases. The first part of this report has been devoted to determining the validity of this assumption.

Table 4. 1 summarizes the effects of the translunar parameters on the incoming $\overline{v}_\infty$ vector. To substantiate the simplification discussed above, it is only necessary to consider the effects due to the pericynthion altitude and the lunar landing site location. These values should be considered as representative of general effects. A complete analysis has been presented in Section 3. 2. As can be noted from these values, the location of the lunar

Table 4.1. Summary of Outbound Trajectory Parameters

28 January 1968

Parameter	Range	Nominal	Effects on $\overline{V}_\infty$ Type 5			Type 6		
			ΔV_∞ (ft/sec)	$\Delta \mu_\infty$ (deg)	$\Delta \lambda_\infty$ (deg)	ΔV_∞ (ft/sec)	$\Delta \mu_\infty$ (deg)	$\Delta \lambda_\infty$ (deg)
Trip Time	60 - 100 hr	range	-1490.0	-3.15	-35.9	-1640.0	+0.4	-36.6
Launch Azimuth (t_o = 70 hr)	72-108 deg	90 deg	+ 52.3	-0.45	- 0.5	+ 4.9	+0.95	$\pm$ 0.14
Parking Orbit vary by + 1 rev (t_o = 70 hr)	0.5-3.0 rev	1.75 rev(T-5) 2.07 rev(T-6)	$\pm$ 4.3	$\pm$0.42	$\pm$ 0.07	$\pm$ 1.5	$\mp$0.25	$\pm$ 0.08
Pericynthion Altitude (t_o = 70 hr)	50-150 n mi	50 (reference) 80 nominal	+ 2.92	+0.008	+ 0.06	+ 2.88	-0.001	+ 0.055
Lunar Landing Site Location for Inplane Deboost (t_o = 70 hr)	$\pm$ 45° long. $\pm$ 30° lat	+ 45° long. 0° lat	- 29.0	-0.75	- 1.0	- 23.0	+1.2	- 0.82

landing site for inplane deboost has the greatest effect on the $\overline{v}_{\infty}$ vector, that is, about 30 feet per second in velocity magnitude and one degree in selenographic position. If these variations are within the limits of acceptability, then the assumption that the $\overline{v}_{\infty}$ vector may be taken as a free vector is valid.

The variations of the $\overline{v}_{\infty}$ vector with trip time, launch azimuth, and length of the parking orbit also are shown in Table 4. 1. The purpose here is to determine the effects of the other independent translunar variables. Time of flight, which is related to energy, is the principal determinant of the position and magnitude of the $\overline{v}_{\infty}$ vector. The launch azimuth and parking orbit duration do not have nearly as large effects. The relatively small variation of these parameters on the $\overline{v}_{\infty}$ vector leads to the possibility that, in a complete parametric study, each may be limited to a nominal value, such as a 90-degree launch azimuth, and type 5 and 6 parking orbits.

Due to the lunar phase symmetry in the outbound and return trajectories, the variations of transearth parameters on the return $\overline{v}_{\infty}$ vector will be similar. For a transearth injection date of February 1, 1968 and the complete range of lunar sites, the magnitude, latitude, and longitude of the $\overline{v}_{\infty}$ vector vary less than 15 feet per second, 1 degree, and 0. 5 degree, respectively. These variations may be expected to remain essentially the same throughout the lunar orbital period (Section 3. 3). As with the translunar trajectory, the lunar parking orbit altitude has a negligible effect on the $\overline{v}_{\infty}$ vector. The transearth geocentric trajectory inclination ranging from 30 to 40 degrees, has a small but significant effect on the $\overline{v}_{\infty}$ vector. The magnitude and position of the $\overline{v}_{\infty}$ vector has a maximum variation throughout the lunar cycle of about 100 feet per second and 3 degrees, respectively. One conclusion that may definitely be stated is that the inclusion of both northern and southern earth landing sites, such as San Antonio, Texas, and Woomera, Australia, will be required in the final study. The limitation on the reentry maneuver angle seems to be the main deciding factor as to which earth landing site will be used. However, on those dates when both sites would have requirements within the reentry range limitations, that site requiring less transearth injection velocity would probably be chosen.

The second question this report proposes to answer is the procedure by which the lunar operations phase may be computed. The method chosen to separate the three phases of the Apollo trajectory lends itself directly to this problem. Specifically, for definite values of the Group 1 and Group 3 parameters discussed in Section 2. 1, the approach and departure $\overline{v}_{\infty}$ vectors will be defined. Each lends itself to two degrees of freedom in position, assuming for the moment that only non-free-circumlunar trajectories are being considered. These degrees of freedom have been translated into degrees of freedom in the inclinations and pericynthion altitudes of the approach and departure hyperbolas. Then, assuming that a lunar landing site has been specified, these free paramaters plus the orientation of the SM orbit are found which minimize the total fuel requirements of the Service Module. If an alternate landing site is chosen, a different amount of propellant will generally be required. Considering the fuel requirements for the complete range of landing sites, propellant contours may be drawn specifying those sites for which the fuel required is the same. Such contours have been drawn and studied for the launch date of January 28, 1968. Although the study is necessarily limited, a great deal of insight and generalization have been derived. Summaries of this information may be found in Sections 1, 2, and 3.

This study of the lunar phase for unrestricted translunar trajectories has been informative not only for deriving the above mentioned properties for this mode of operation but also for leading to methods of analysis applying to other sets of constraints. Thus, the idea of degrees of freedom of the $\overline{v}_{\infty}$ vectors is directly applicable to the free circumlunar case. In the past, Reference 1 for example, analyses of free circumlunar trajectories have been restricted to pericynthion deboost. The possibility exists, however, of having a variable pericynthion altitude. This will provide an additional degree of freedom, which may be used to minimize the total SM propellant requirement. Thus, the nominal free circumlunar translunar trajectory may be targeted to 60 nautical miles instead of the SM orbit altitude of 80 nautical miles if this is more favorable. The other characteristics of the translunar trajectory will change only slightly and the degree of freedom consisting of the transearth inclination with the earth's equator would still be available.

Another alternative that is derivable from the $\bar{v}_\infty$ vector concept is the following:

a) First, analyze a particular mode of operation in the lunar phase with respect to the $\bar{v}_\infty$ vectors alone. Thus, a parametric study of propellant requirement may be based on the positions and magnitudes of the two $\bar{v}_\infty$ vectors.

b) Analyze the translunar and transearth phases of the mission from the standpoint of developing the more favorable $\bar{v}_\infty$ magnitudes and directions.

For example, in Section 3.3 and for the range of variables considered here, it has been deduced that lengthening the stay time on the moon generally results in a decrease in the total SM propellant requirement.

With this approach it is also possible to devise favorable modes of operation in the translunar and transearth phases. For example, the addition of a second major impulse somewhere between the earth and the moon need be analyzed only from the view of its effect on the position and velocity of the approach or departure $\bar{v}_\infty$ vector. A parametric analysis of the lunar phase with respect to the $\bar{v}_\infty$ vectors will determine whether this second impulse is favorable or unfavorable.

REFERENCES

1. Johnson, R. W., "Analysis of Apollo Trajectories for the Period 20 January - 17 February, 1968." STL Report No. 8408-6034-RC-000 dated December 27, 1963. (Conf.)

2. Egorov, V. A., "Certain Problems of Moon Flight Dynamics," Russian Literature of Satellites, Part I, International Physical Index, Inc., 1958.

APPENDIX

MAXIMUM ALLOWABLE STAY TIME ON THE LUNAR SURFACE

In trying to develop a method for computing the maximum allowable lunar surface stay time, it soon became apparent that the use of spherical trigonometry was going to involve the use of a series of cumbersome trigonometric equations. Thus, an approach using vector analysis was tried, which resulted in a rather simple expression of lunar surface stay time as a function of the LEM plane change requirement at liftoff, lunar parking orbit inclination, and latitude of lunar landing site. The technique first involves finding the shortest distance between a point (the landing site some time after touchdown) and a plane (the parking orbit plane). Rearrangement of this equation resulted in the desired expression. Following is the derivation of this expression.

Define the coordinate system with origin at the center of the moon such that,

x-axis is positive in the direction of the parking orbits ascending node

y-axis is in the lunar equatorial plane and rotated 90^{o} counterclockwise from the x-axis

z-axis is such that a right handed cartesian system is formed

Letting the radius of the moon be unity, the CM/SM orbital plane can be defined by any three points (A, B, and C) not is a straight line (see Figure 1). Thus, let

$A = (0, 0, 0) =$ origin

$B = (1, 0, 0) =$ ascending node

$C = (0, \cos i, \sin i) =$ maximum declination

The landing site is the point P with coordinates (x_p, y_p, z_p) of

$$x_p = \cos \mu_L \cos (\Delta\lambda_o + \omega t + \dot{n}t)$$

$$y_p = \cos \mu_L \sin (\Delta\lambda_o + \omega t + \dot{n}t)$$

$$z_p = \sin \mu_L$$

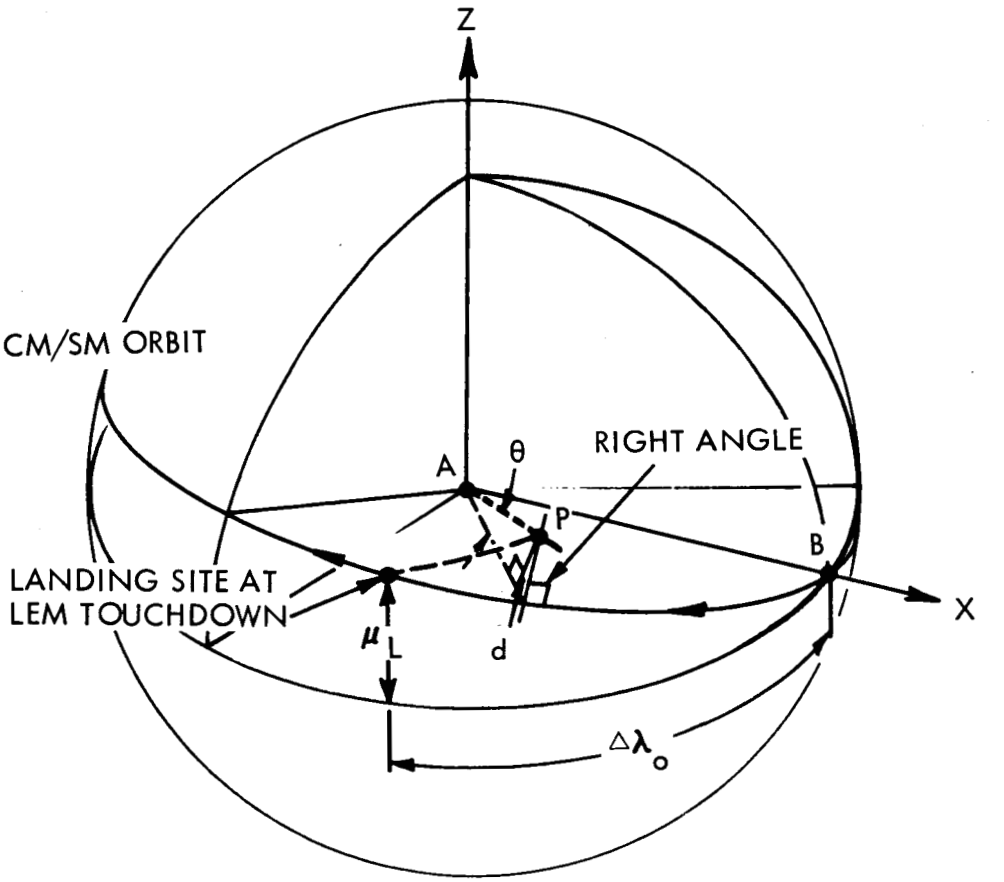

Figure 1. Geometry for Computing Stay Time on the Lunar Surface

where

μ_L = latitude of landing site

$\Delta\lambda_o$ = longitude difference between ascending node and landing site at the time of LEM touchdown

$= \sin^{-1}\left(\frac{\tan \mu_L}{\tan i}\right)$ for $\Delta\lambda_o < 90^o$ and equals $-\sin^{-1}\left(\frac{\tan \mu_L}{\tan i}\right)$ for $\Delta\lambda_o > 90^o$

ω = axial rotation rate of moon = 0.549 deg/hr

$\dot{n}$ = nodal regression rate of lunar parking orbit

$\approx 0.0465 \cos i$ deg/hr

t = stay time on lunar surface

The normal to the parking orbit plane is found from

$$\overline{AB} \times \overline{AC} = (1, 0, 0) \times (0, \cos i, \sin i) = (0, -\sin i, \cos i) = \bar{n}$$

Since the vectors AB and AC are orthogonal, the resultant cross-product of AB and AC is a unit vector, say n. The perpendicular distance from the landing site, P, to the orbit plane is then

$$d = \bar{n} \cdot \overline{PA} = (0, -\sin i, \cos i) \cdot (-x_p, -y_p, -z_p)$$

$$= y_p \sin i - z_p \cos i$$

$$= \sin i \cos \mu_L \sin (\Delta\lambda_o + \omega t + \dot{n}t) - \cos i \sin \mu_L$$

The angle θ between the landing site and the orbital plane is now simply

$$\theta = \sin^{-1}(d)$$

or

$$\theta = \sin^{-1}\left[\sin i \cos \mu_L \sin (\Delta\lambda_o + 0.549t + 0.0465t \cos i) - \cos i \sin \mu_L\right]$$

This is the great circle distance between the LEM landing site and the CM/SM ground track at LEM liftoff, and thus is equivalent to the plane change required by the LEM for rendezvous with the CM/SM. Note that

this expression is only valid for time less than the time required for one-quarter rotation of the moon on its axis and for $\theta < 90^{\circ}$. Thus rearranging the above expression and solving for t gives

$$t = \frac{\left| \sin^{-1}\left[\frac{\sin\theta + \cos i \sin\mu_L}{\sin i \cos\mu_L}\right] - \sin^{-1}\left(\frac{\tan\mu_L}{\tan i}\right) \right|}{0.549 + 0.0465 \cos i}$$

The value of θ is either positive or negative, depending on whether the difference in longitude between the ascending node and landing site at the time of touchdown is less than or greater than 90°, respectively.

Figures 2 and 3 were then developed by setting $\theta = \pm 4^{\circ}$ (the maximum allowable LEM plane change requirement), and running through the possible orbit inclinations and latitudes of the lunar landing site. These curves were then used for obtaining the contours of maximum allowable lunar surface stay time in Section 3.4. The possibility of choosing an inclination which would result in no plane change for a given stay time was not considered. Also, near these "optimum" inclinations, the expression above for the stay time results in the unique solution for $\theta = \pm 4^{\circ}$ and the stay time less than 48 hours.

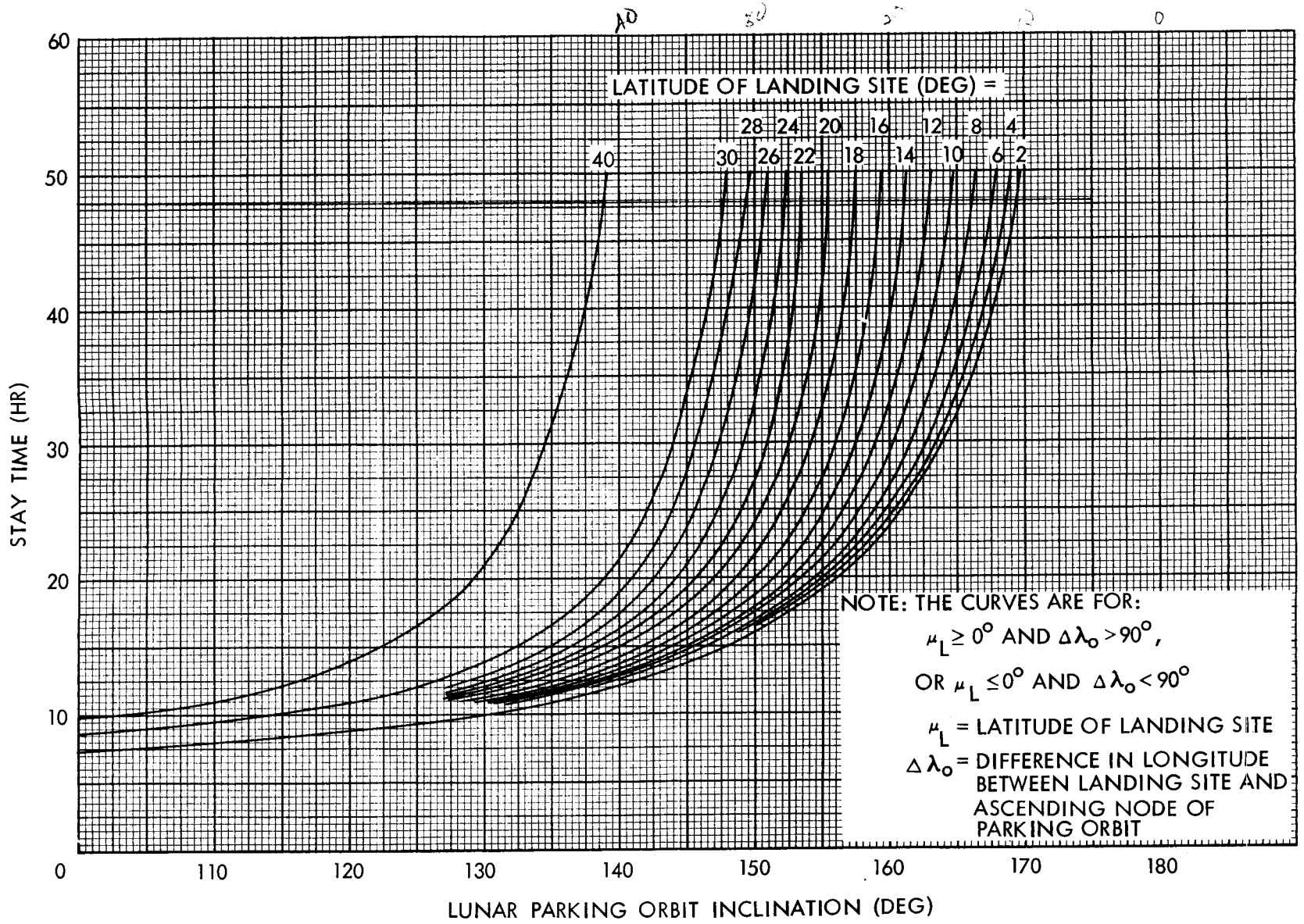

Figure 2. Lunar Surface Stay Time Requiring a 4° Plane Change at LEM Liftoff

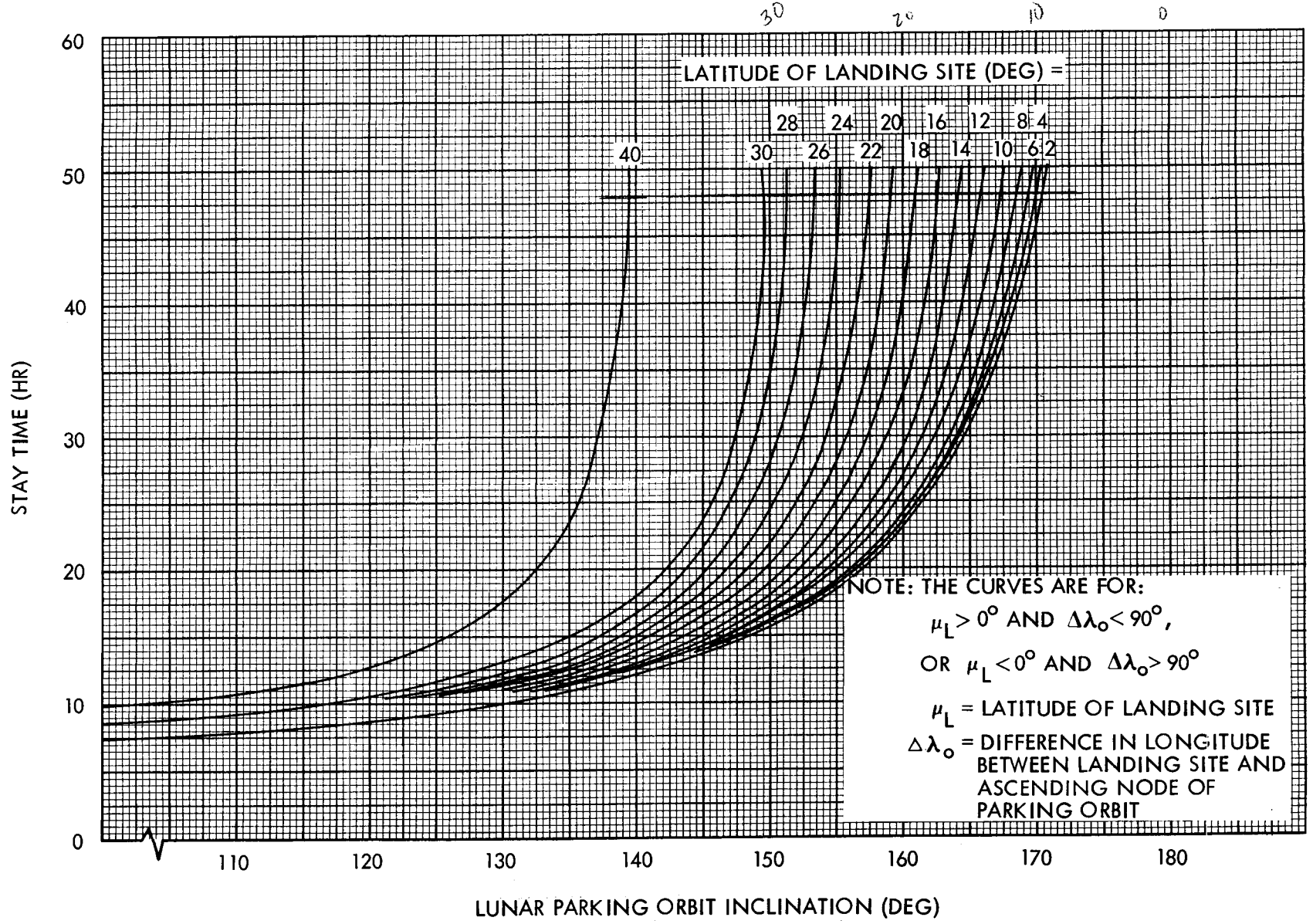

Figure 3. Lunar Surface Stay Time Requiring a 4° Plane Change at LEM Liftoff